The tracking detector of the MEG II experiment.

Dottorato di ricerca Fisica e Nanoscienze

XXIX° ciclo

PhD student:
Gianluigi Chiarello

Tutors:
Prof. M. Panareo
Dott. F. Grancagnolo

Outline

- Flavor violation
- Signal and background
- MEG experiment
- MEG I
- MEG II Detector
- MEG II CDCH
  - Design
  - Front End Electronics
  - Construction
  - Wiring Robot
  - Assembly
  - Performance
- Conclusion

Flavour violation

Lepton flavour is preserved in the SM naturally violated in SM extensions

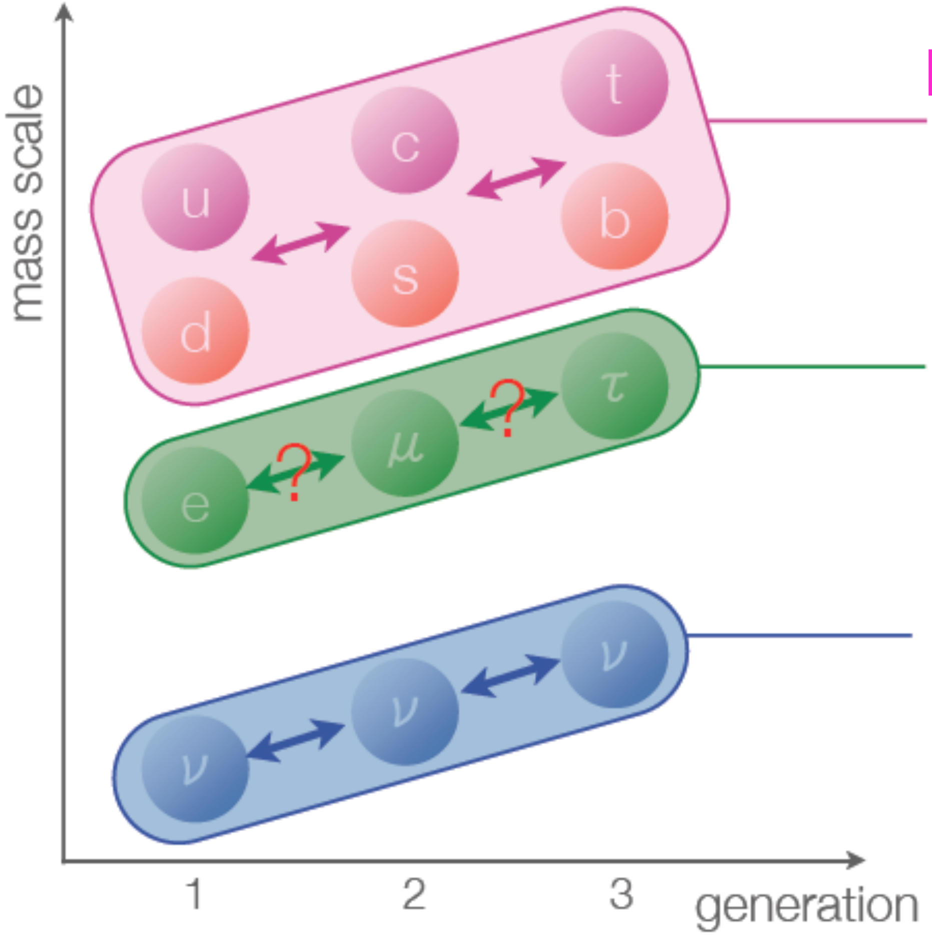

☑ Quarks

- Quark mixing observed by various accelerator experiments
- Standard Model: *CKM mixing matrix*

☐ Charged lepton flavor violation

- Not observed

☑ Neutrinos

- Neutrino oscillations observed by various neutrino experiments
- Standard Model: *PMNS mixing matrix*

charged Lepton Flavour Violation

STANDARD MODEL: cLFV are strongly suppressed even in the MSM extension with neutrino masses and oscillation

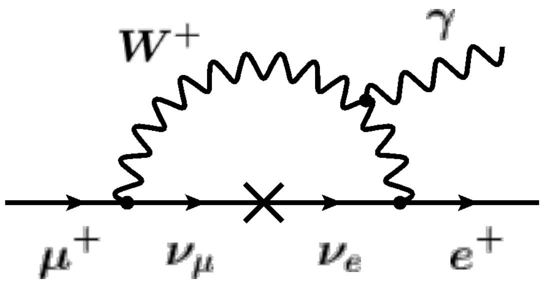

$$\mathrm{Br}(\mu \to e\gamma) = \frac{3\alpha}{32\pi} \sum_i \left| U^*_{\mu i} U_{ei} \frac{m^2_{\nu_i}}{m^2_W} \right|^2 \approx 10^{-54}$$

Experimentally not measurable !

NEW PHYSICS: Many new physics scenarios (SUSY and variation...) predict an enhanced probability, through mixing between new particle of the theory.

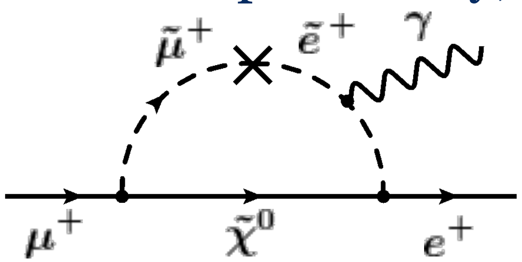

$$\mathrm{Br}(\mu \to e\gamma) \approx \frac{\alpha^3}{G_F^2} \frac{(\delta_{\mathrm{LL}})^2_{e\mu}}{m^4_{\mathrm{SUSY}}} \tan^2(\beta) \approx 10^{-11} \sim 10^{-14}$$

An experimental evidence is a clear signature of New Physics and strongly constraints the NEW PHYSICS scenarios

charged Lepton Flavour Violation:70 years history

Annu. Ref. Nucl. Part. Sci. 2008. 58:315-41 W. J. Marciano, T.Mori, and J. M. Roney

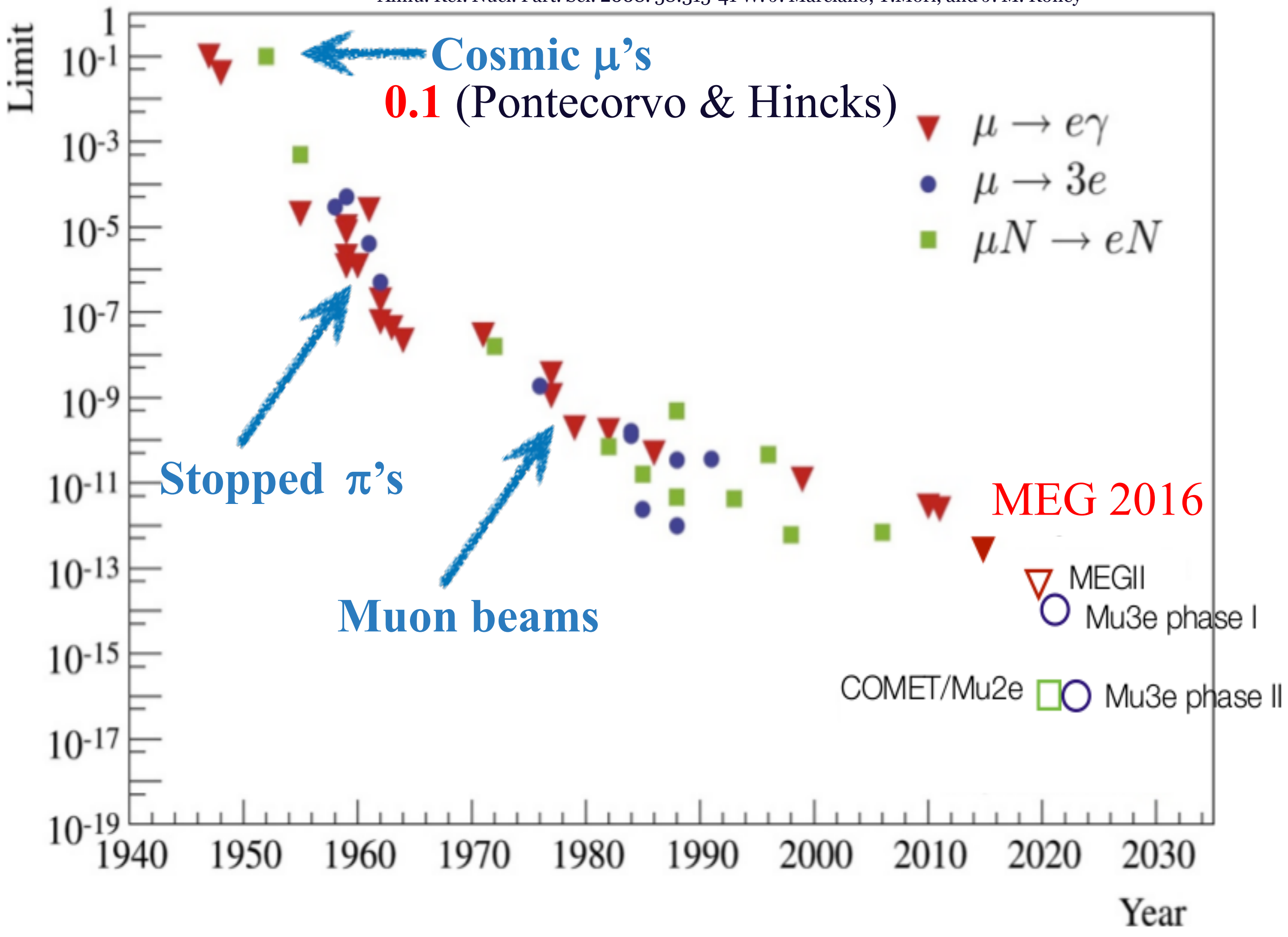

Processes involving muons are best constrained: Muons are copiously produced at high-intensity proton accelerators and have precisely measurable final states

MEG event kinematic

Signal

$t_e = t_\gamma$
$E_e = E_\gamma = 52.8$ MeV
$\theta_{e\gamma} = 180º$

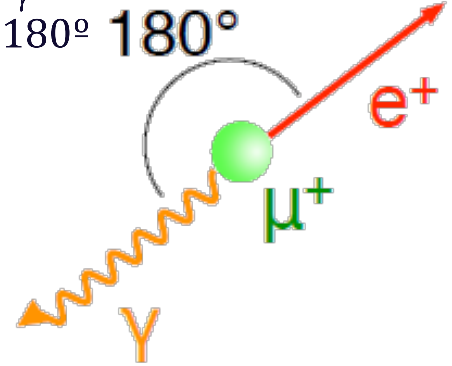

RMD

$t_e = t_\gamma$
$E_e = E_\gamma < 52.8$ MeV ($\pm\delta E$)
$\theta_{e\gamma} < 180º$

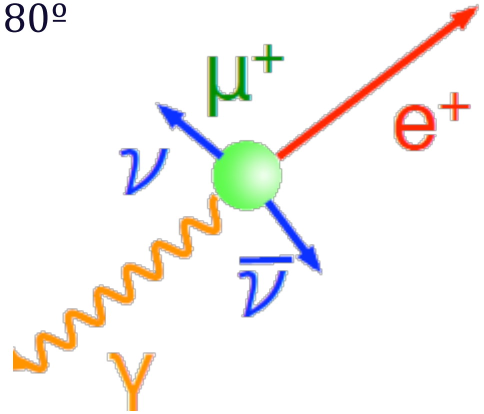

Accidental

$t_e = t_\gamma \pm \delta$
$E_e \sim E_\gamma \sim 52.8$MeV ($\pm\delta E$)
$\theta_{e\gamma} \sim 180º$

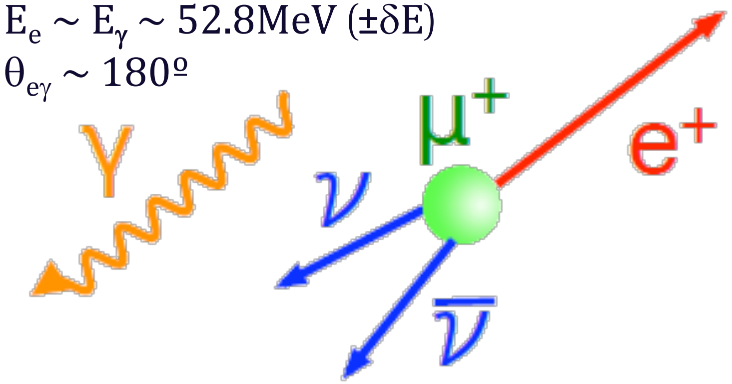

- $\mu \to e\gamma$ **signature**: photon and positron simultaneously emitted back-to-back and with equal energies in the Center-Of-Mass system.
- radiative decay $\mu \to e\nu\nu\gamma$: two neutrinos have low energy and γ and e emitted back-to-back with high energy (rare)
- "accidental": e and γ from different sources but with compatible kinematics to the $\mu \to e\gamma$ (e.g. e^+ from Michel decay, γ from RMD, e^+e^- annihilation…)

To distinguish the signal from the background it is necessary to have a high resolution detector and an efficient algorithm

The MEG experiment

Detector location is at the *Paul Scherrer Institut* near Zürich, Switzerland

- The MEG experiment, at the PSI searches $\mu \to e\gamma$ decay with the most intense muon beam available(10^8 μ/s).
- The most recent measured limit is **4.2×10^{-13}@90% CL**

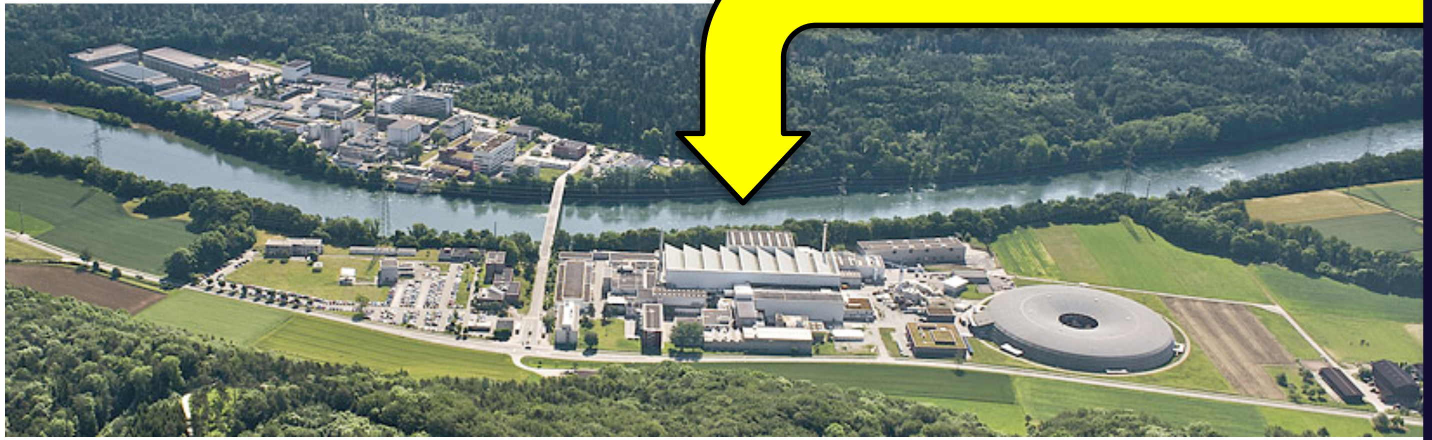

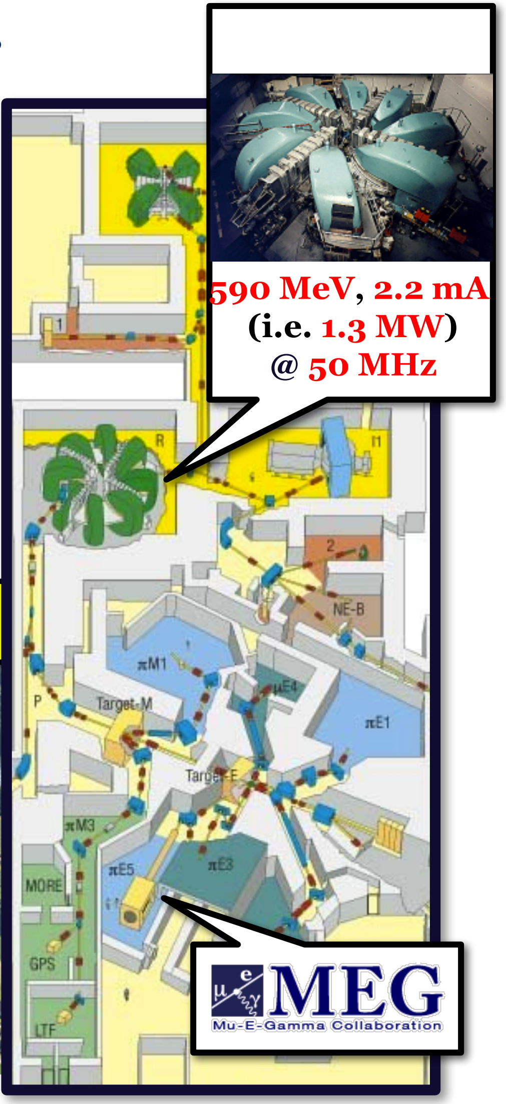

The MEG I Detector

3D view:

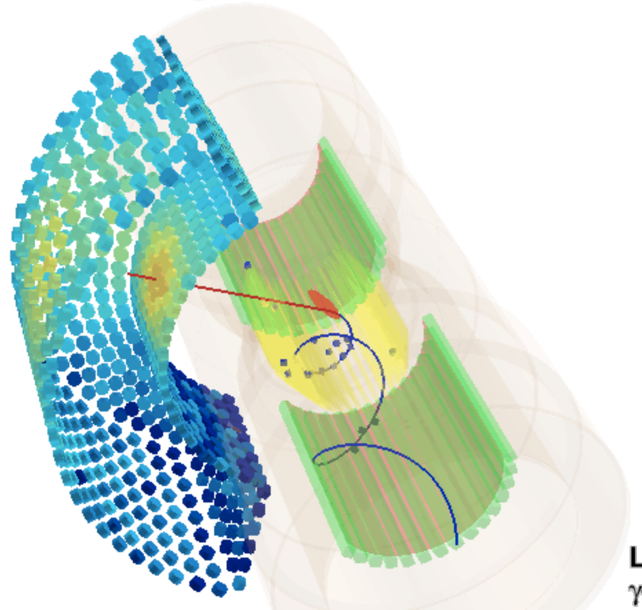

Lateral view:

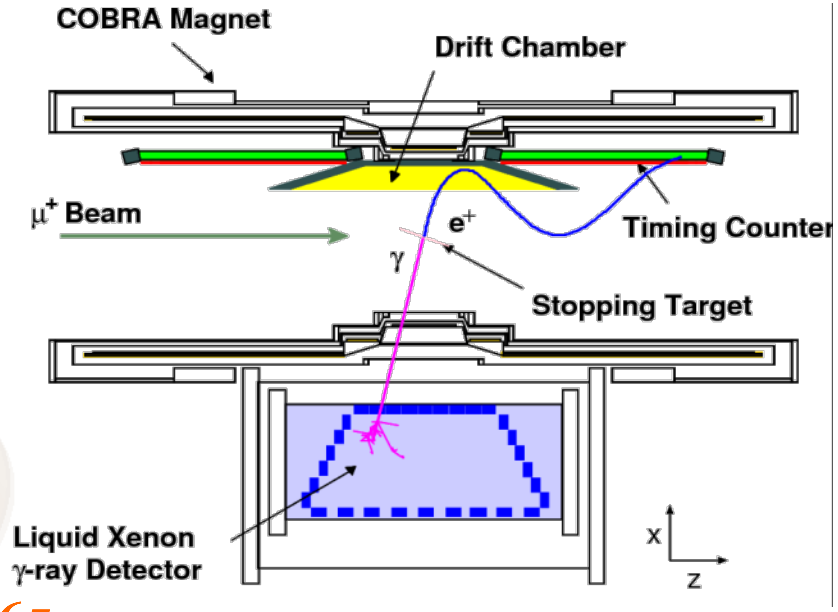

Front view:

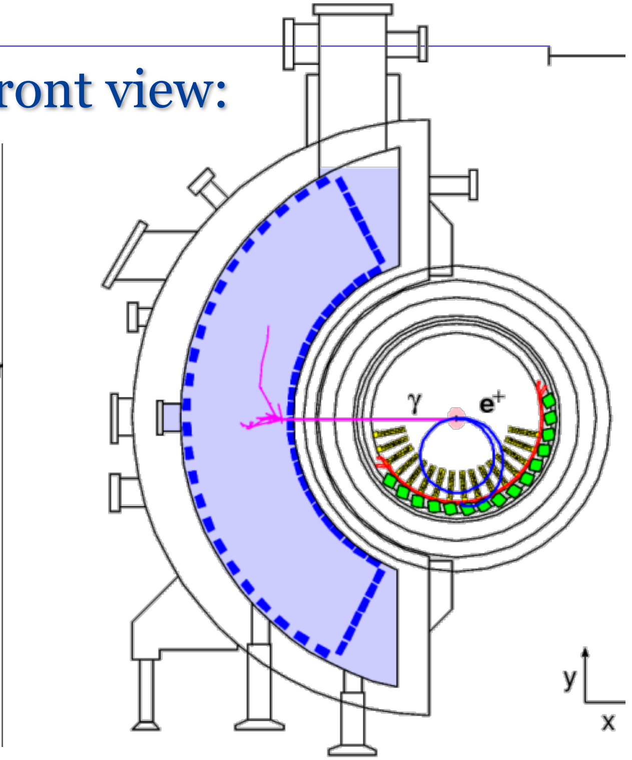

Eur. Phys. J. C 73 (2013) 2365

Dedicated detector with non-symmetric coverage ($\Omega_{MEG}/4\pi = 11\%$):

1. Photon detector with excellent spatial, time & energy resolutions
2. Positron spectrometer with excellent energy & timing capabilities
3. Stable and well monitored & calibrated detector (multitude of calibration & monitoring tools)
4. High performance DAQ system (multi-GHz waveform digitization of nearly all 3k channels)

MEG I: Analysis Result

Combined 2009-2013 analysis resulting in a factor 30 improvement of the world's most stringent BR($\mu \to e\gamma$) respect to MEGA (1999)

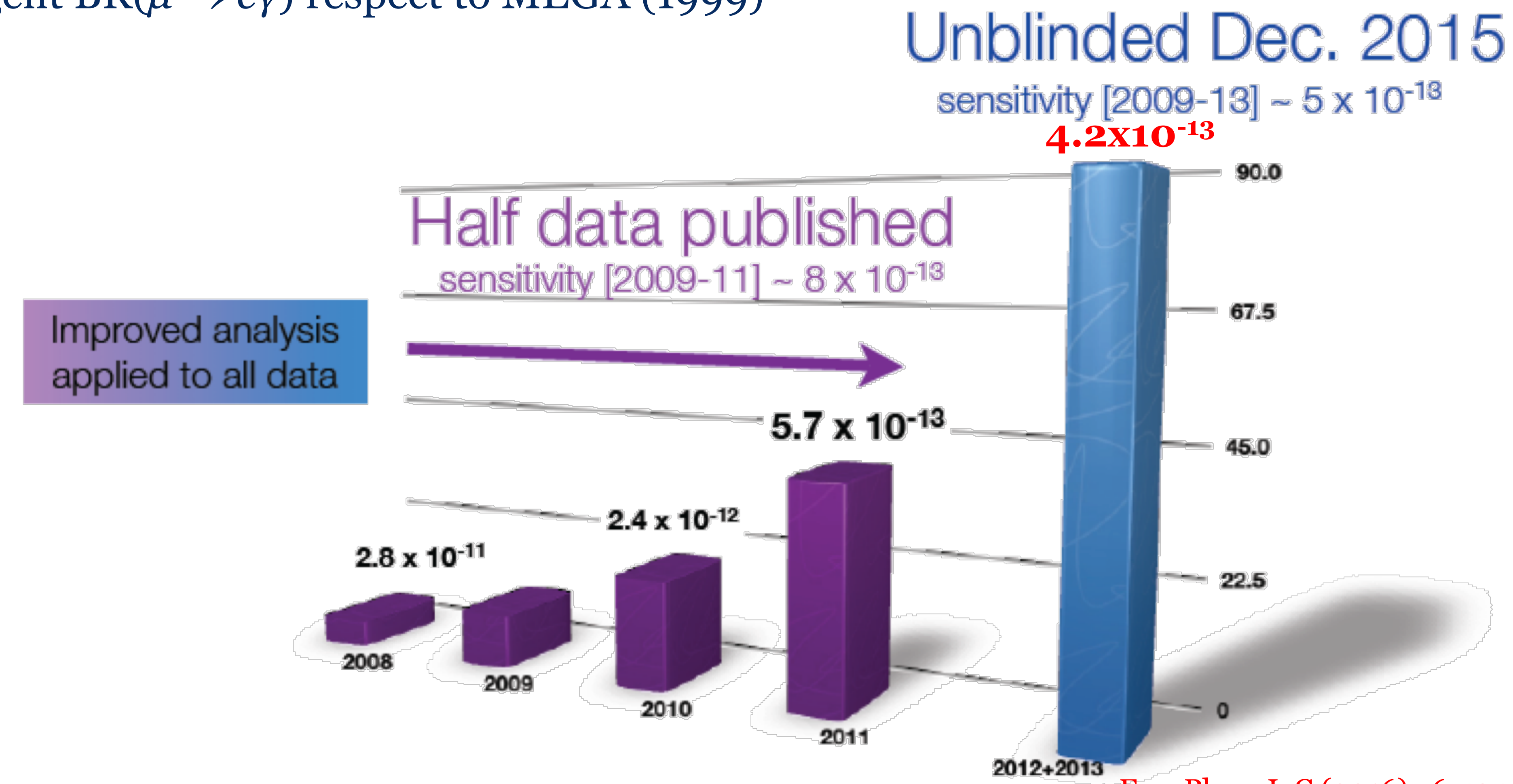

Eur. Phys. J. C (2016) 76:434

MEG II vs MEG I

arXiv:1301.7225

Goal: 10x improvement in sensitivity ($\sim 5 \times 10^{-14}$)

Upgrades:

1. **Increased beam intensity ($7 \times 10^7\ \mu^+/s$)**
2. **Thinner target (140 μm)**
3. **New single-volume cylindrical Drift Chamber**
4. **Pixelated TC with SiPM readout**
5. **New high-bandwidth DAQ boards**
6. **LXe with SiPM readout on front face**
7. **RMD counters**

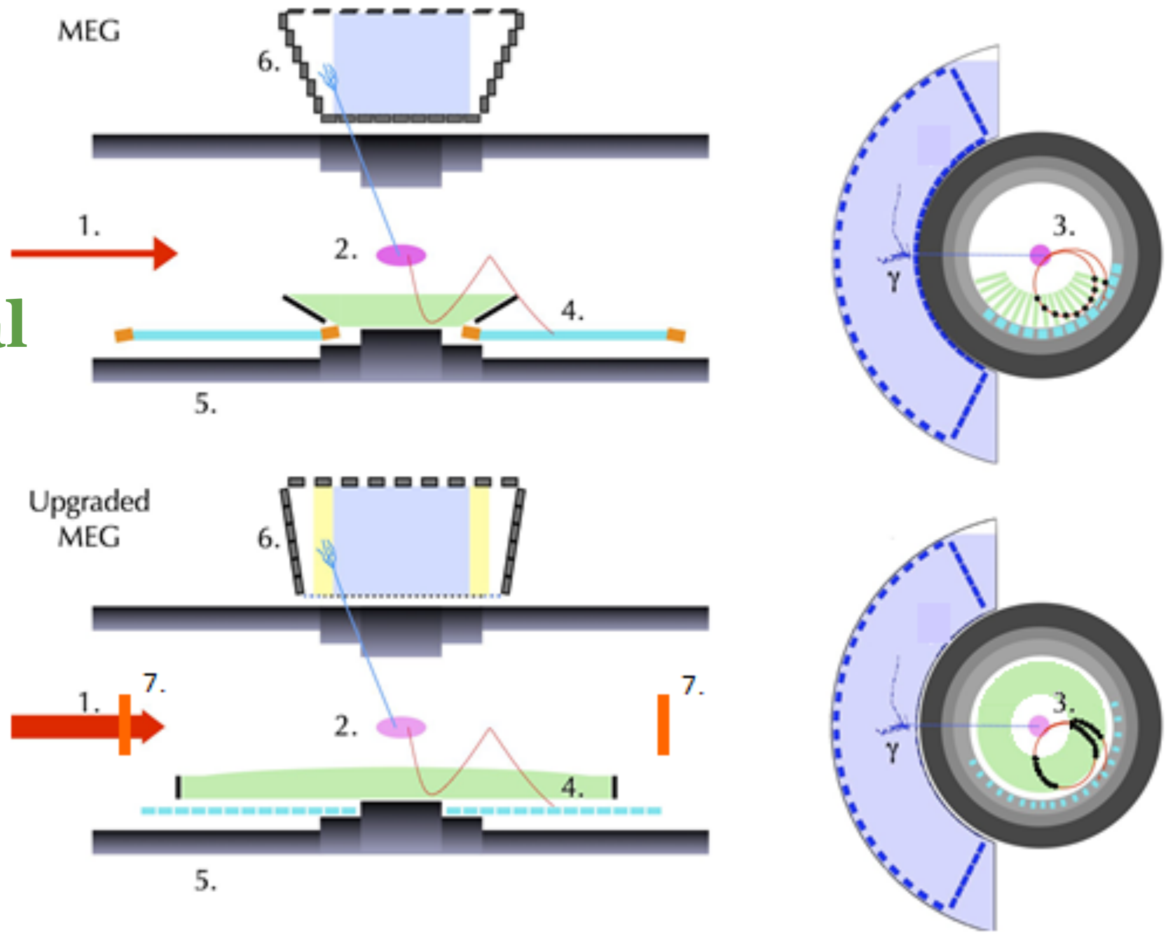

MEG I DC vs MEG II CDCH

Variable	Foreseen MEG	Obtained MEG	Foreseen MEG^{UP}
$\Delta E_\gamma (\%)$	1.2	1.7	1.0
Δt_γ (ps)	43	67	–
γ position (mm)	$4(u,v)$, $6(w)$	$5(u,v)$, $6(w)$	$2.6(u)$, $2.2(v)$, $5(w)$
ΔP_e (keV)	200	306	130
e^+ angle (mrad)	$5(\varphi_e)$, $5(\vartheta_e)$	$8.7(\varphi_e)$, $9.4(\vartheta_e)$	$5.3(\varphi_e)$, $3.7(\vartheta_e)$
Δt_e (ps)	50	107	–
$\Delta t_{e\gamma}$ (ps)	65	122	84
e^+ efficiency (%)	90	40	88
γ efficiency (%)	> 40	63	69
trigger efficient(%)	~99	~99	~99

MEG I DC did not perform as expected.

Main problems were:

- Few hits on the positron track (8-16)
- Active volume of the detector only partly instrumented
- Unmatched coverage with Timing counter
- Large track extrapolation to Timing counter

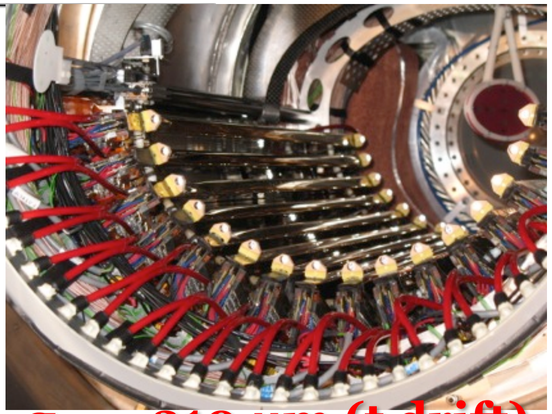

σ_{xy} ~ 210 µm (t drift)
σ_Z ~ 800 µm (Vernier)

MEG II Detector

arXiv:1301.7225

Liquid xenon with SiPM

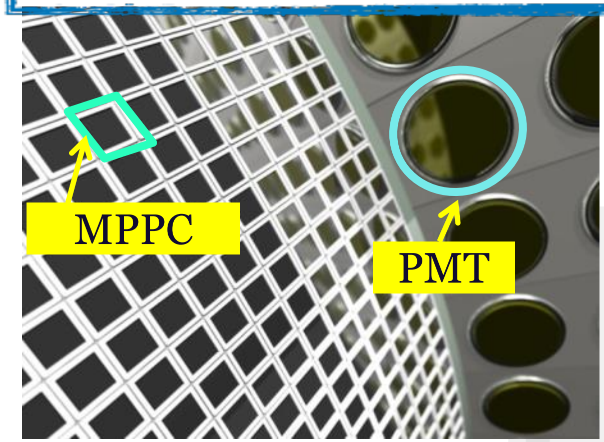

Drift chamber

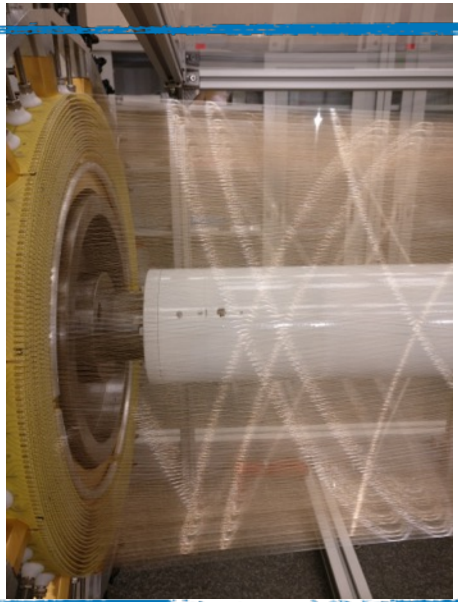

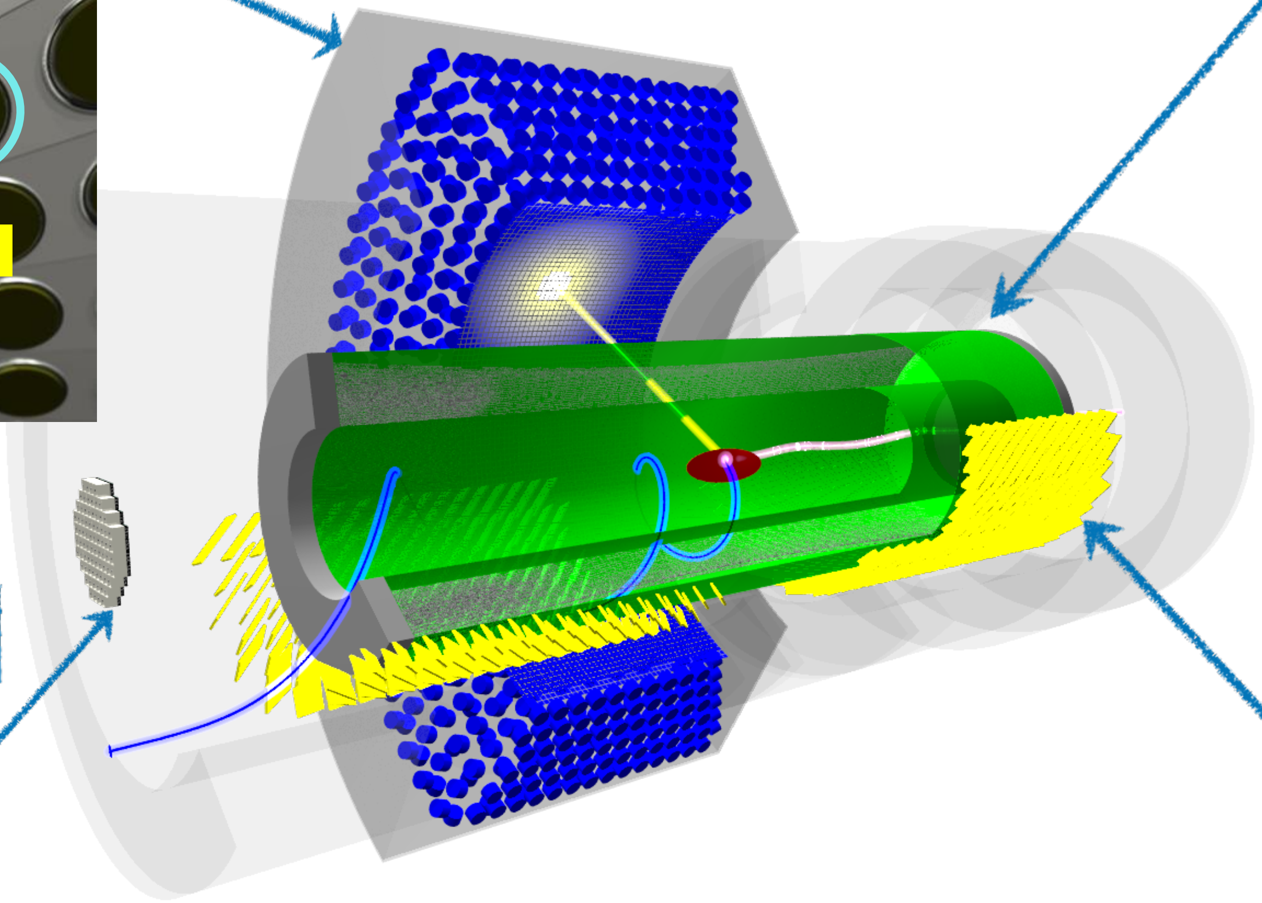

RDC

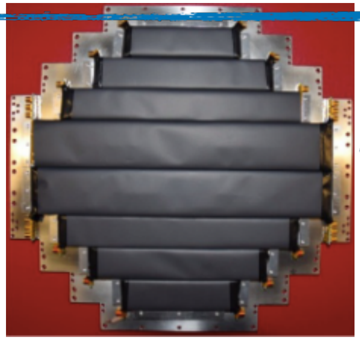

Pixelated Timing

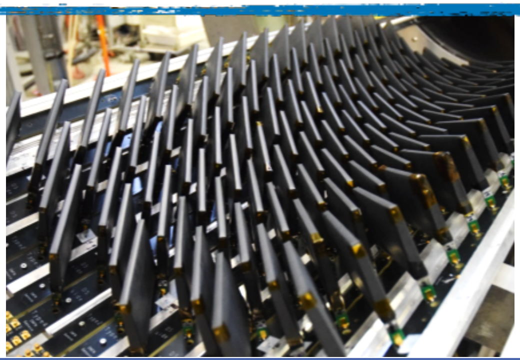

MEG II CDCH: Design I

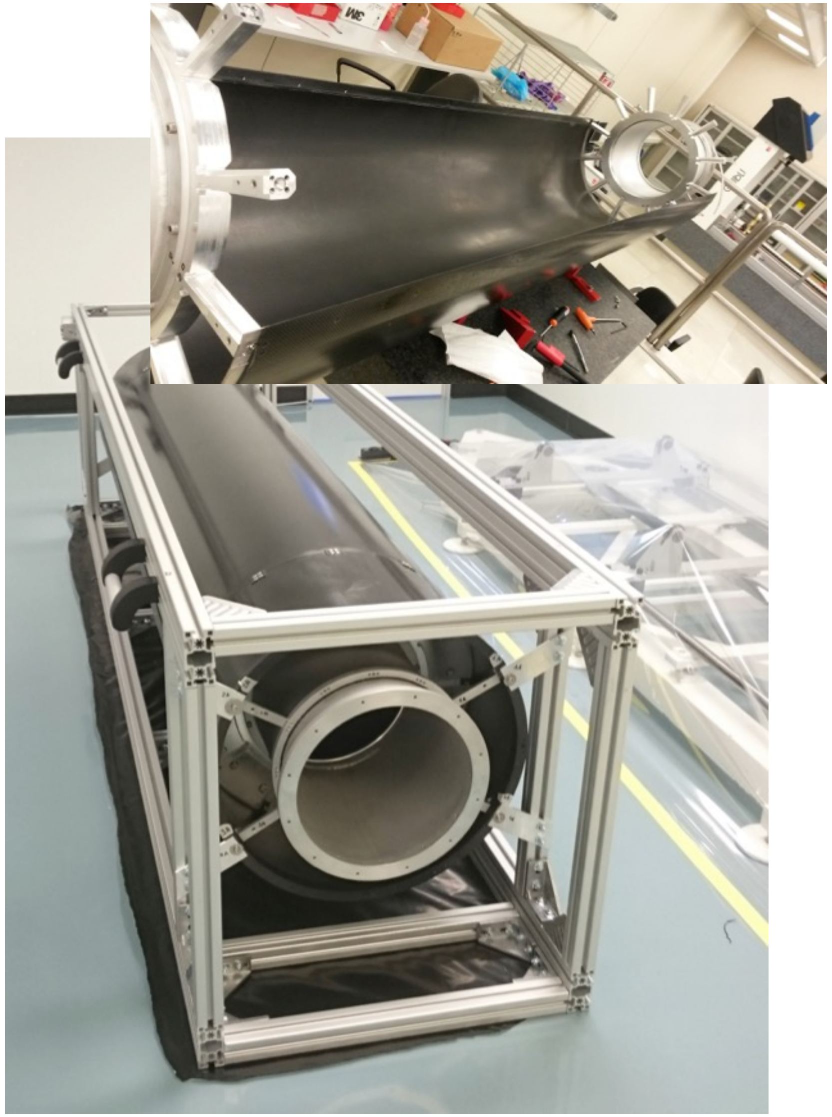

- The **MEG II positron tracker** is a **unique volume, cylindrical drift chamber**, with the axis parallel to the muon beam.
- The external radius of CDCH is 284 mm.
- The internal radius 196 mm.
- The CDCH length (193cm) is dictated by the necessity of:
  - **avoiding any material along the positrons path** to the timing counter in order to increase the positron efficiency;
  - **tracking the positrons trajectories as close as possible to the TC**.

MEG II CDCH: Stereo angle

$L \tan \varepsilon_i = 2 r_i \sin \alpha$
stereo angle, $\boldsymbol{\varepsilon_i}$

Drop $\delta_{i0} = r_i - r_{i0} = r_i(1 - \cos \alpha)$

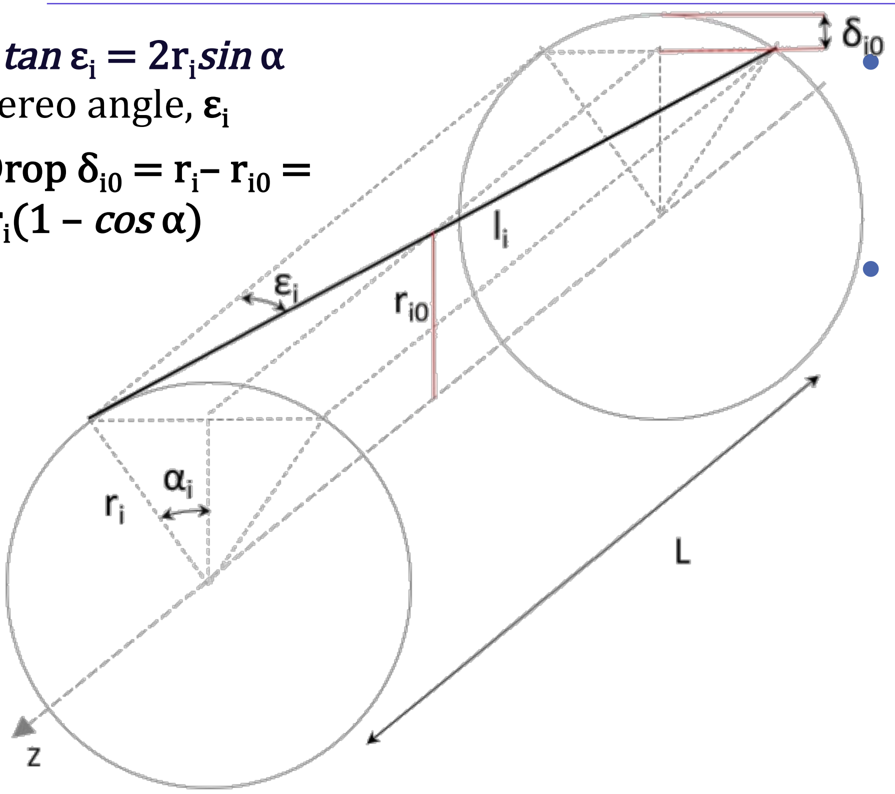

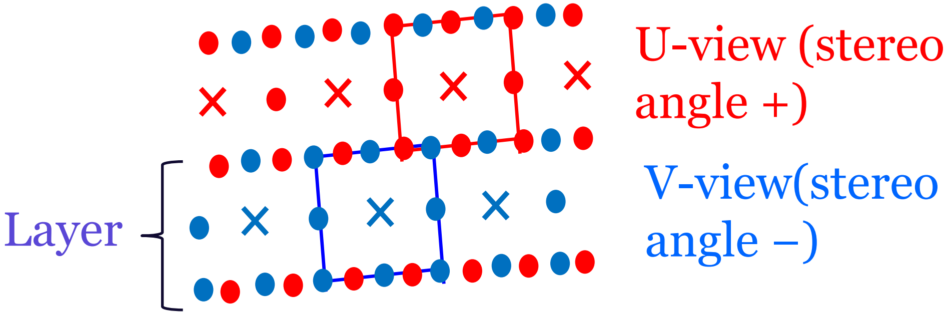

- A limiting factor of a drift chamber is the poor z resolution.

- The stereo layers can be arranged in:
  - **constant stereo angle (ε_i)** with the advantage of having the same view for all wires;
  - **constant projection angle (α_i)** to preserve the cell aspect ratio for all layers;
  - **constant drop (δ_o):** in this configuration the radial extent of the cell is constant for all layers (KLOE).

- The MEG II CDCH uses the constant projection angle configuration.
  - Small square cells **(5.8÷7.8 mm)**

MEG II CDCH: Wires

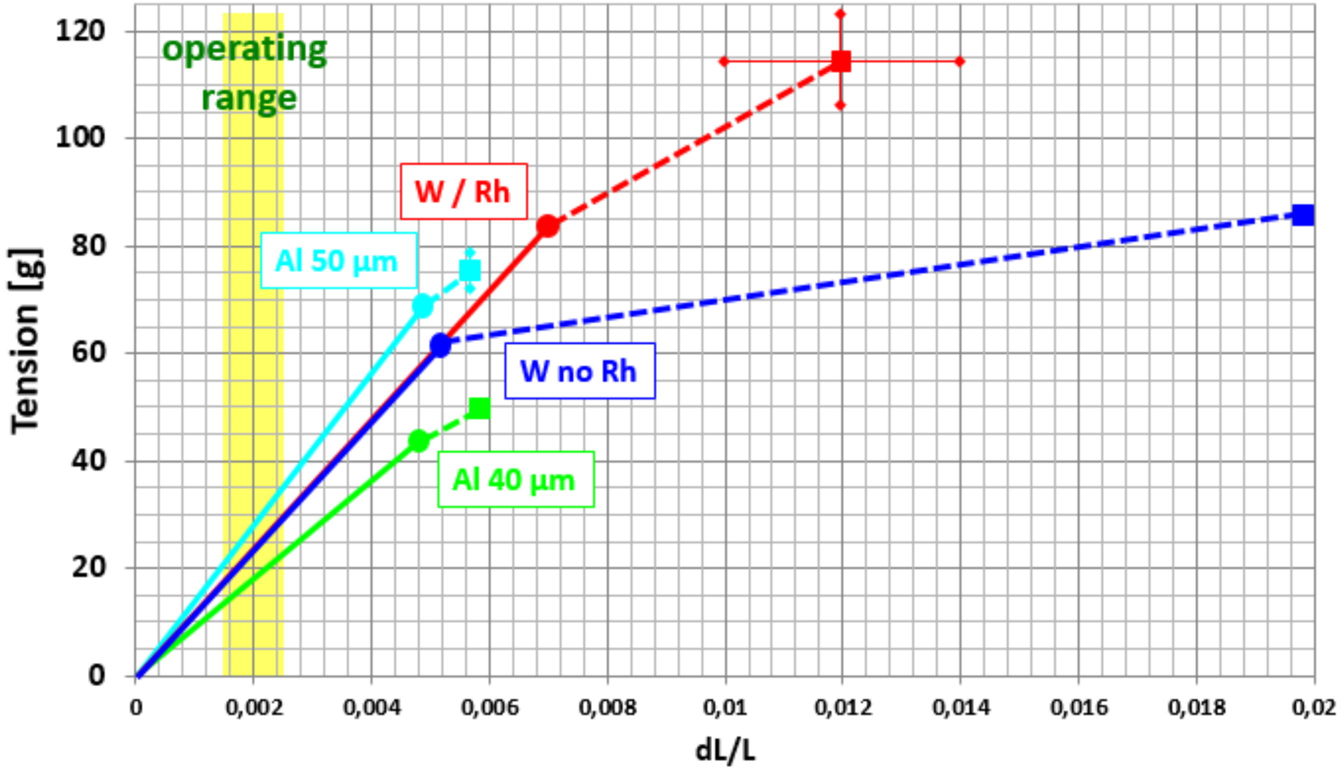

Thype	Sagitta(μm)	Mechanical Tension (g)
20 μm W-Au pltd	115	24.52
40 μm Al-Ag pltd	91	19.25
50 μm Al-Ag pltd	93	29.64

The choice of the wire size is dictated by electrostatics considerations.

- a gas gain 3×10^5
- the electric field on the sense wires is about 2×10^5 V/cm

Therefore, in CDCH are used:

- Sense wires: 20 μm diameter W(Au)
- field wires: 40 μm diameter Al(Ag)
- Guard wires: 50 μm diameter Al(Ag)

The operating point is chosen at an absolute elongation **of 4 mm for the 2 m long wires**, corresponding to a relative elongation **of 0.2%** at about 40% of the elastic limit for all wires.

MEG II CDCH: Design II

- MEG CDCH uses an **ultra-low mass gas mixture**
  - Helium and Isobutane (85:15) in this configuration produces about **14.5 ionization** clusters/cm.
- The accurate reconstruction of the **positron tracks** is strongly influenced by **Multiple Columb Scattering**. Its minimization is critical in order to achieve high momentum and angular resolution.

Item	Description	Thickness(10^{-3} X_0)
Target	140 μm Polyethylene	0.21
Sense wires	20 μm W	0.16
Field wires	40 μm and 50 μm Al	0.33
Inner gas	He	0.06
CDCH gas	85He:15iC_4H_{10}	0.53
Inner foil	20 μm Mylar	0.14
Total	1 full turn (without) target	1.49(1.28)

MEG II CDCH: Design III

Chamber characteristics:

- **10 layers**
  - 12 30° sectors
  - **16 cells** per sector
- **12288 wire**
  - 1920 sense wires: W(Au) 20 μm
  - 7680 field wires: Al(Ag) 40 μm
  - 2688 guard wires: Al(Ag) 50 μm
- full stereo with large stereo angles **(102÷147 mrad)**
- small square cells **(5.8÷7.8 mm at z=0, 6.7÷9.0 at z=±L/2)**
- A large field to sense wires ratio (5 : 1) allows for thinner field wires.

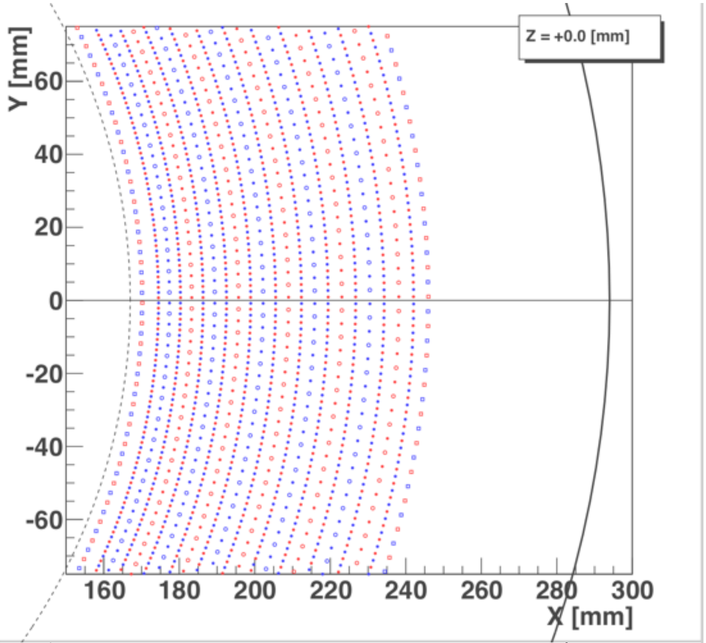

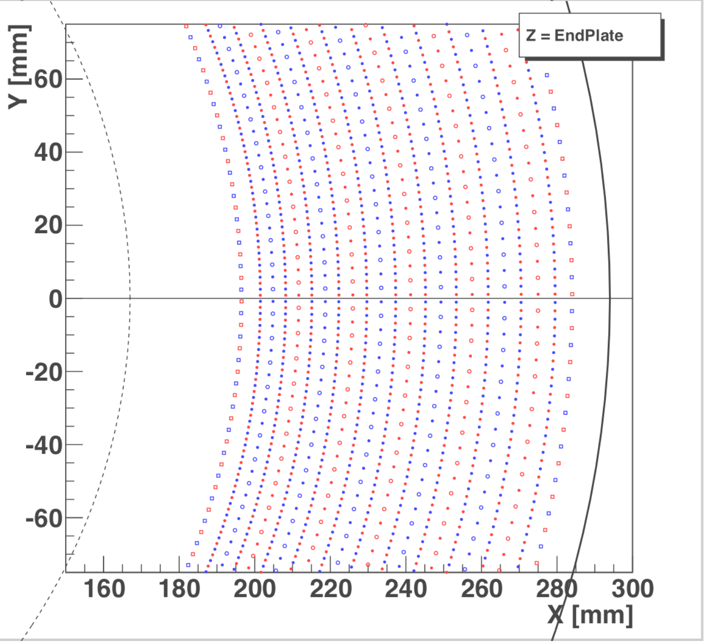

MEG II CDCH: Design IV

- **2-mm thick carbon fiber** cylindrical support at the outer radius
- an **aluminized mylar foil, 20 μm** thick at the inner radius

MEG II CDCH: Front End Electronics

1280 out of 1920 channels (2/3) readout on both ends

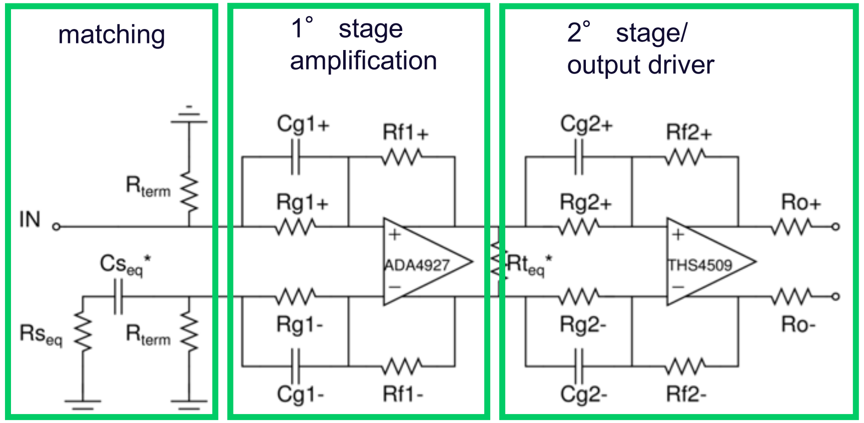

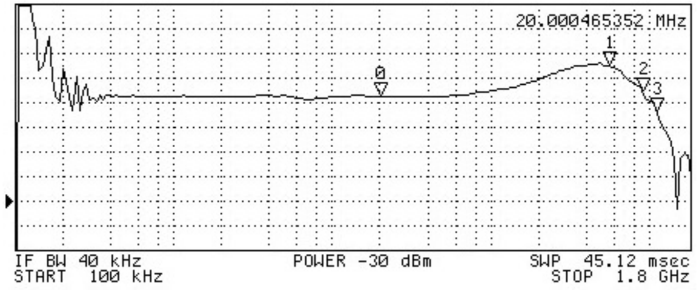

N	SWP PARAM	VAL
0	20.000465352 MHz	21.236 dB
1	554.109452707 MHz	27.458 dB
2	899.74895028 MHz	22.206 dB
3	1.099455926016 GHz	18.203 dB

Layout:

- **2 stage amplifiers**
- **Pre-emphasis** implemented on both stages in order to balance the attenuation of output cable
- High overall (*after 5m of cable*) bandwidth (FE input to DRS WaveDream input): ~1GHz
- Low power: **60mW** @ ±2.5V

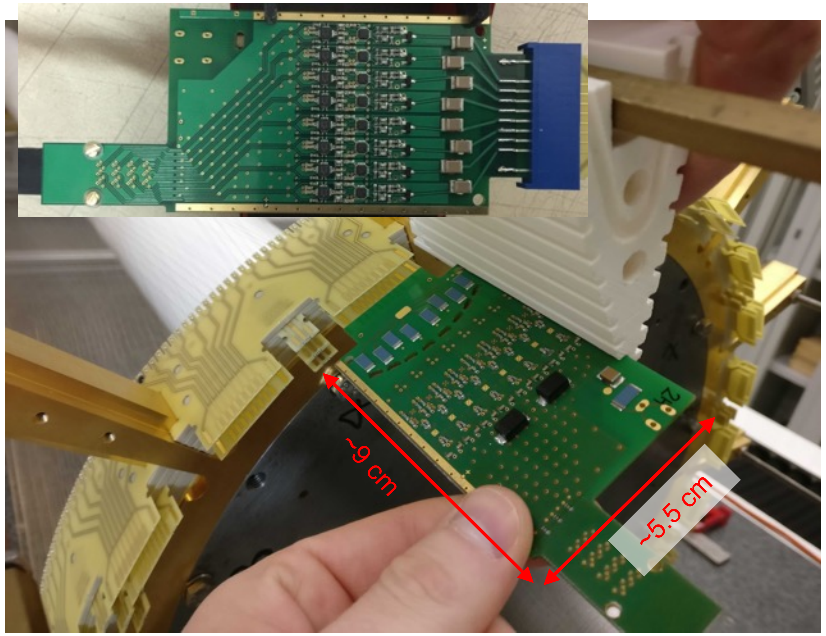

MEG II CDCH

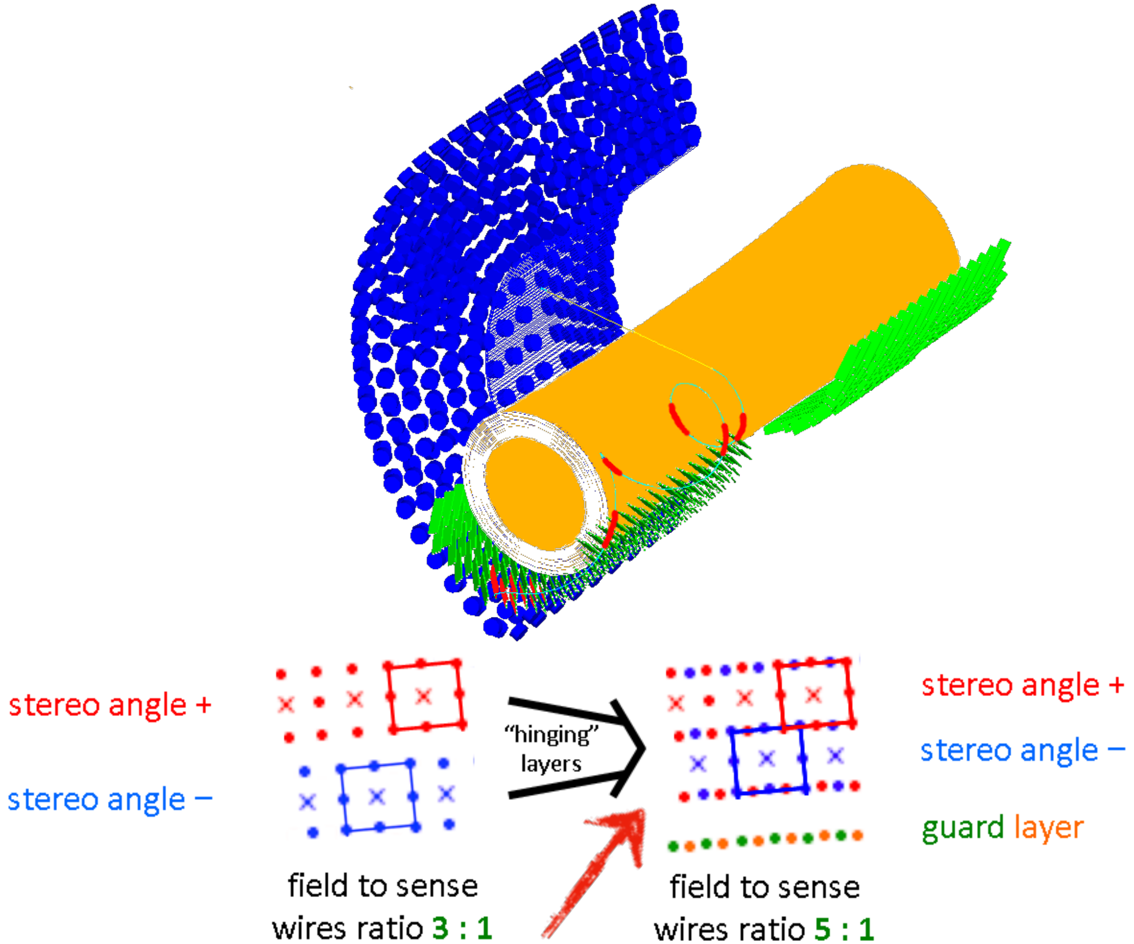

The wire net created by the combination of + and – orientation generates a more uniform equipotential plane

- Single volume, small cells, full stereo cylindrical drift chamber;
- A large field to sense wires ratio (5 : 1) allows for thinner field wires, thus reducing the **wire contribution to multiple scattering** and the **total wire tension** on the the end-plates.
- Light gas mixture **(85% He – 15% iC_4H_{10})**
- Positron efficiency > 90% (better coupling with TC, very short extrapolation needed);
- Cluster Timing readout capabilities **(high bandwidth, high sampling rate) to** further reduce spatial resolution

High wire densities, anyway, require complex and time consuming assembly procedures and need novel approaches to a feed-through-less wiring

MEG II CDCH: Construction

The traditional technique

“A cylindrically symmetric gas volume with (para-)axial wires defining a strong electric field, strung under mechanical tension for electrostatic stability and fixed at their extremities to the end walls by means of feed-through.”

CONSTRAINTS:

- The **end walls**, holding the feed-through (which limit the chamber granularity), the FE electronics and the relative cabling, must be rigid enough to transfer the load due to the wire tension (of the order of several Tons) to the **outer cylindrical wall**, without deforming.

- The **gas tightness** relies on the hermetic properties of all surfaces and of all their relative joints.

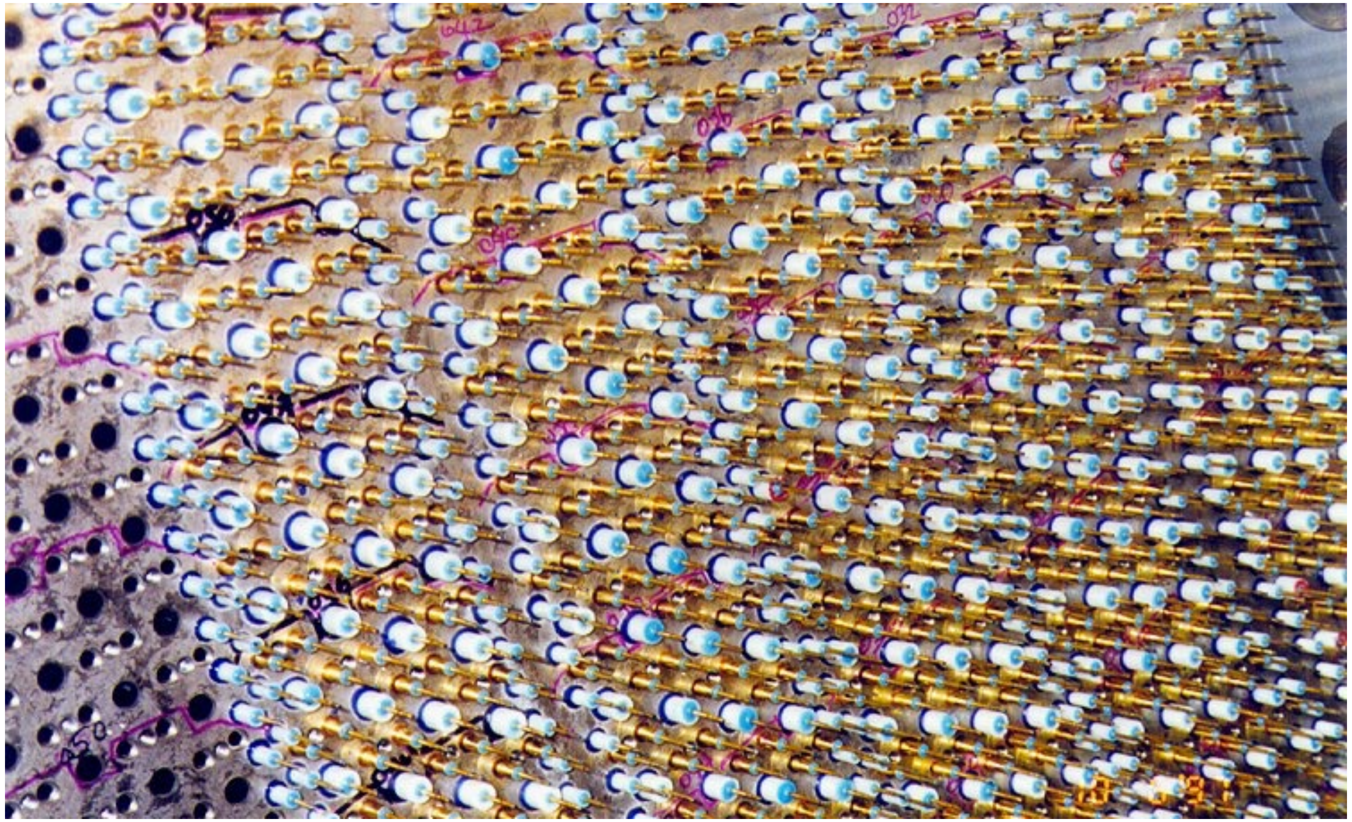

MEG II CDCH: Construction

The innovative technique

- Separating **gas containment** from **wire support** functions: the **Gas envelope** can freely deform without affecting the internal wire position and tension
- This scheme does not require **wire feed-through** thus allowing for denser wire spacing, i.e. **smaller cells** (finer chamber granularity) and for **larger field to sense wires ratios**.
- **Larger field to sense wires ratio** and, therefore, **thinner field wires**, help reducing **multiple scattering contribution** and **total wire tension** on support structure.
- Large number of wires and small cells, however, require complex and cumbersome **assembly procedures**, which call for a **novel approach** to the wiring problem.

MEG II CDCH: Construction

The **solution** found for MEG II:

- ✓ end-plates numerically machined from solid Aluminum (mechanical support only);
- ✓ Field, Sense and Guard wires placed by Wiring Robot with better than one wire diameter accuracy;
- ✓ wire PC board layers (yellow) radially spaced by numerically machined peek spacers (gray) (*accuracy < 20 μm*);
- ✓ wire tension defined by homogeneous winding and wire elongation (ΔL *= 100μm corresponds to ≈ 0.5 g*);
- ✓ Drift Chamber assembly done on a 3D digital measuring table;

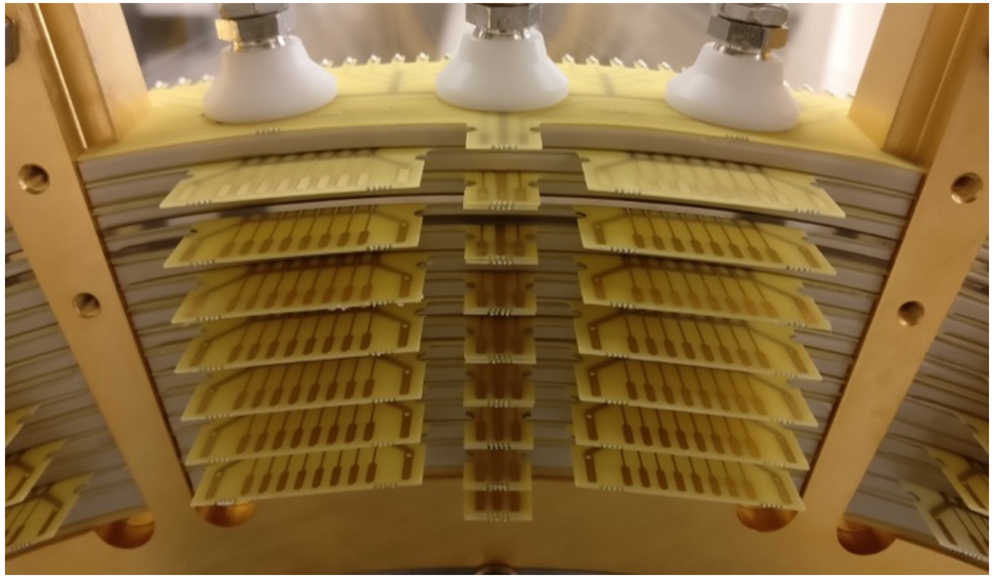

MEG II CDCH: The wire PCBs

- The wire PCBs are made of 400 μm thick FR4 board with 35 μm gold plated copper traces.
- Three types of wire PCBs have been produced:
  - guards
  - cathodes
  - anodes
- All wire PCB pads are oriented along the stereo angle ⇒ two versions of wire PCB (upstream and downstream)
- The US and DS wire PCB are coupled together in a single FR4 board for a precise alignment during the wiring procedure

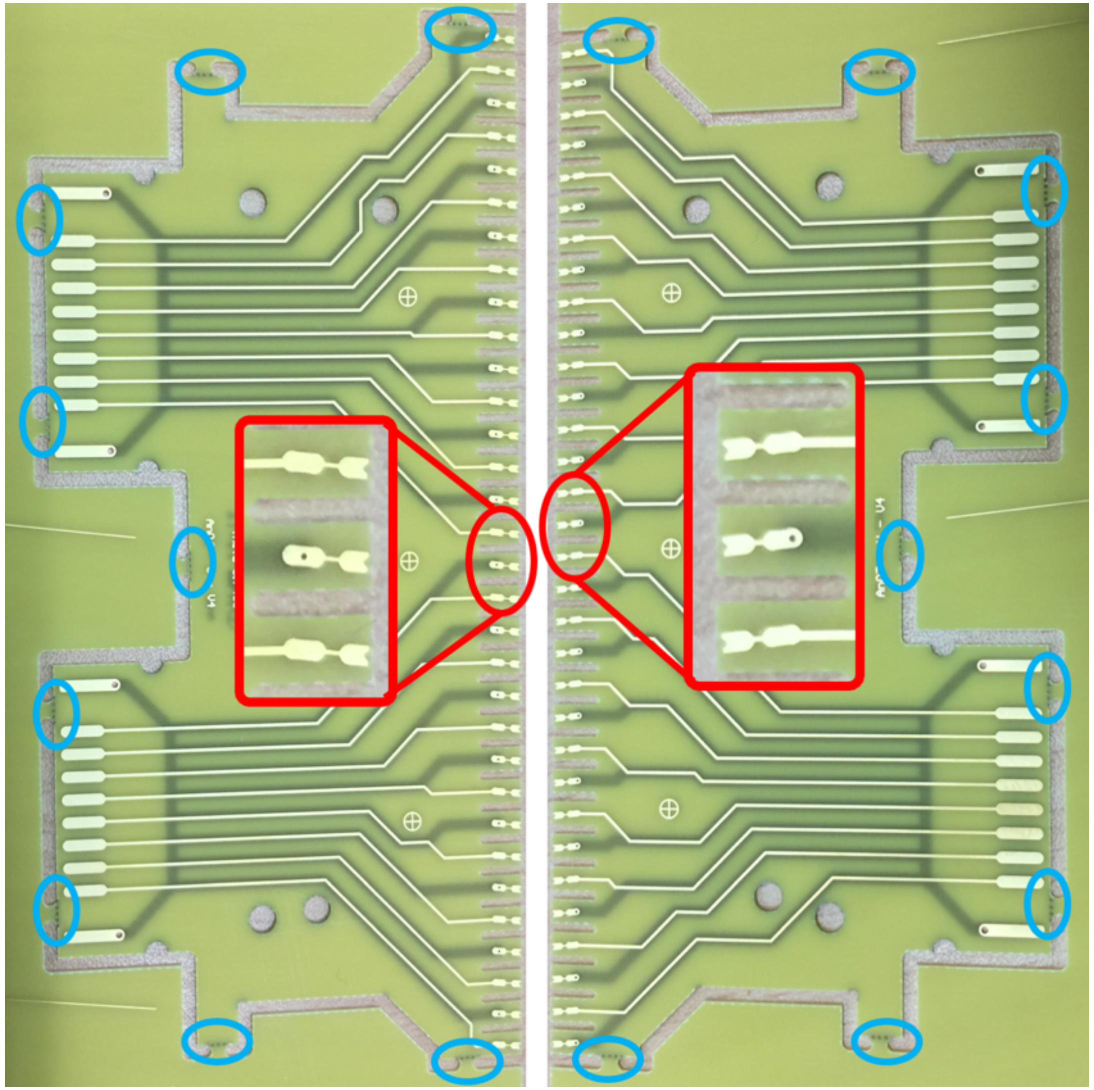

MEG II CDCH: The wiring robot

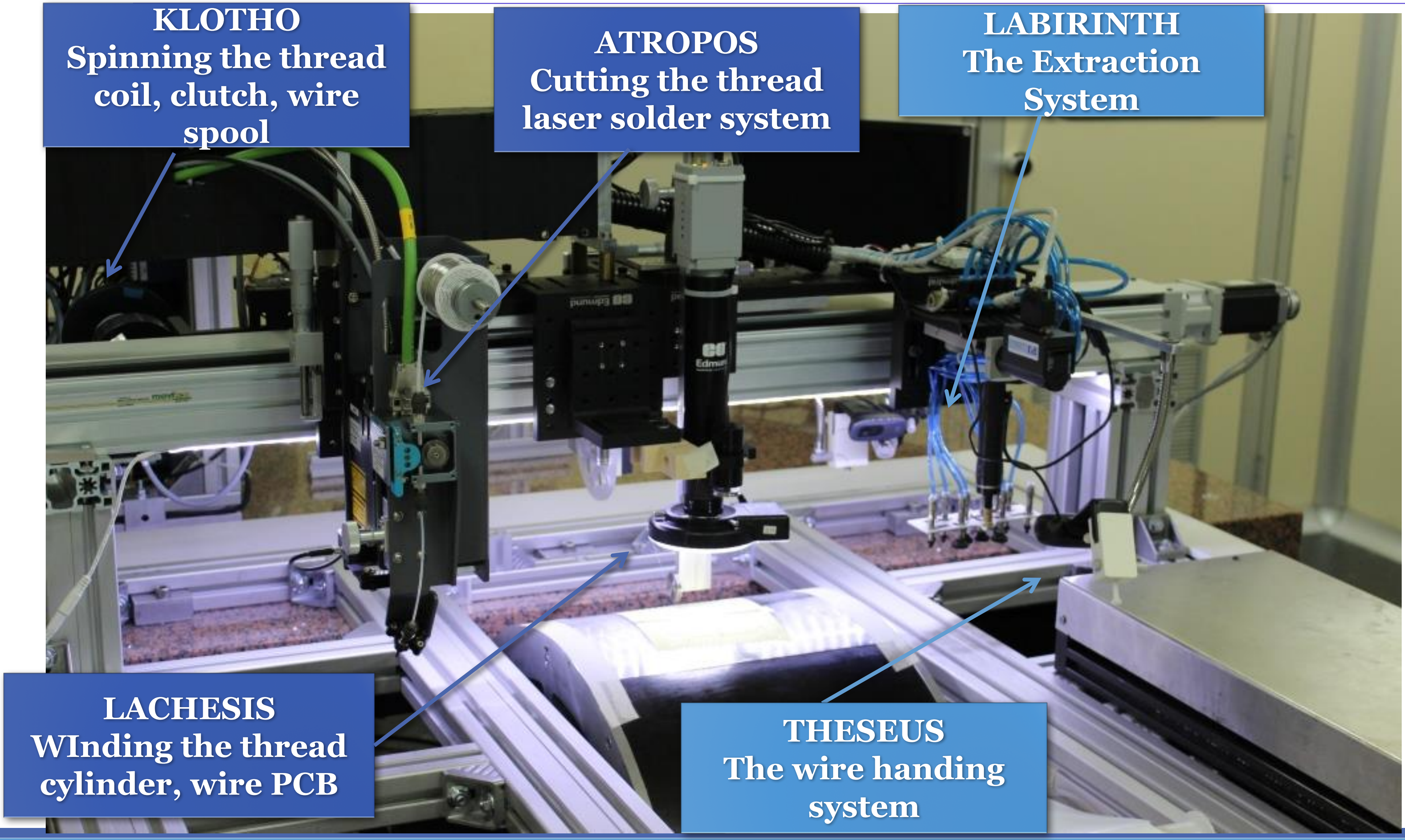

The wiring robot is required to manage the positioning of a large quantity of wires with precise alignment and mechanical tension.

The DAQ

Software LabVIEW

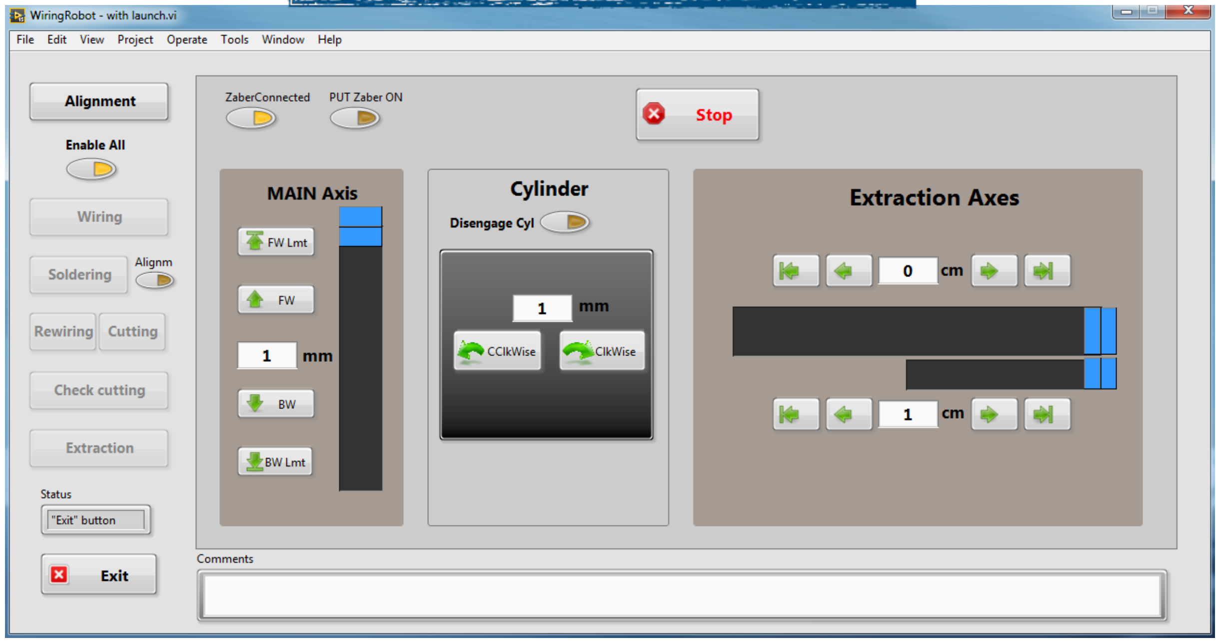

Hardware

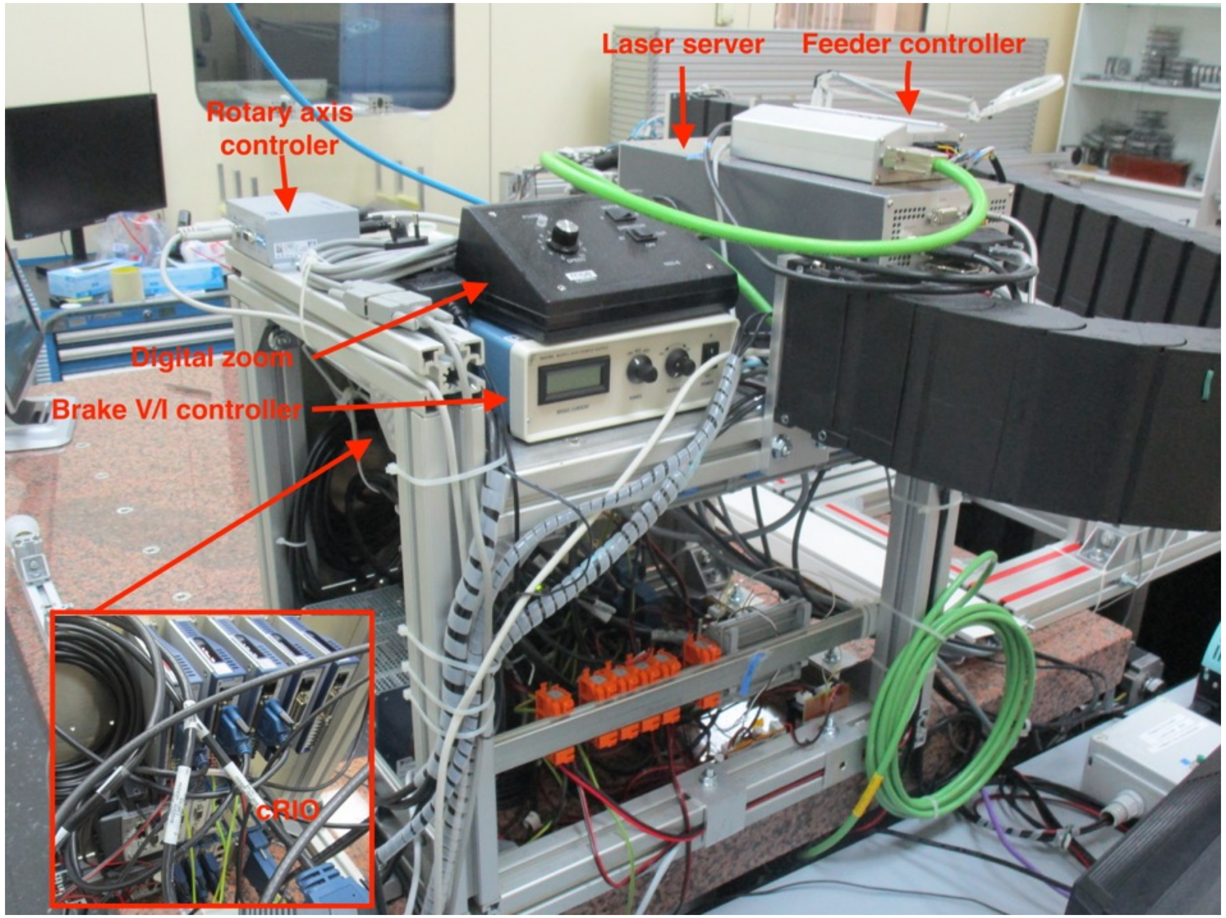

WIRING SYSTEM (*Klotho and Lachesis*)

The **wiring system** has the task of distributing the wire along a **helicoidal trajectory (32 parallel wires)** with high precision and with a constant pre-defined mechanical tension.

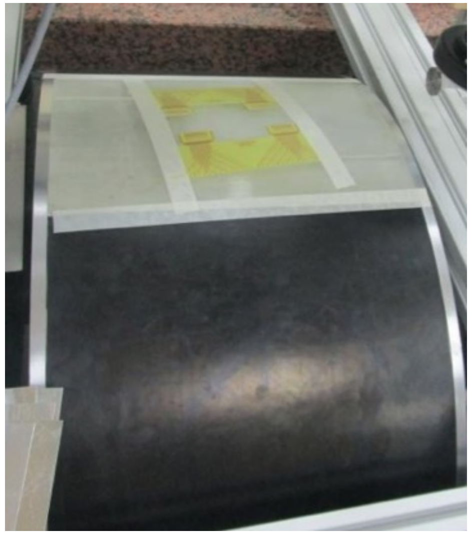

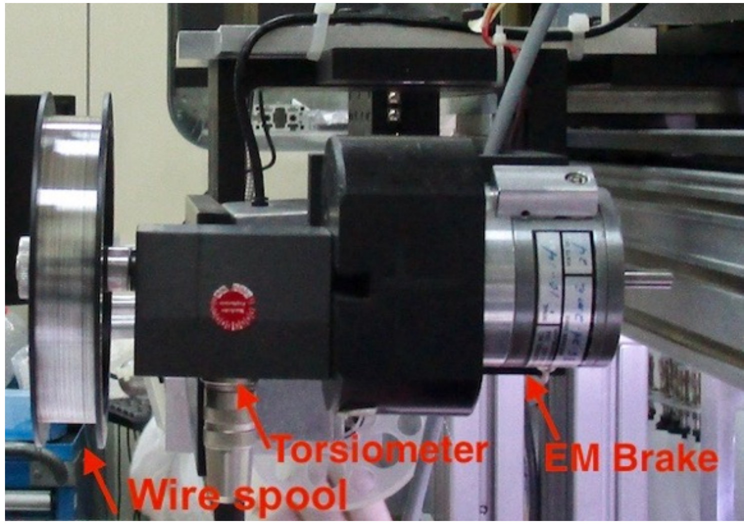

The wiring system is composed from:

- **a rotating cylinder**
- **wire spool holder**
- **a pulley system.**

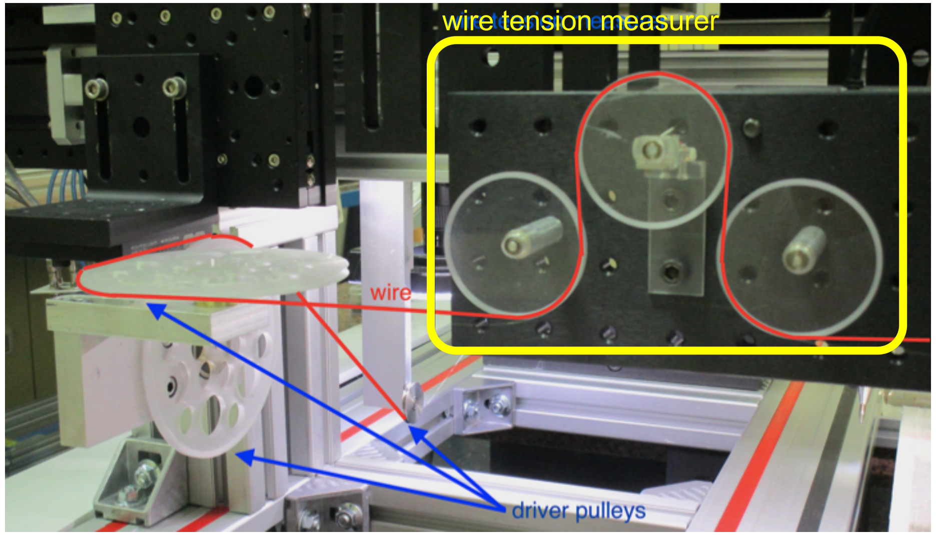

WIRING SYSTEM (***Klotho and Lachesis***): feedback

The wire mechanical tension is delivered by an electromagnetic clutch and its on-line monitored by a high precision strain gauge, a real-time feedback system correct any variation.

- The feedback system reduces the wire tension variations to less then $\pm 0.05\ g$.
- The systematic difference in tension between two adjacent wires is about 0.005 g

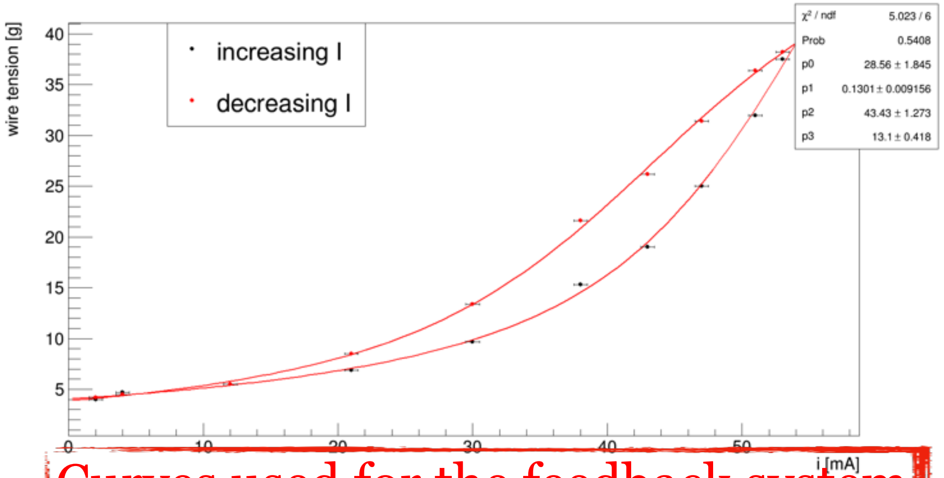

Curves used for the feedback system

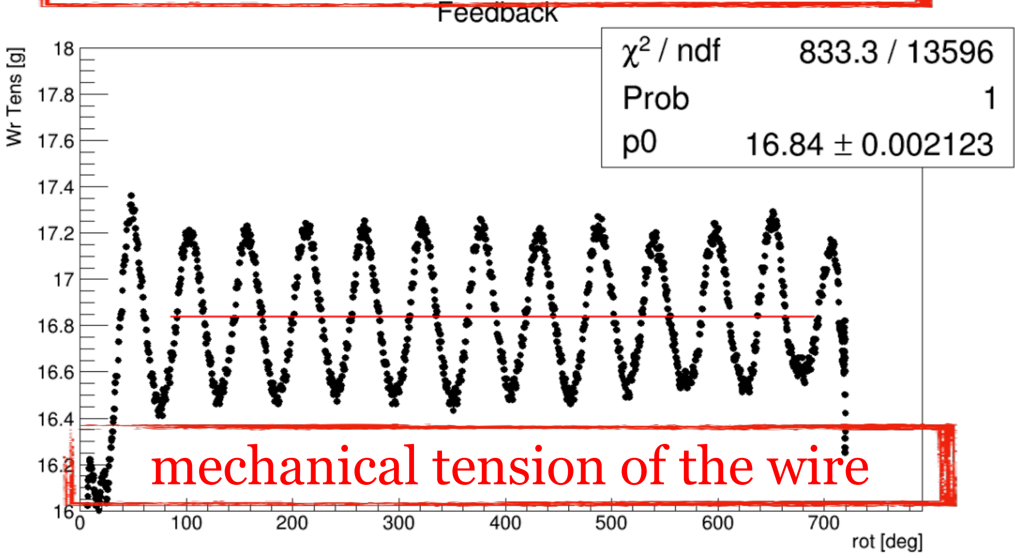

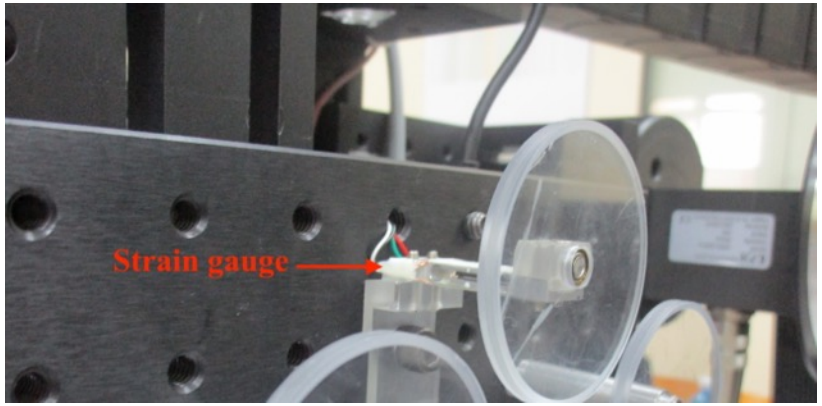

WIRING SYSTEM (*Klotho and Lachesis*): wire tension

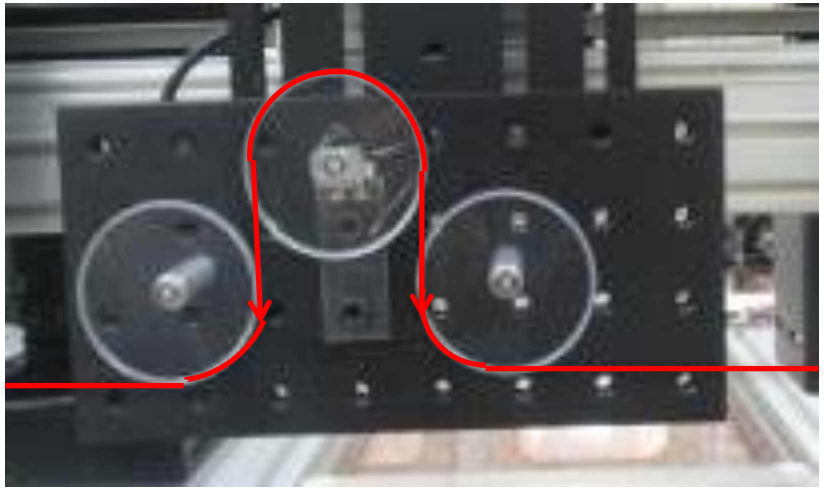

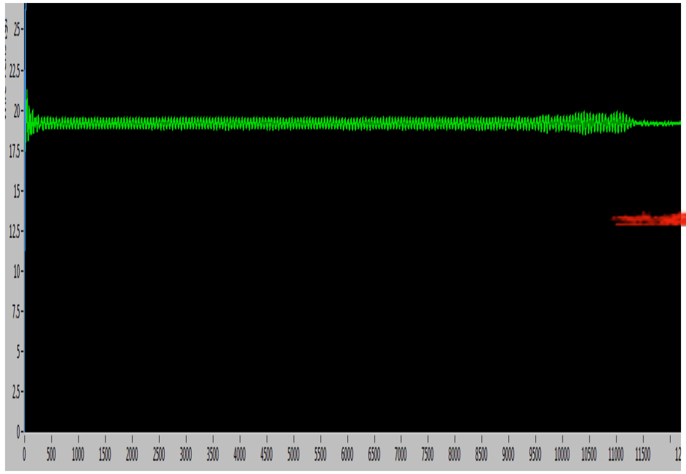

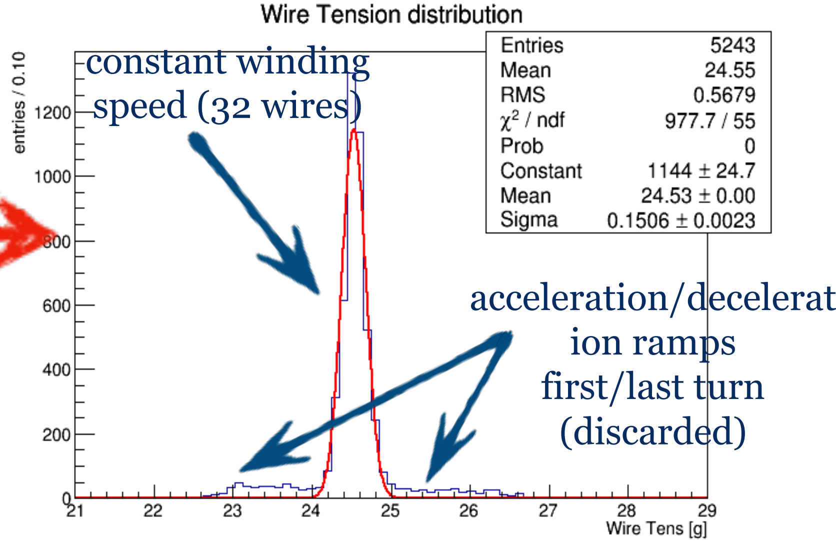

mean wire tension is stable at the level of 0.05 g

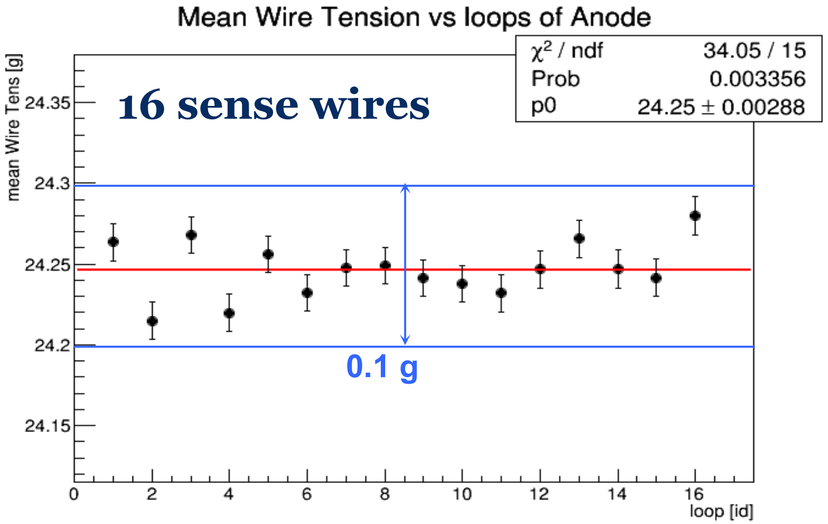

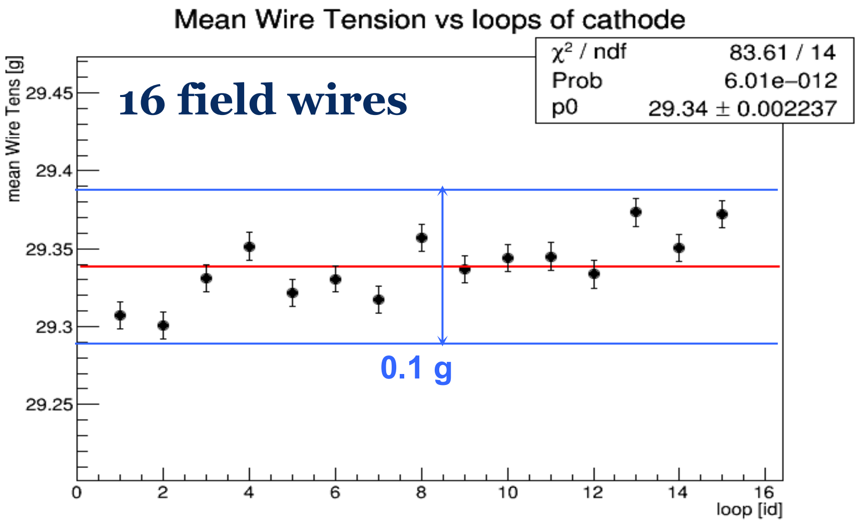

WIRING SYSTEM (***Klotho and Lachesis***): wire position

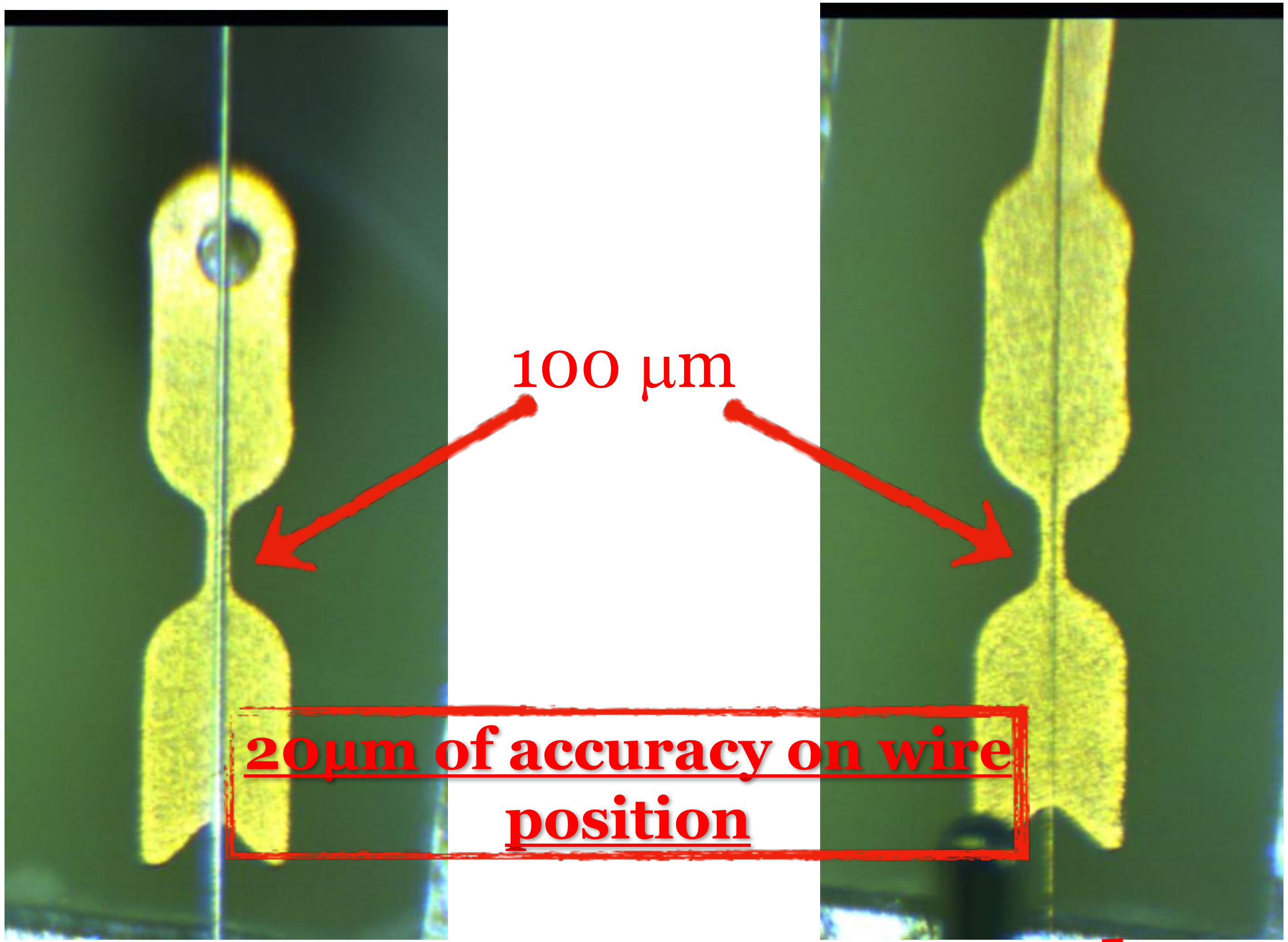

cathode **anode**

SOLDERING SYSTEM (***Klotho and Lachesis***)

- Each wire is fixed at both ends on the pads of the wire PCB, while still constrained around the rotating cylinder under its own tension.
- The soldering phase is accomplished by an LASCON 501 IR laser soldering system.
- The laser system is controlled by the NI Compact RIO and is synchronized with the positioning system.

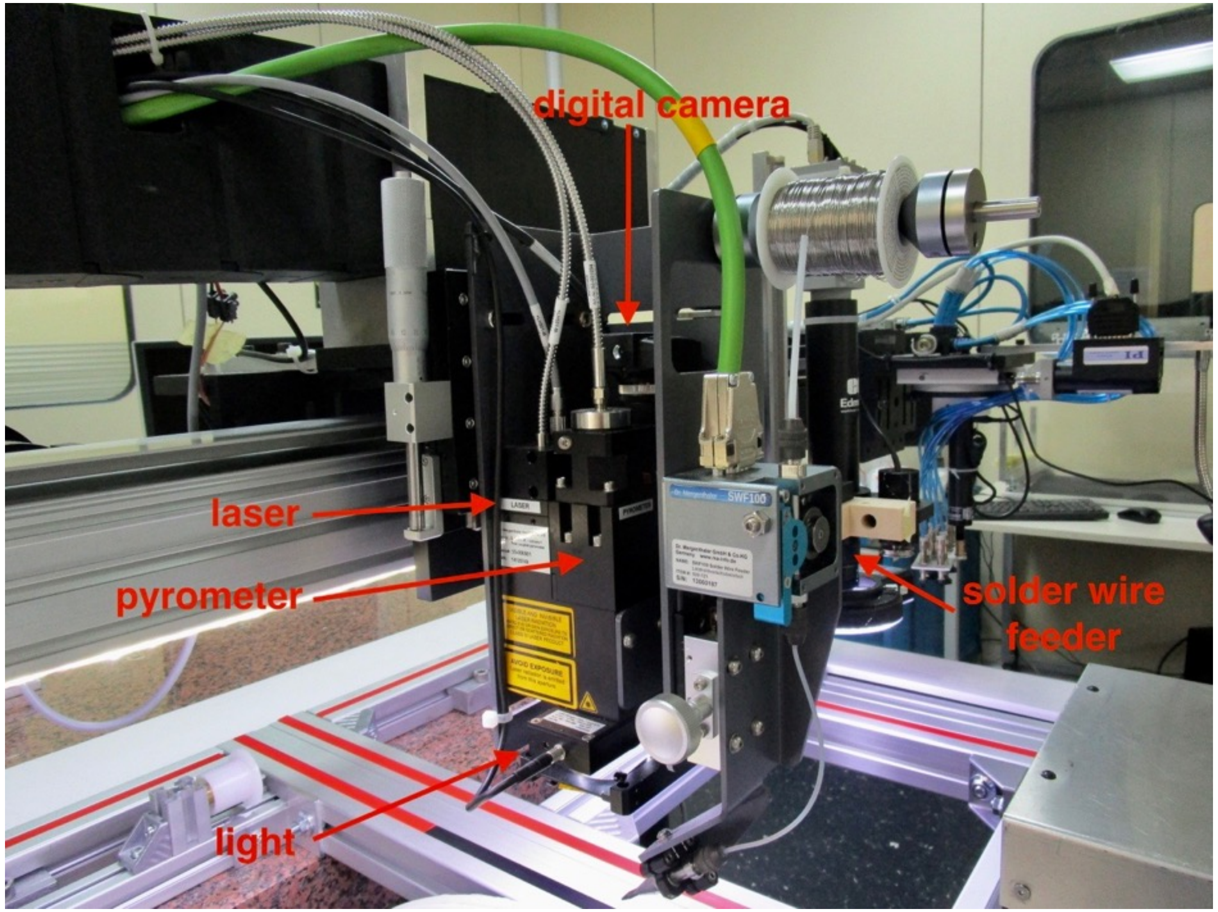

SOLDERING SYSTEM (*Klotho and Lachesis*)

- The solder wire used has a low melting point of 160◦ C to avoid damages to the wire Ag plating and low outgassing in order to avoid contaminating the CDCH gas during operation.

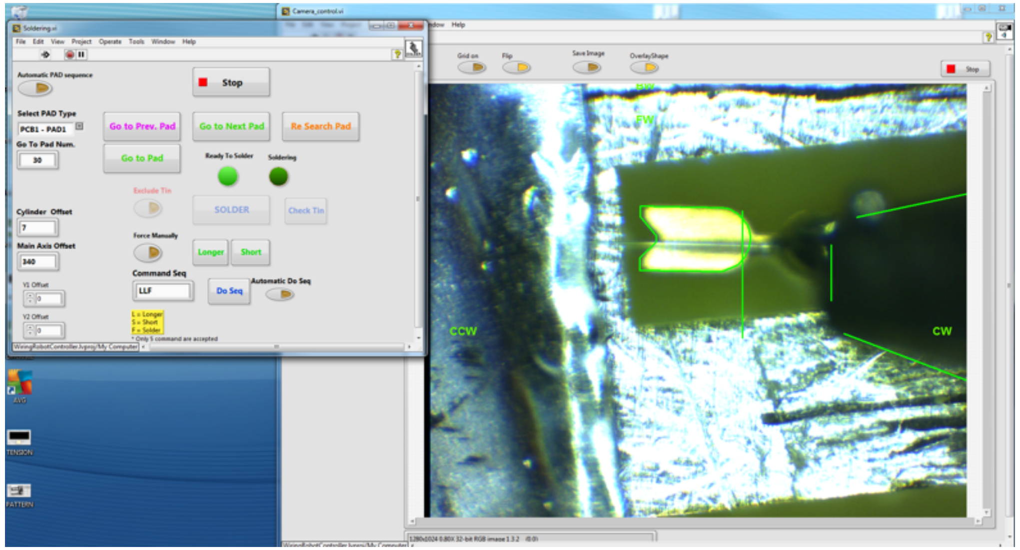

- The wires, during the soldering phase, are protected with a Mylar foil to avoid flux splashing.

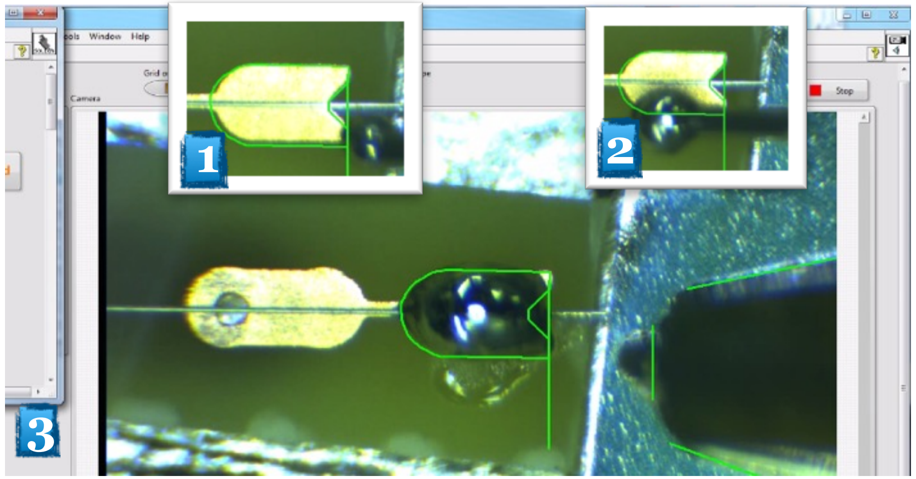

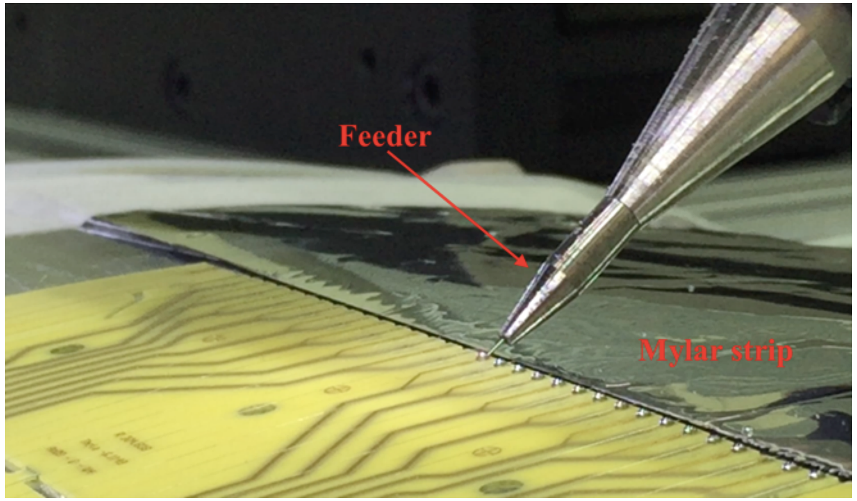

EXTRACTION SYSTEM (***Labirinth and Theseus***)

The wound layer of soldered wires must be unrolled from the winding drum and de-tensioned for storage and transport to the assembly station at the INFN Pisa.

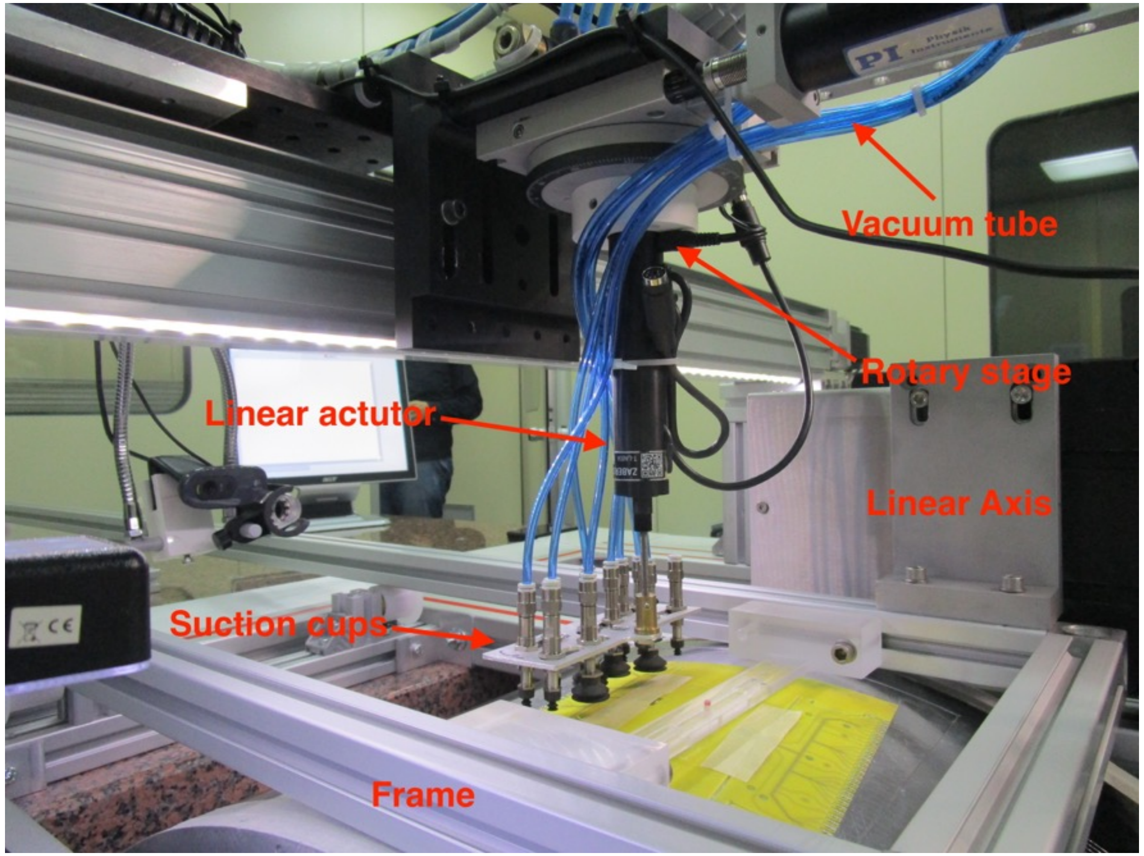

EXTRACTION SYSTEM (***Labirinth and Theseus***)

The wire PCBs are lifted off from the cylinder surface with a linear actuator connected to a set of vacuum operated suction cups and placed on the storage and transport frame.

The US and DS wire PCB supports are made of plexiglass and they are dedicated to hold the wire PCBs at correct positions by means of teflon screws.

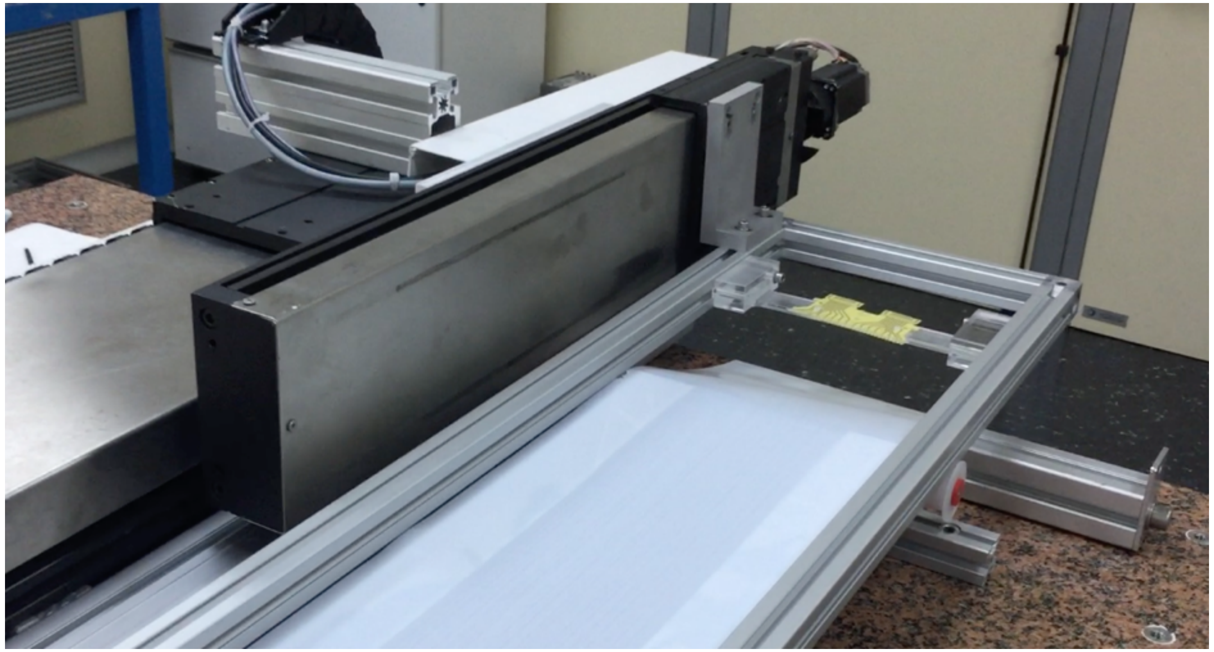

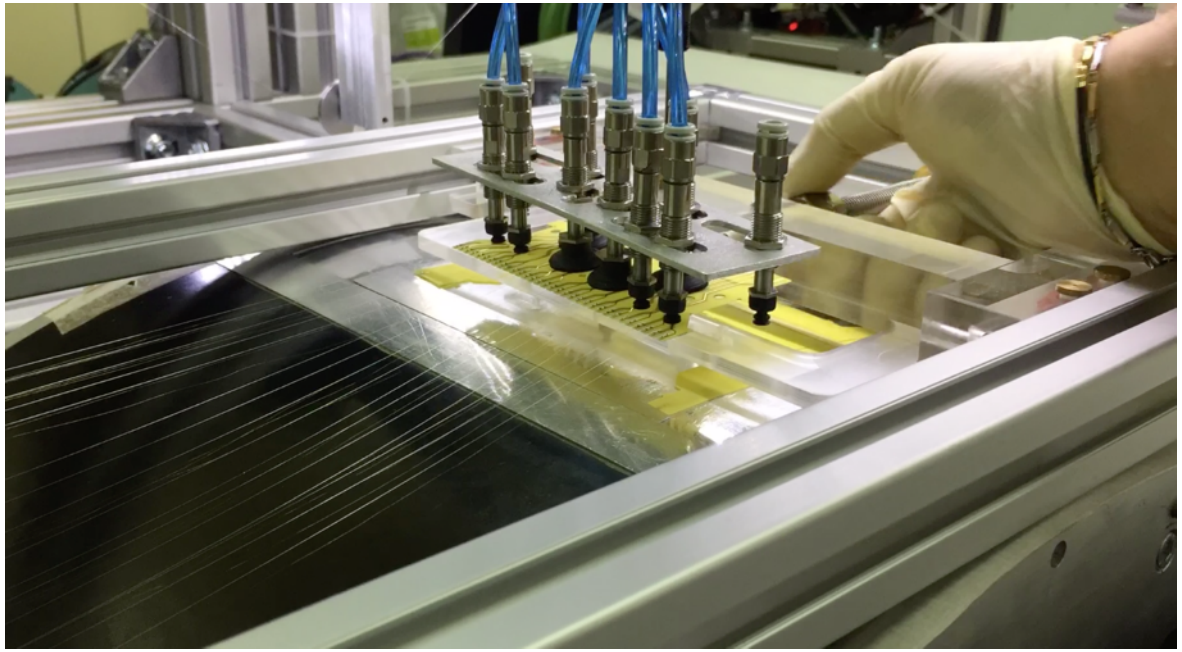

CHECK MECHANICAL TENSION WIRE

The measurement of the wire mechanical tension is performed with the method of the resonant oscillation induced on the wires. The first nominal resonant frequency of a wire is given by:

$$f = \frac{1}{2L}\sqrt{\frac{Tg}{\rho}}$$

T - wire tension (in g), L - wire length (in meters),
ρ - density(in g/m)

A system has been developed to measure the variation of the capacitance C_{ww} :

$$C_{ww} = \frac{2\pi\varepsilon}{\ln\left(\frac{4H}{d}\right)} \Longrightarrow |\delta f| \approx \frac{C_{ww}}{4\pi C\sqrt{LC}} \frac{\frac{2}{3}}{\ln\left(\frac{2H}{d}\right)} \frac{dH}{H}$$

The system induces oscillation in a wire by means of a pulsed HV signal and measures the frequency of the first harmonic resonance of wire by measuring the variation of its capacitance

Wire	μ (10^{-6}g/m)	T (g)	f (Hz)
50 μm Al (Ag)	6.53	29.64	54.74
40 μm Al (Ag)	4.38	19.25	53.83
20 μm W (Au)	6.04	24.51	51.74

CHECK MECHANICAL TENSION WIRE

The system shows the ability to resolve each frequencies of two field wires in a system made by two field wires and one sense wire placed in the middle

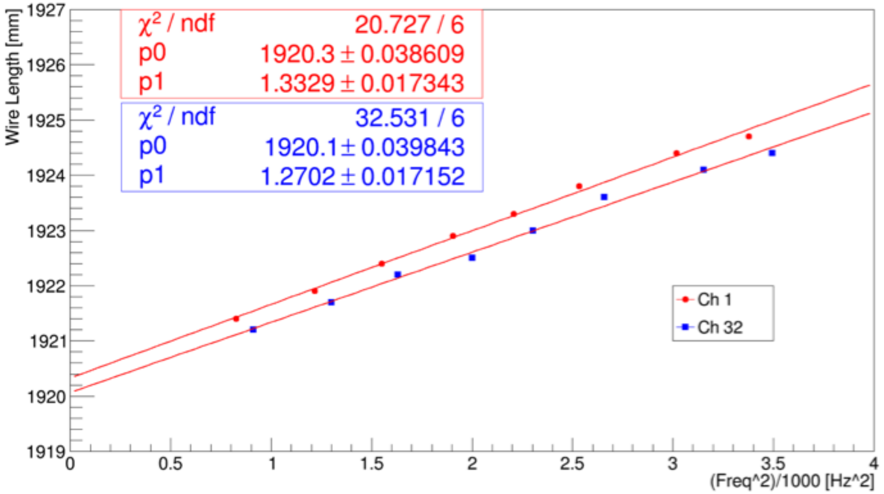

the wire length vs (f[Hz])² curves

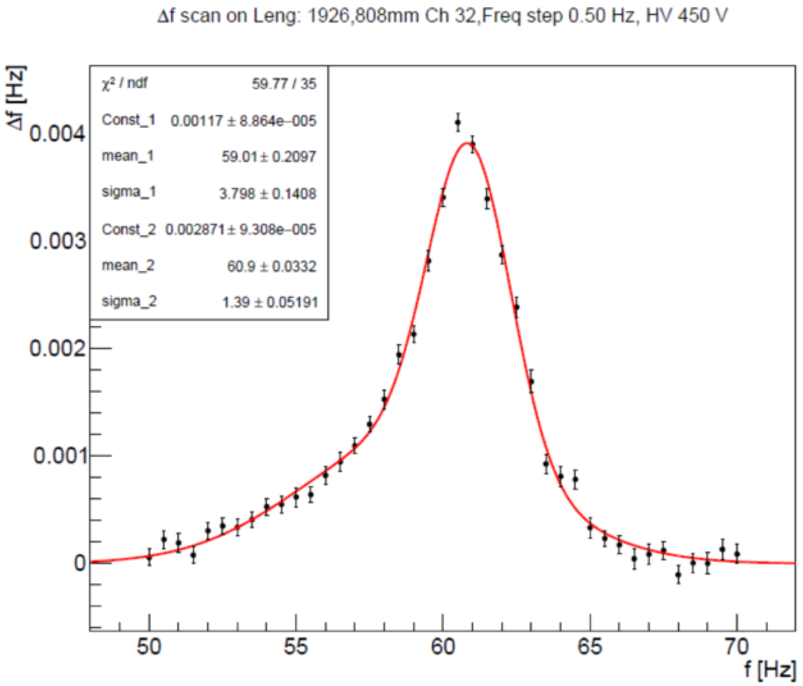

the resonant oscillation frequency for a fixed length of the multi-wire plane

TRASPORT TO INFN PISA

During transport, the 3 sets of 13 frames are wrapped in a welded seal bag to avoid contamination from outside and equipped with valves in order to be flushed with dry gas (to avoid water vapor condensation)

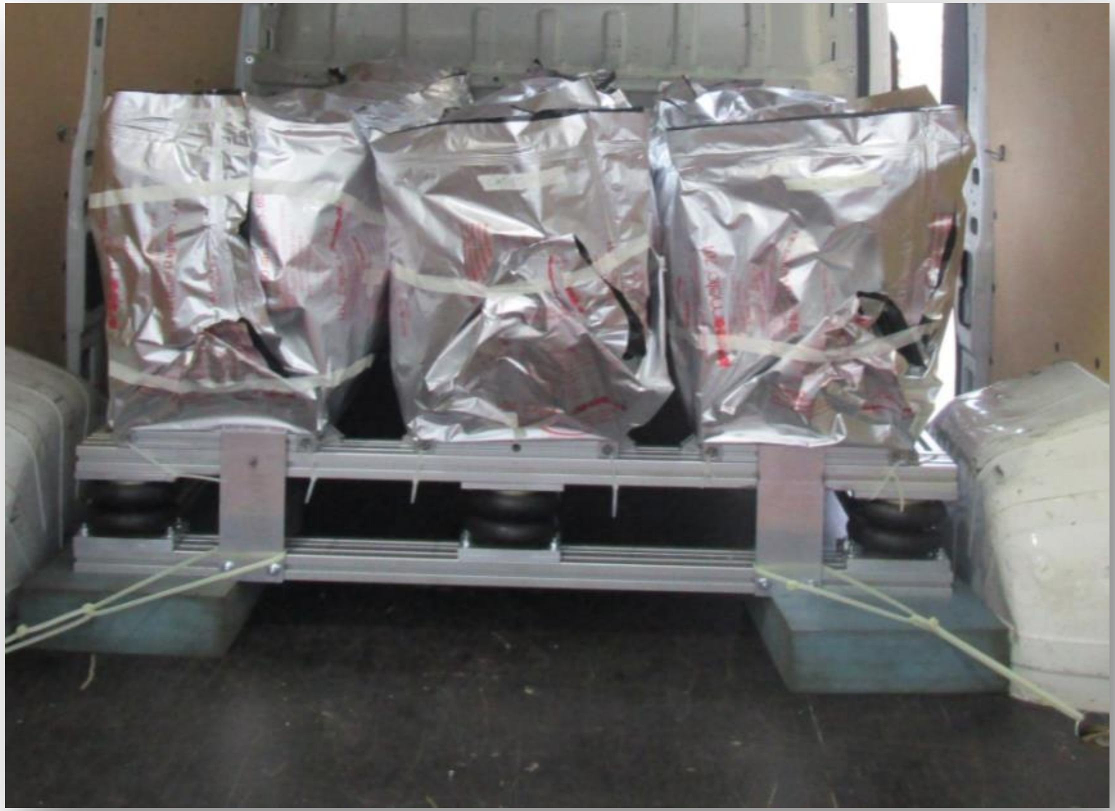

CDCH ASSEMBLY I

During the assembly phase, the endplates are placed at a shorter distance than nominal to avoid stressing the wires

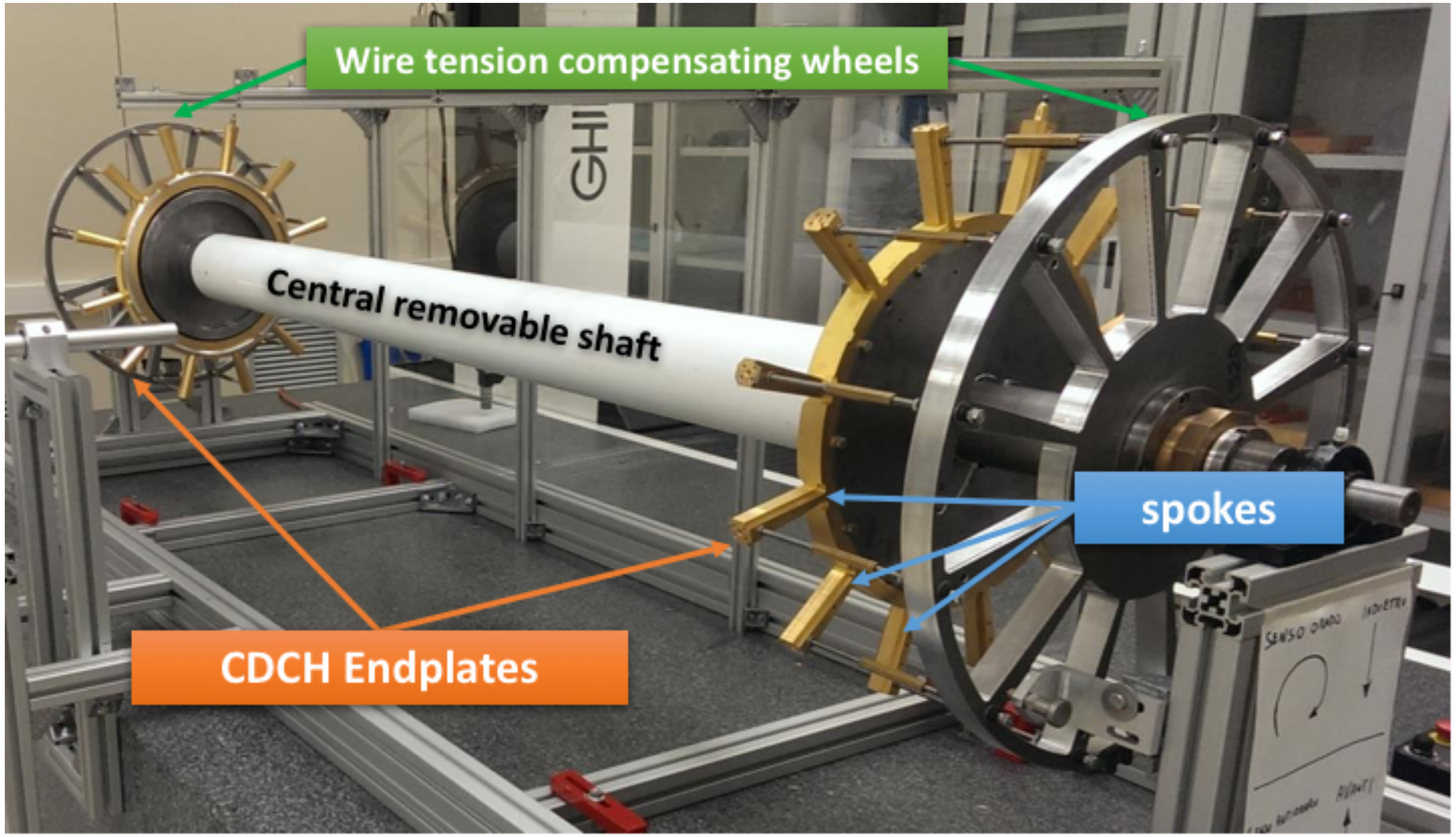

CDCH ASSEMBLY II

- The mounting procedure is performed with an adjustable arm and a flipping arm which is used to flip layers;
- The wire-PCBs, fixed on the transport frame, are anchored to the mounting arm with a clip and released from the frame.

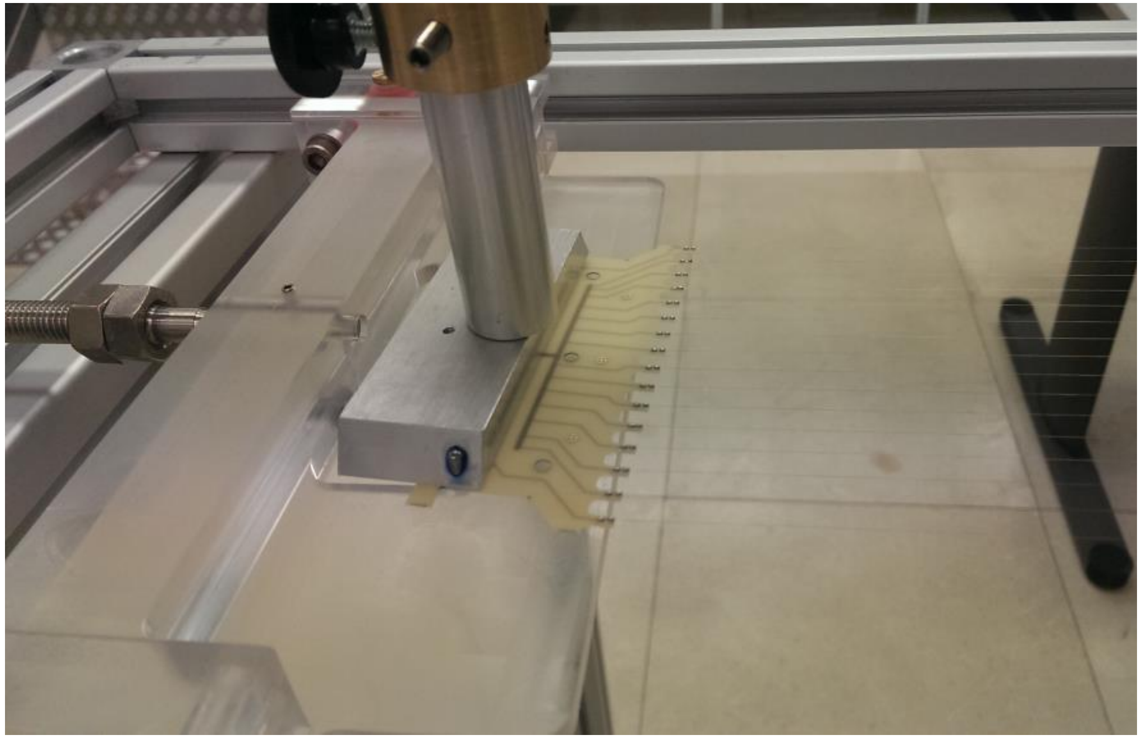

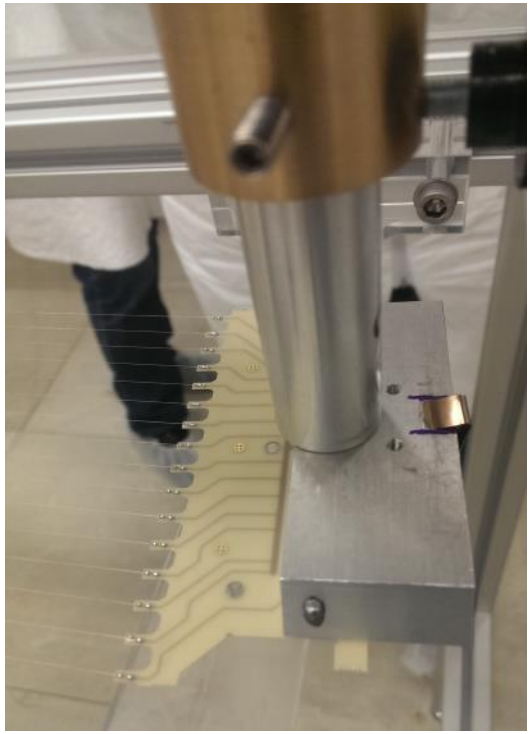

CDCH ASSEMBLY III

- The mounting arm (with the multi-wire layer) is then placed next to the end plates for the engagement procedure.
- The mounting arm is fixed to a support structure to prevent damaging the wires.
- This structure transfers the multi-wire layer on the end plates between two spokes.

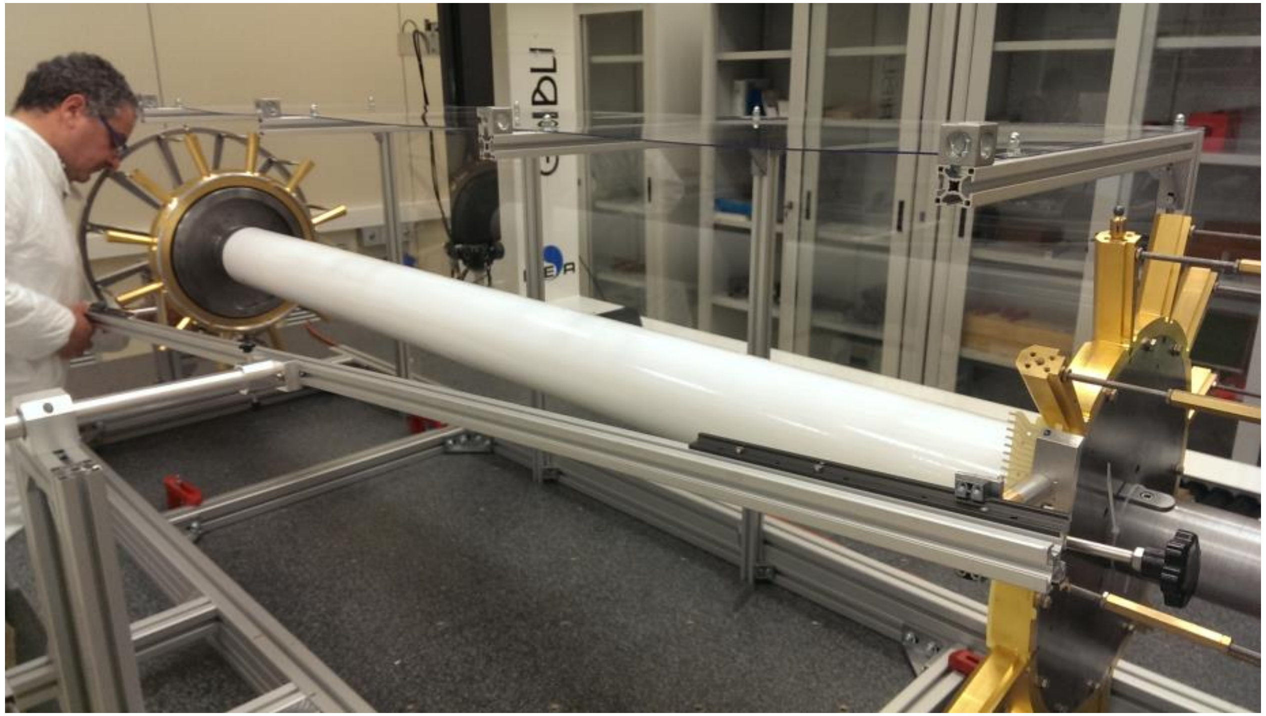

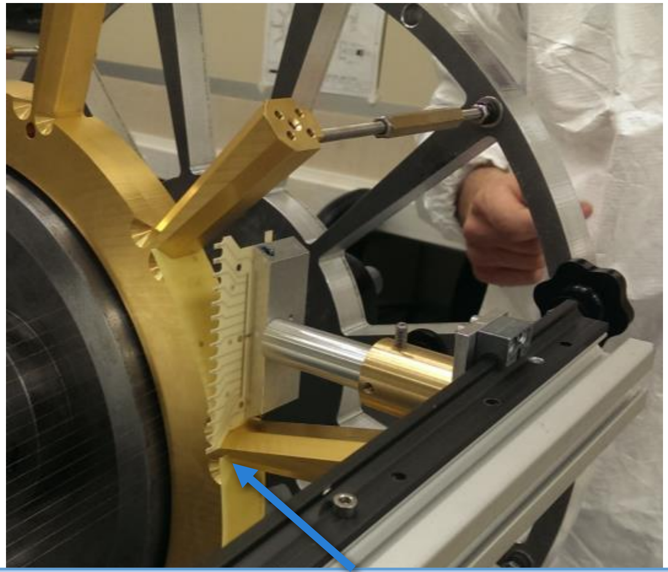

Spoke used as reference for the alignment of the pcb

CDCH ASSEMBLY IV

- This procedure is repeated for each of the 12 sectors.
- After completing the installation of one layer, a survey is performed on the radial layer position
- Spacers, to separate the successive layer, are pressed and glued in position.
- The procedure is repeated for all the layers

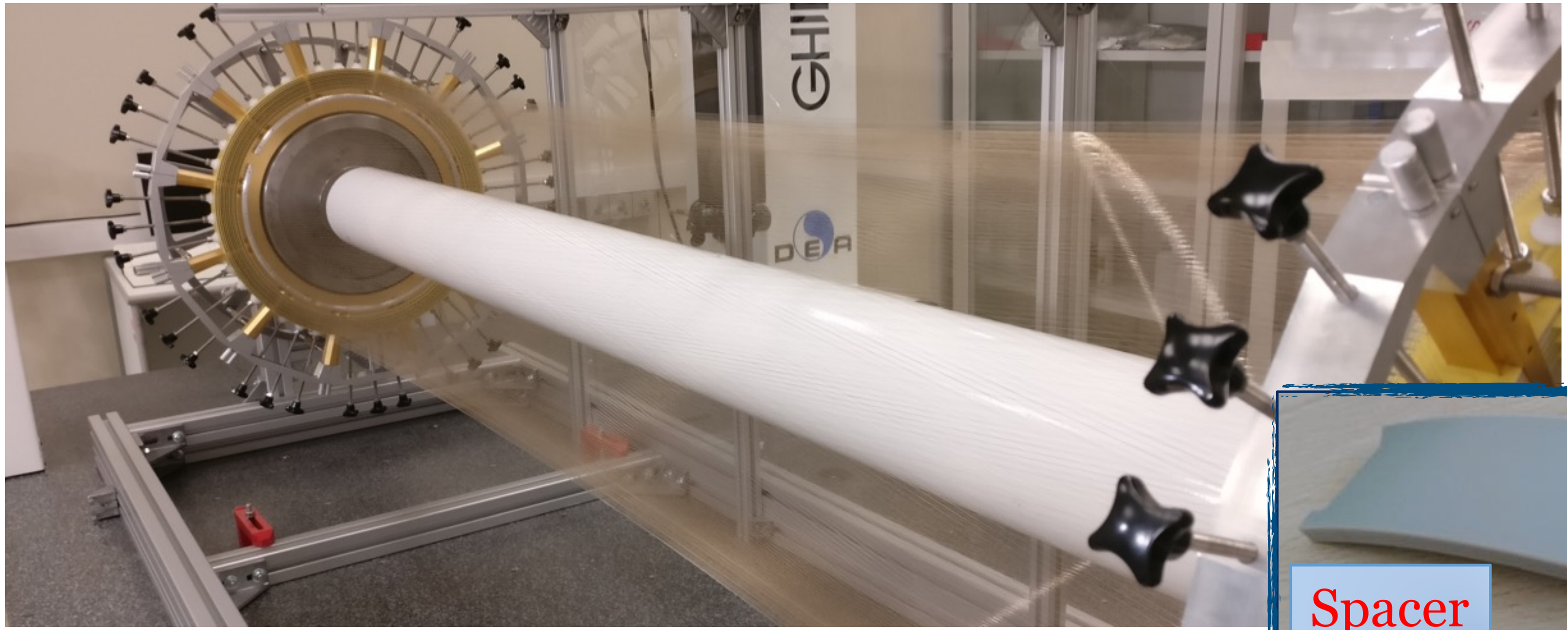

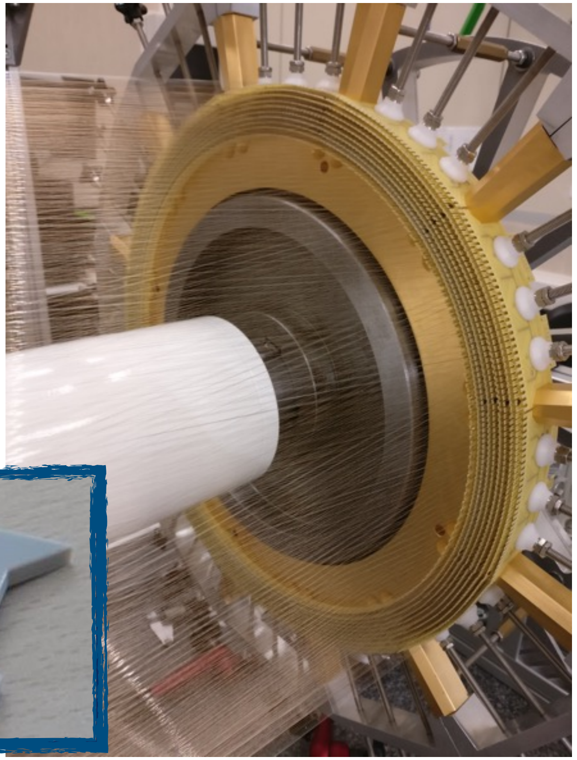

CDCH ASSEMBLY V

- After assembling all the layers, the CDCH is closed with a carbon fiber panels.
- CDCH will be lifted up 90 degrees to seal the end plates (wire-pcb and spacer);
- After the sealing is completed, the mechanical supports for the electronics and finally the extender structure will be mounted
- Before of the transport to PSI, some tests on the CDCH will be done

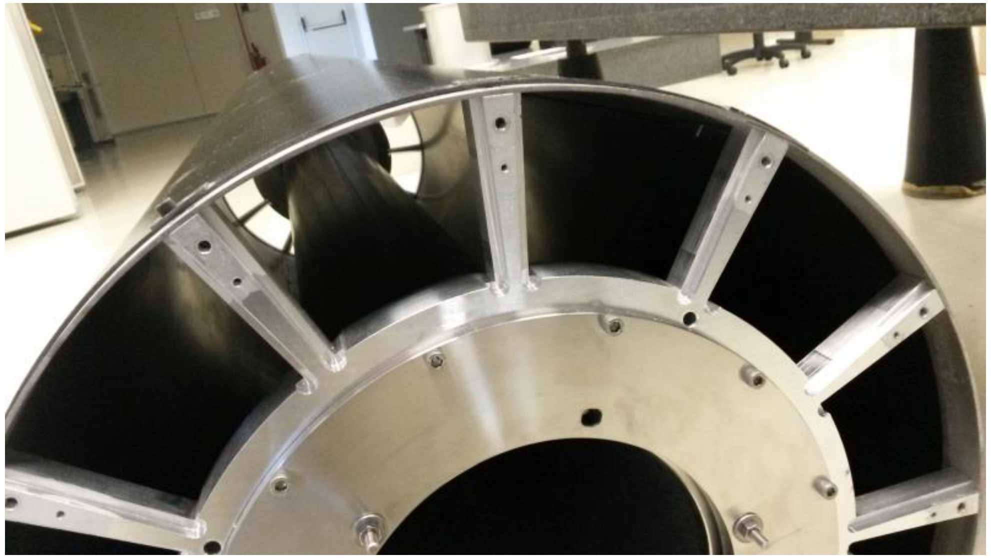

CDCH STATUS

The CDCH wiring is now ~80% and the assembling is ~70%

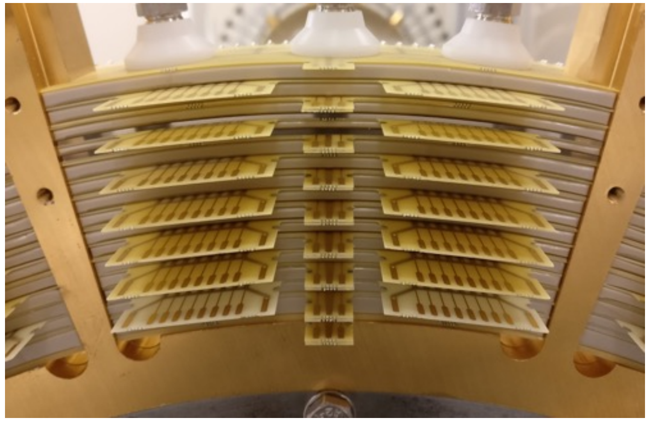

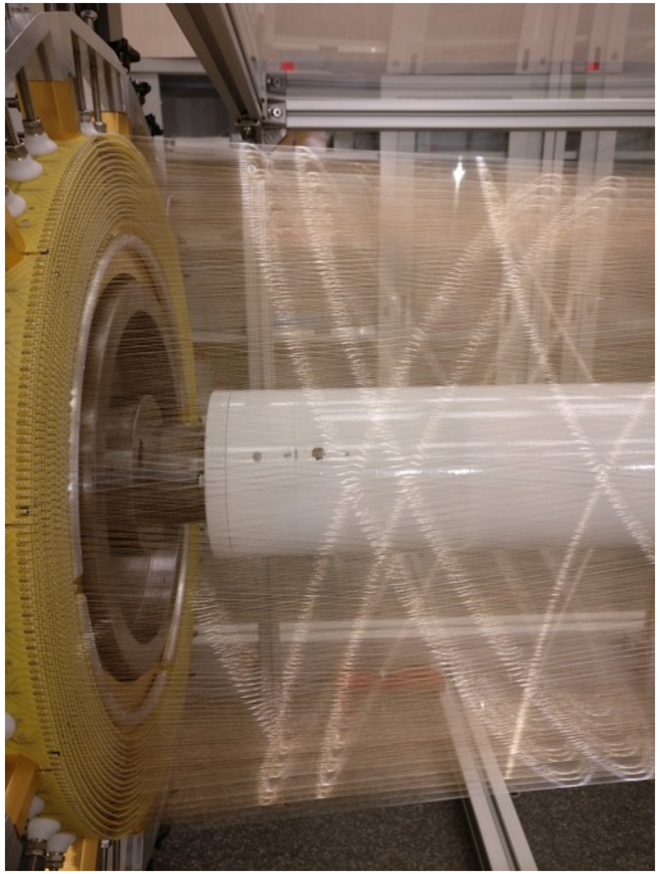

The end of the wiring is planned for August

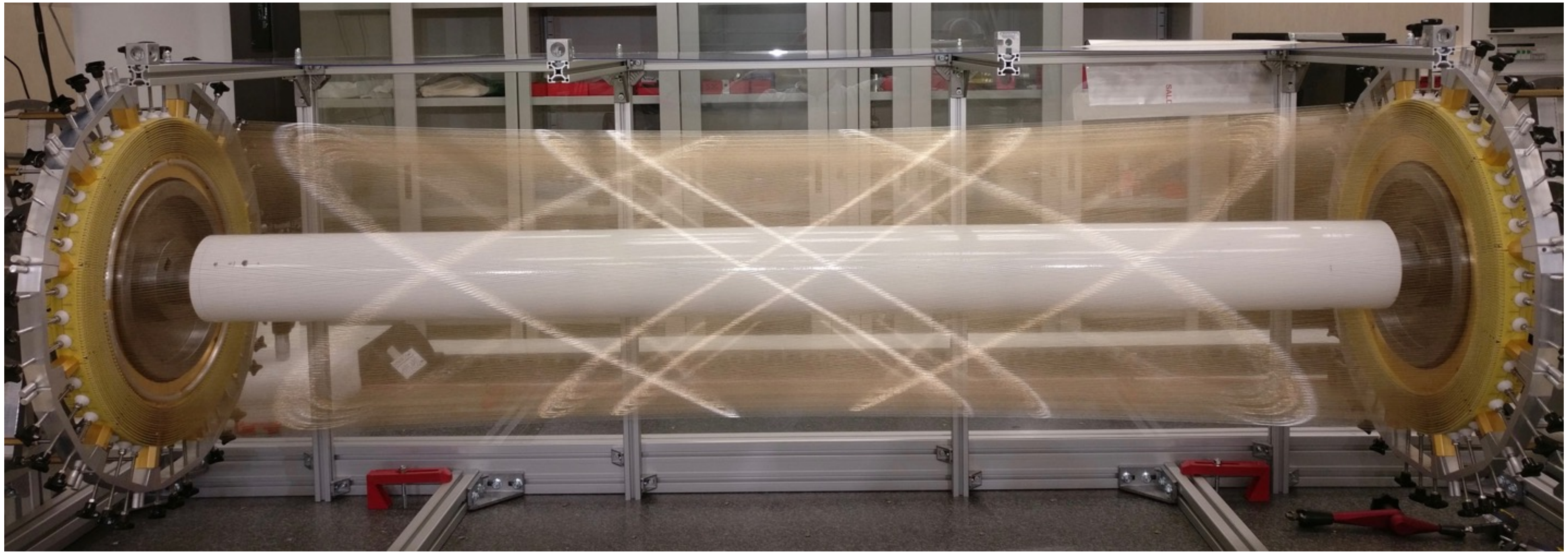

MEG II CDCH: expected performance

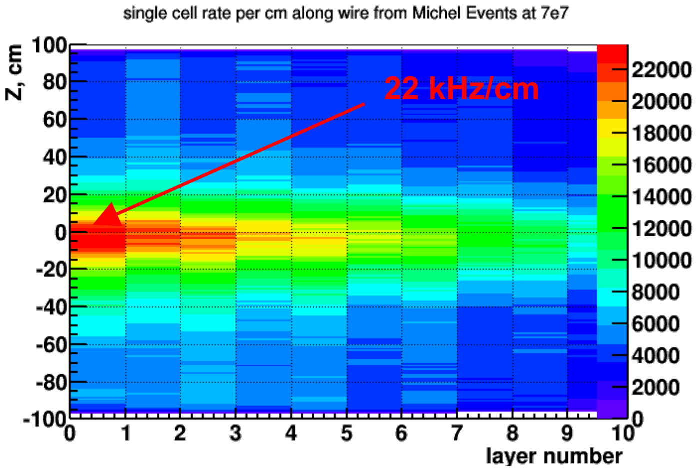

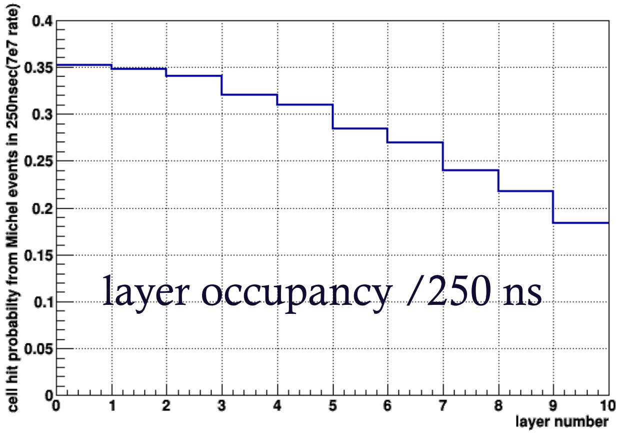

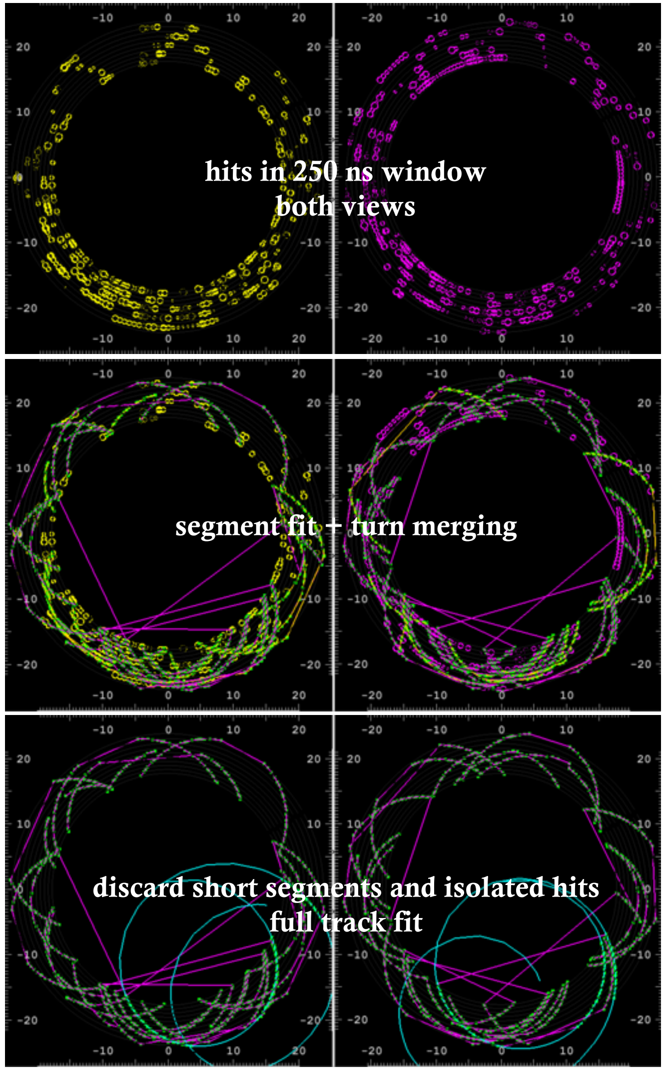

3D
track finding
and fit

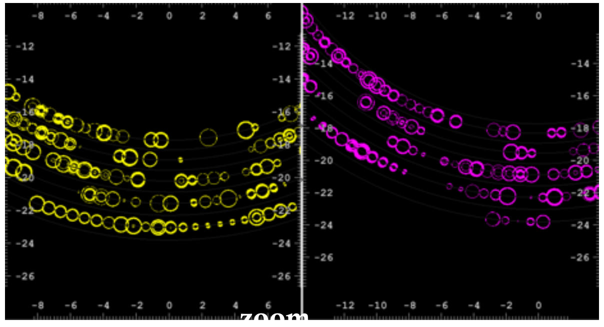

signal track

MEG II CDCH: Performance

From montecarlo simulation, with pattern recognition (PR) and applying a Kalman Filter (KF) analysis has been obtained

- $\sigma_{\varphi} = 6.2 \pm 0.10$ mrad
- $\sigma\vartheta = 6.5 \pm 0.09$ mrad
- $\sigma_{P} = 93.41$ keV/c

Preliminary!

The results are a starting point and future improvements in both the PR and KF will enhance the current reconstructed resolutions and efficiency

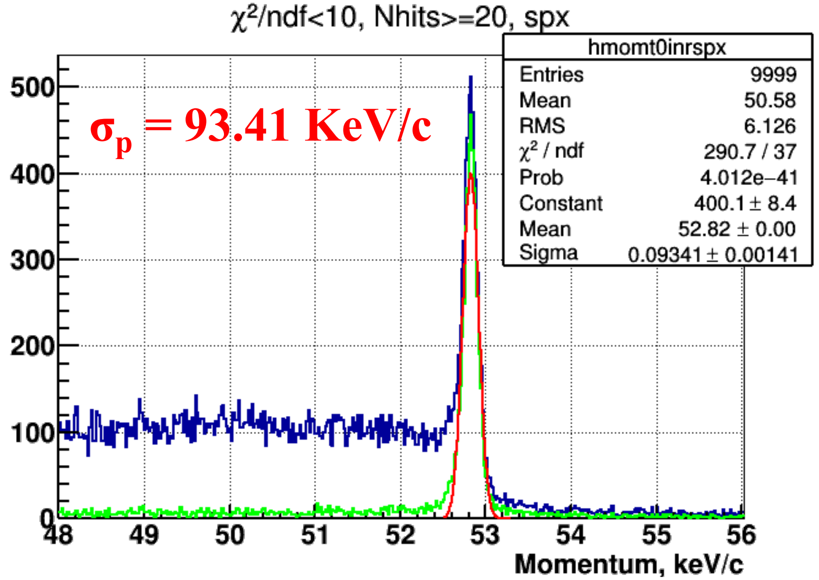

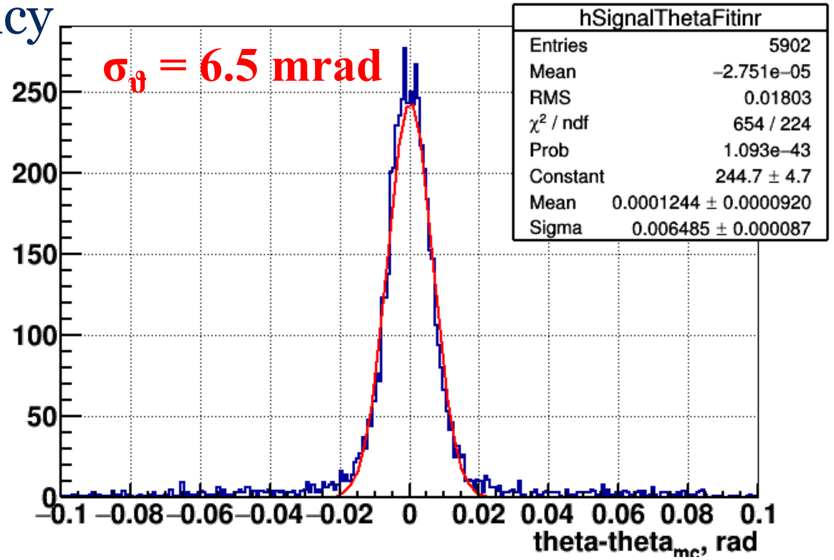

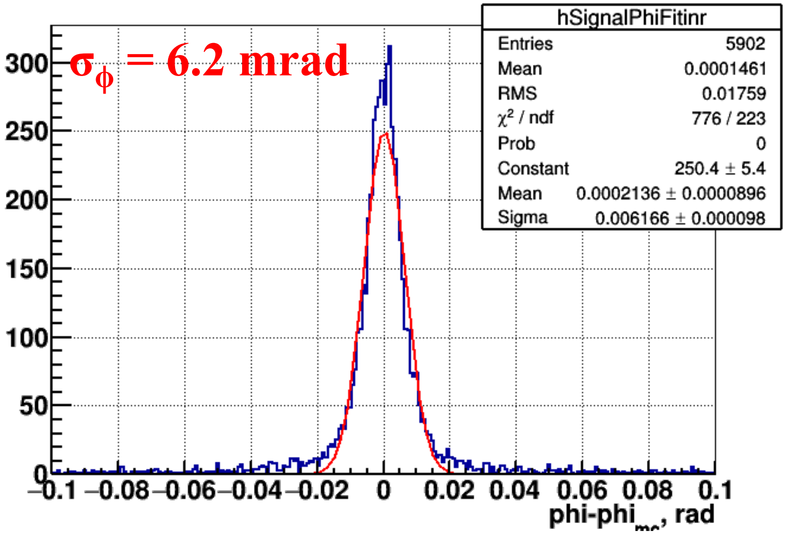

Conclusions

- Strong motivations for an upgraded MEG experiment aiming at setting an upper limit $B(\mu^+ \to e^+ + \gamma) < 5 \times 10^{-14}$.
- The upgrade of the positron tracker consists in a full stereo and high transparency Drift Chamber.
- The high density of wires constituting the CDCH has required a novel approach to the wiring procedure.
- Chamber accuracy obtained:
  - stereo angle < 35 µrad
  - wire position on PCB pad < 25 µm
  - cell width (wire pitch) < 1 µm
  - cell height (spacer) < 50 µm
  - wire tension < 0.1 g
  - PCB offset vs spoke < 50 µm
  - chamber length < 200 µm
- Its expected performance is in line with the requirements.
- CDCH commissioning will start at PSI in fall 2017.

Thank you for your attention!

backup

charged Lepton Flavour Violation

Several LFV processes, sensitive to **New Physics (NP)** through "new" lepton-lepton coupling

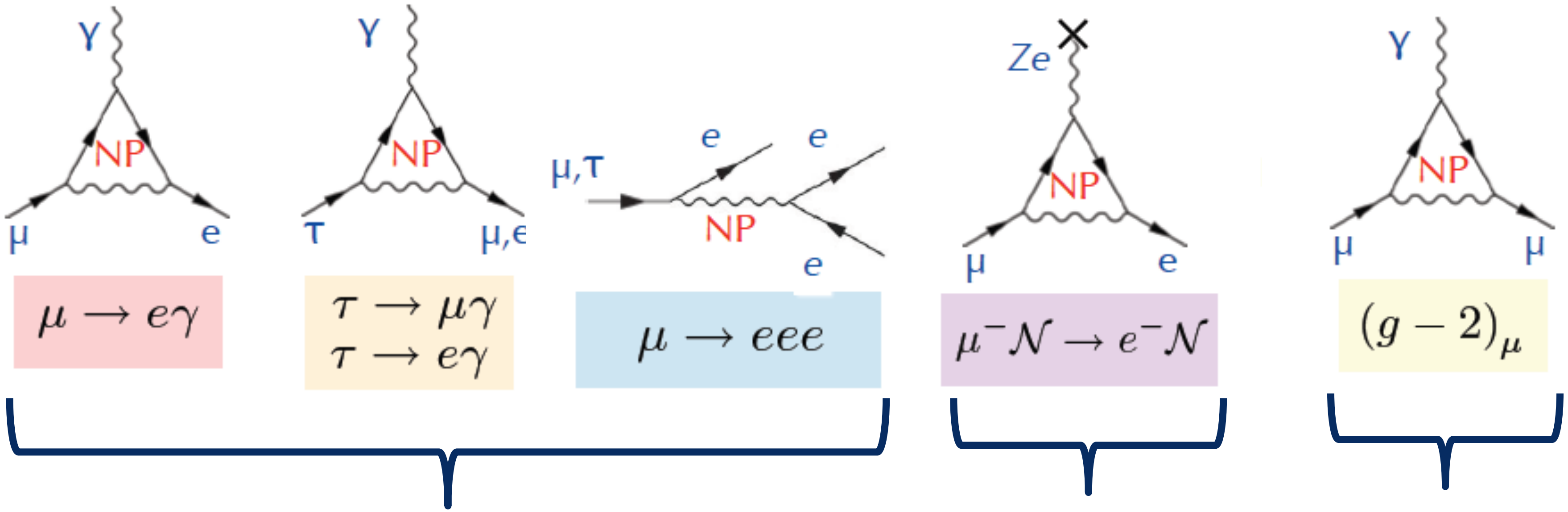

μ,τ anomalous decays

μ → e conversion

Anomalous magnetic moment

Why muon?

Muons are very sensitive probes to study Lepton Flavour Violation:

- **intense muon beams (≈ $10^{7\text{-}8}$ muons/sec)** can be obtained at **meson factories** and **proton accelerators (PSI, LAMPF, J-PARC, Fermilab ...)**;

- **muon lifetime** is rather long **(2.2 μs)**;

- **final states** are **very simple** and can be **precisely measured.**

Analysis of MEG data

PRL 110 (2013) 201801

- Observables: $\vec{x_i} = (E_\gamma, E_e, t_{e\gamma}, \theta_{e\gamma}, \phi_{e\gamma}, \cdots)$
- Search window:

  $48 < E_\gamma < 58$ MeV, $50 < E_e < 56$ MeV,

  $|t_{e\gamma}| < 0.7$ ns, $|\theta_{e\gamma}| < 50$ mrad, $|\phi_{e\gamma}| < 50$ mrad

- Search method:
  - The number of signal ($\boldsymbol{N_{sig}}$), radiative muon decay ($\boldsymbol{N_R}$) and accidental background events ($\boldsymbol{N_A}$) in the analysis window are determined using a **maximum likelihood fit**:

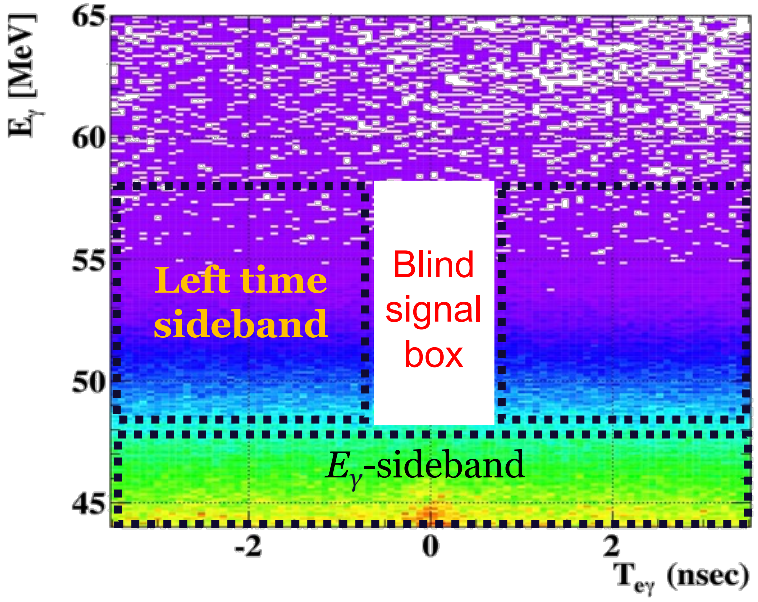

$$\mathcal{L}(N_{\mathrm{sig}}, N_{\mathrm{RD}}, N_{\mathrm{BG}}) = \frac{e^{-N}}{N_{\mathrm{obs}}!} e^{-\frac{(N_{\mathrm{RD}}-\langle N_{\mathrm{RD}}\rangle)^2}{2\sigma_{\mathrm{RD}}^2}} e^{-\frac{(N_{\mathrm{BG}}-\langle N_{\mathrm{BG}}\rangle)^2}{2\sigma_{\mathrm{BG}}^2}} \times \prod_{i=1}^{N_{\mathrm{obs}}} (N_{\mathrm{sig}} S(\vec{x_i}) + N_{\mathrm{RD}} R(\vec{x_i}) + N_{\mathrm{BG}} B(\vec{x_i}))$$

- Blind search: Signal events not used in calculation of PDFs
- Confidence interval of N_{sig}: Frequentist approach using profile likelihood ratio
- Normalization: Number of Michel decays (dedicated trigger) and number of radiative muon decays (E_γ-sideband)

Data taking history

Stable data-taking runs from 2009 until 2013

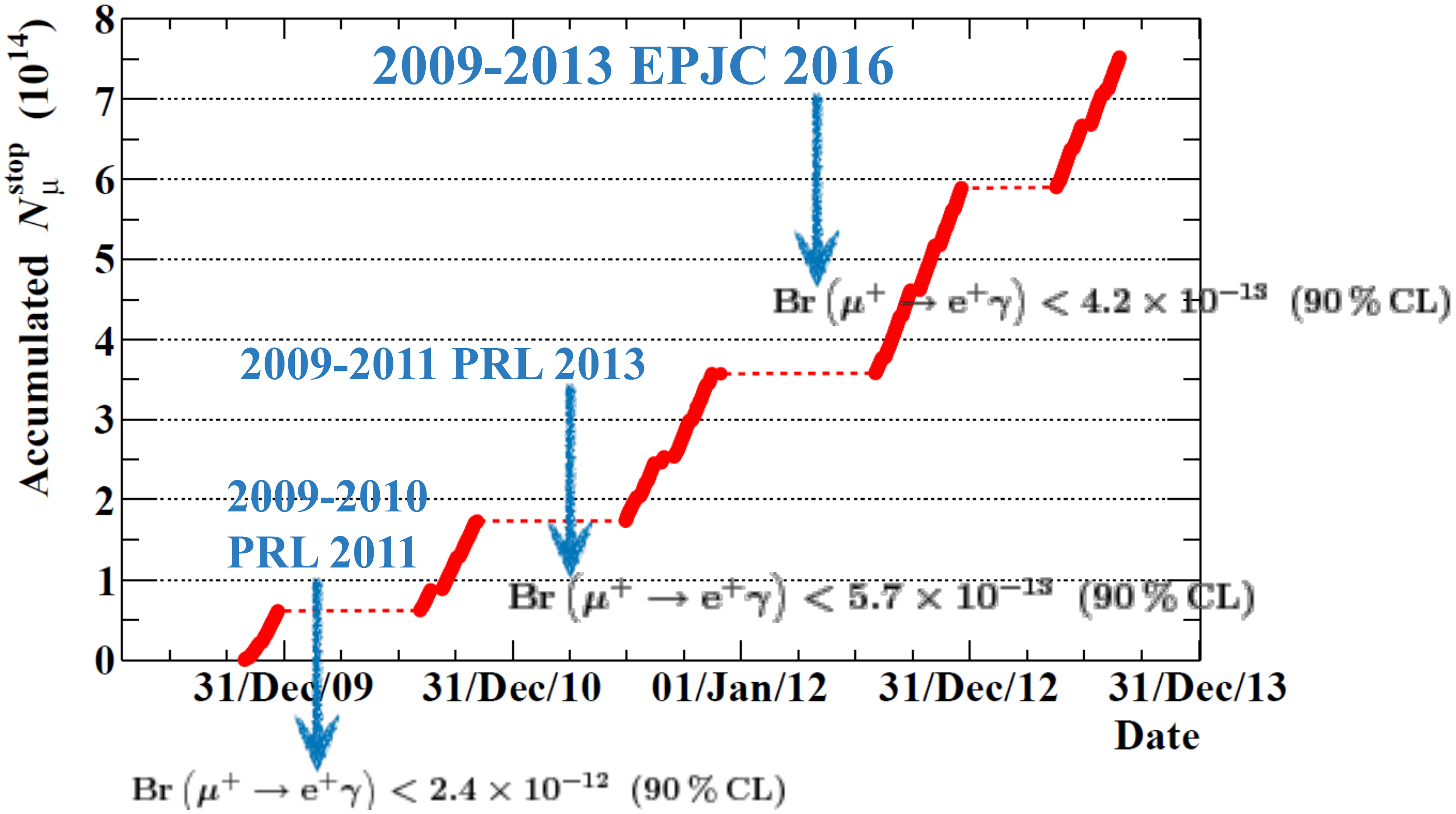

Event distributions

8344 events in the blinding box: **No signal excess observed**

the signal PDF contours (1σ, 1.64σ and 2σ) are also shown

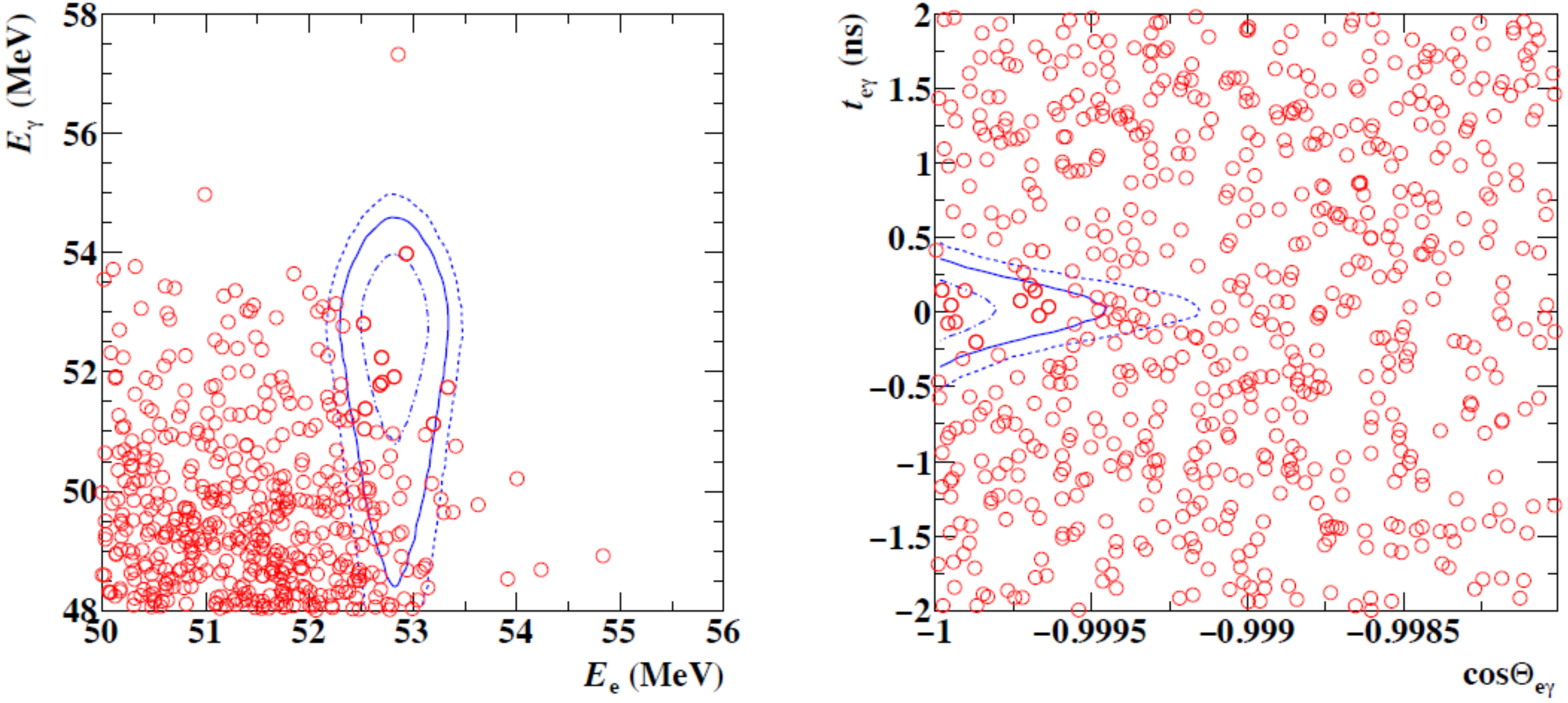

The MEG CoBRa Magnet

- High p_T positrons quickly swept out

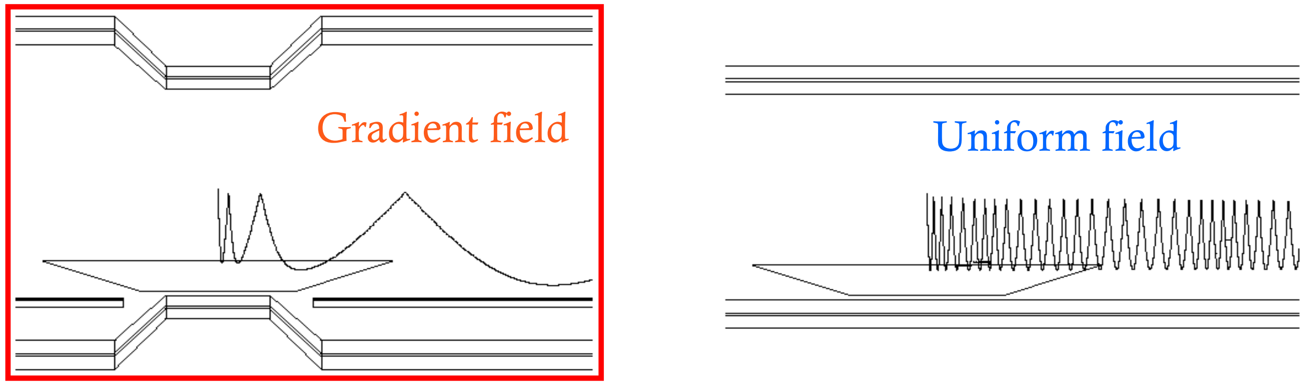

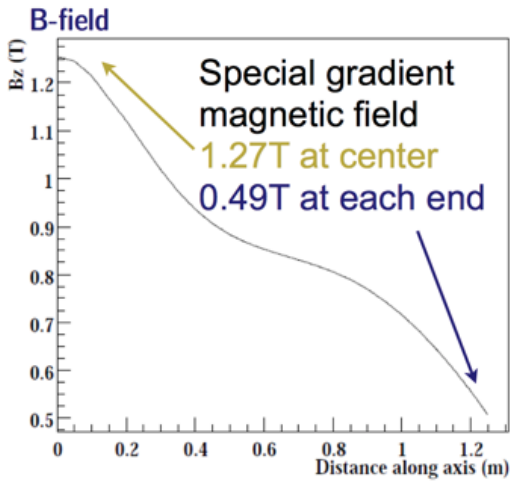

Michel hit rate versus radial distance

- Constant bending radius independent of emission angles

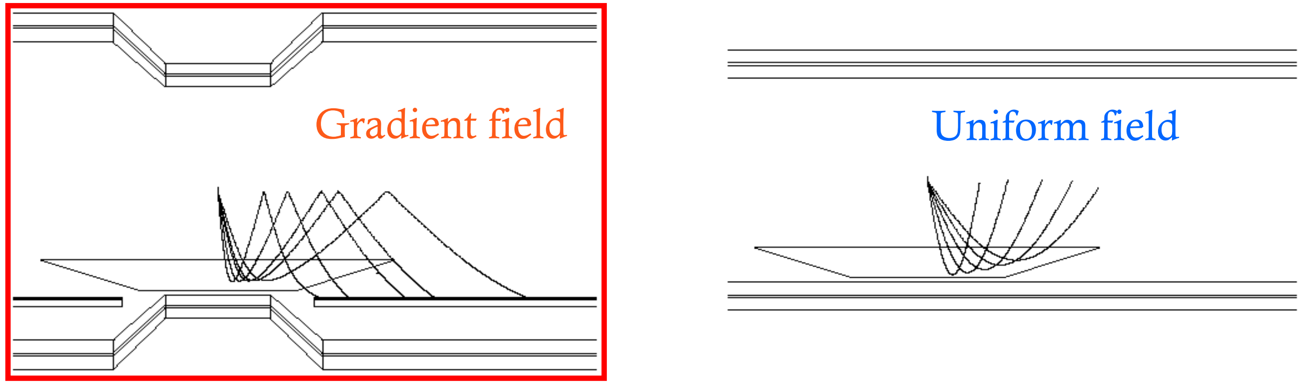

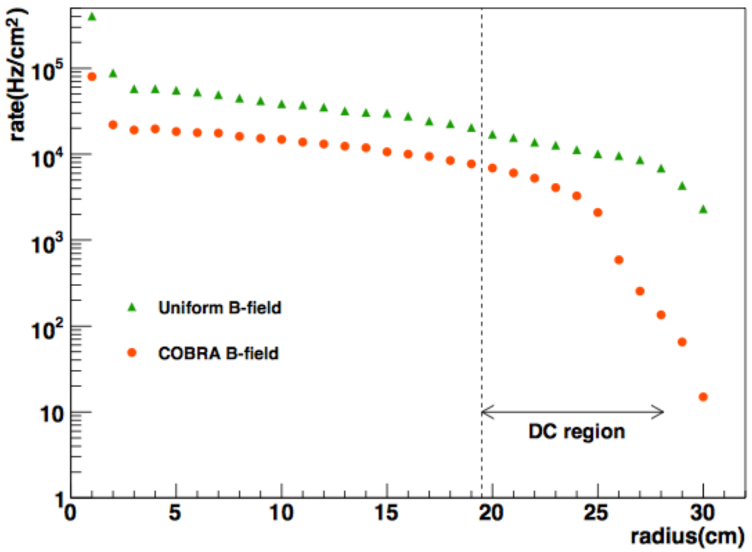

MEG I: Drift Chambers

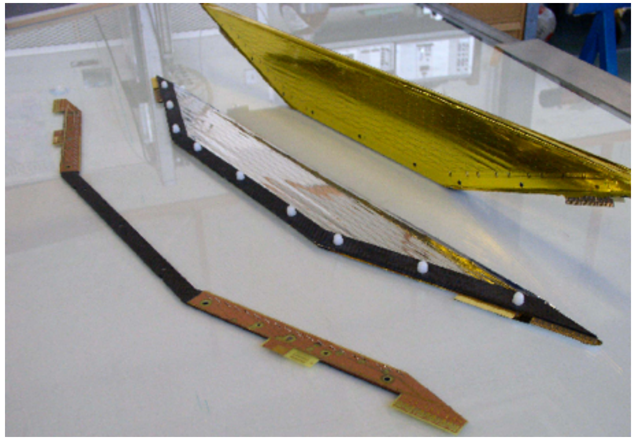

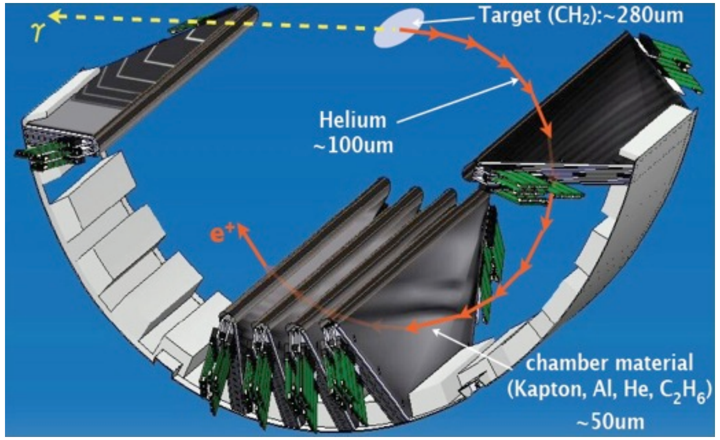

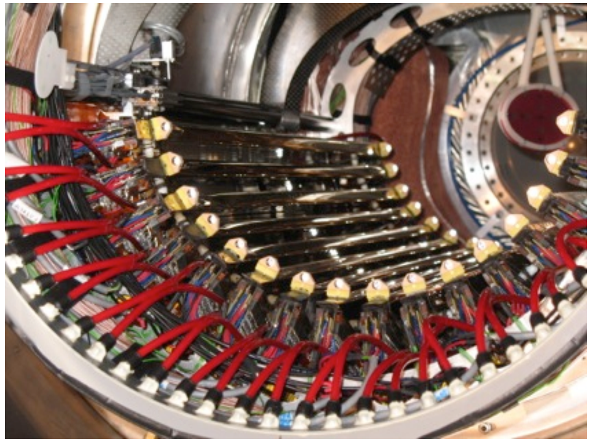

16 chambers

Each chamber is composed of

- 2 straggled arrays of drift cells
- 1 signal wire (25 μm NiCr) and 2x2 Vernier cathode strip made of 15 μm kapton foil and 0,45 μm alluminum strip
- He:C_2H_6 (50/50)

Single chamber ~ 2.3 10^{-4} X_0

Full e+ turn : ~ 1.7 10^{-3} X_0

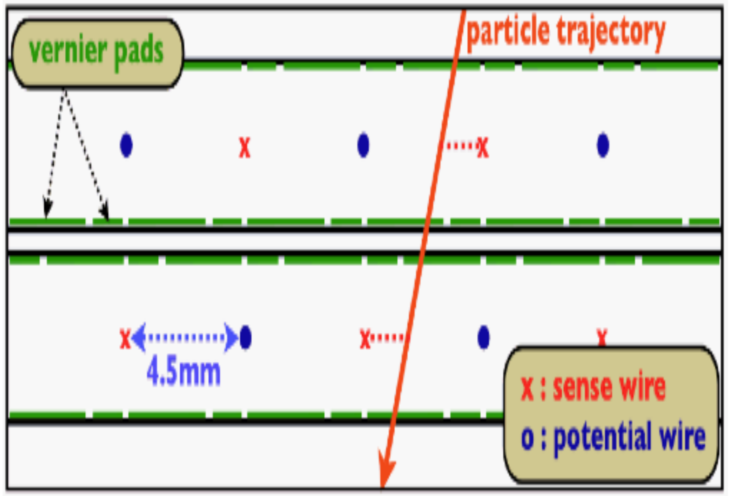

σ_{xy} ~ 210 μm (t drift)

σ_Z ~ 800 μm (Vernier)

MEG II CDCH: Single hit resolution

- Measurements of single-hit resolution made on three different prototypes.
- Results are in agreement, yielding a resolution of about 110 μm averaged throughout the cell.
- Further improvements expected with the implementation of a wider bandwidth front end electronics allowing for the exploitation of the cluster timing technique

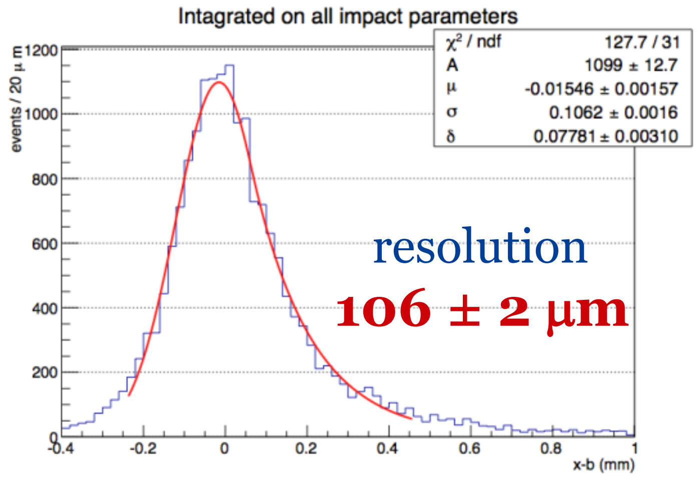

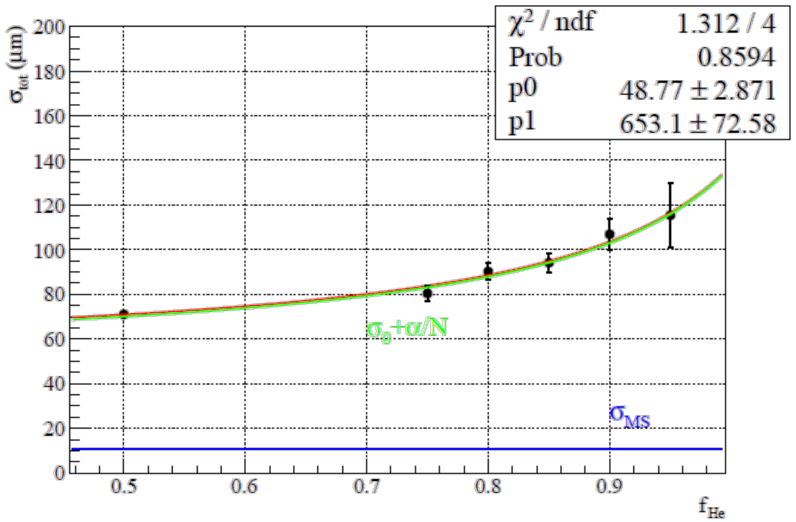

MEG-II DC: expected performance

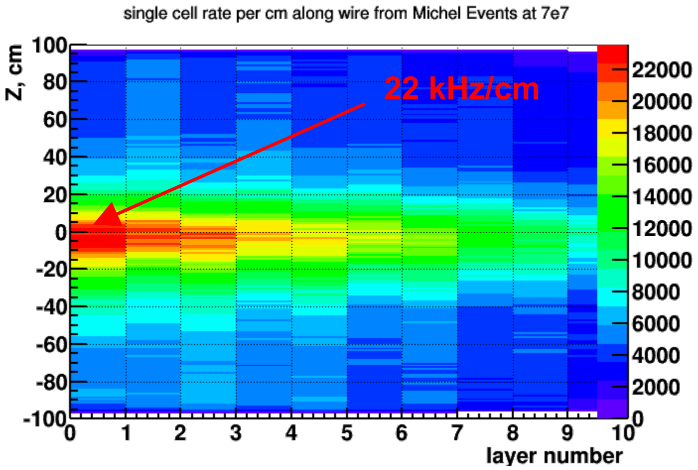

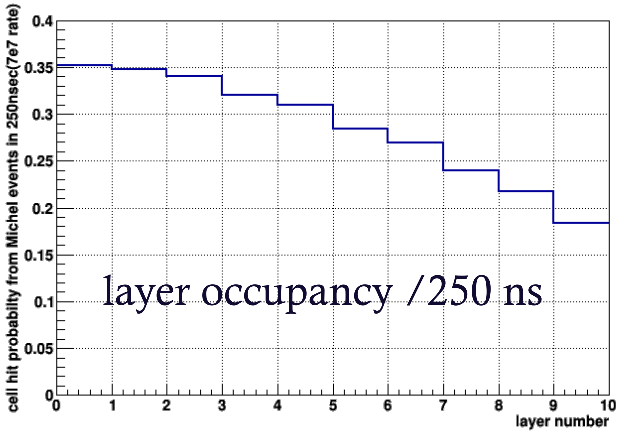

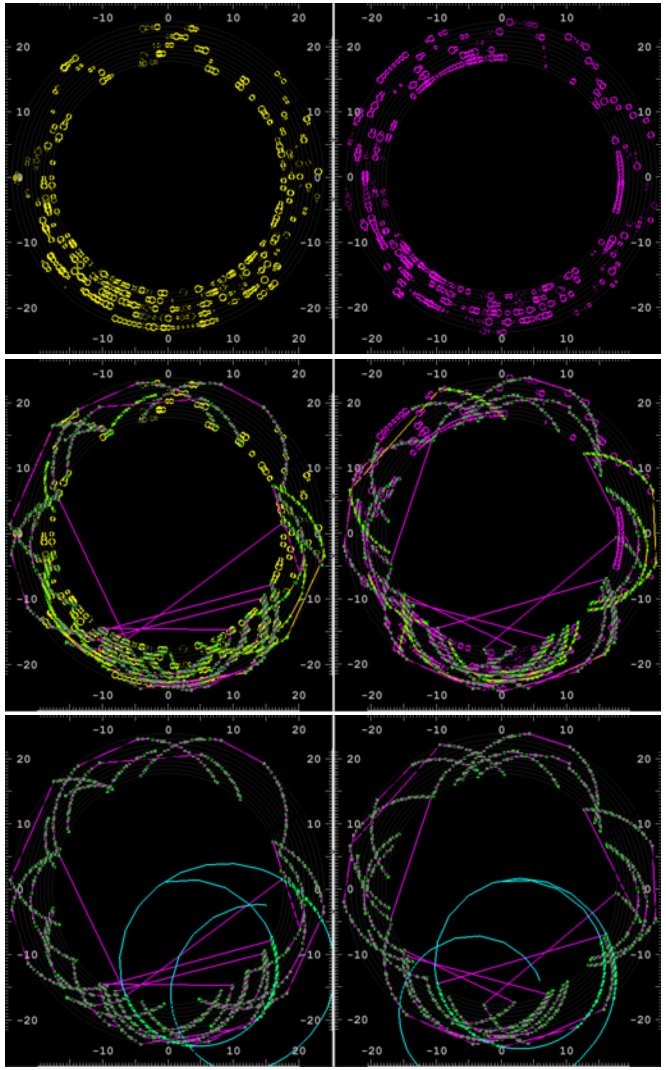

3D track finding and fit

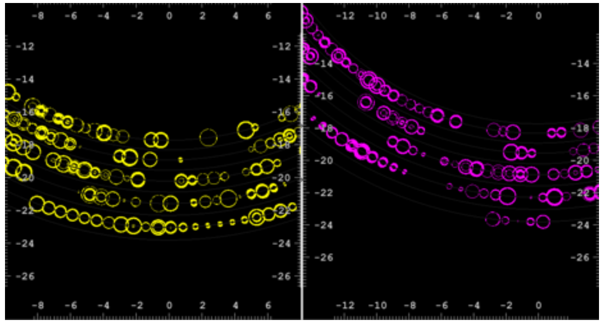

signal track

CUTTING THE WIRE (atropos)

After the soldering phase is completed, the wound multi-wire plane needs to be unrolled from the rotating cylinder and placed on the transport frame during the extraction phase. To this purpose, the excess wire between the wire PCBs must be removed.

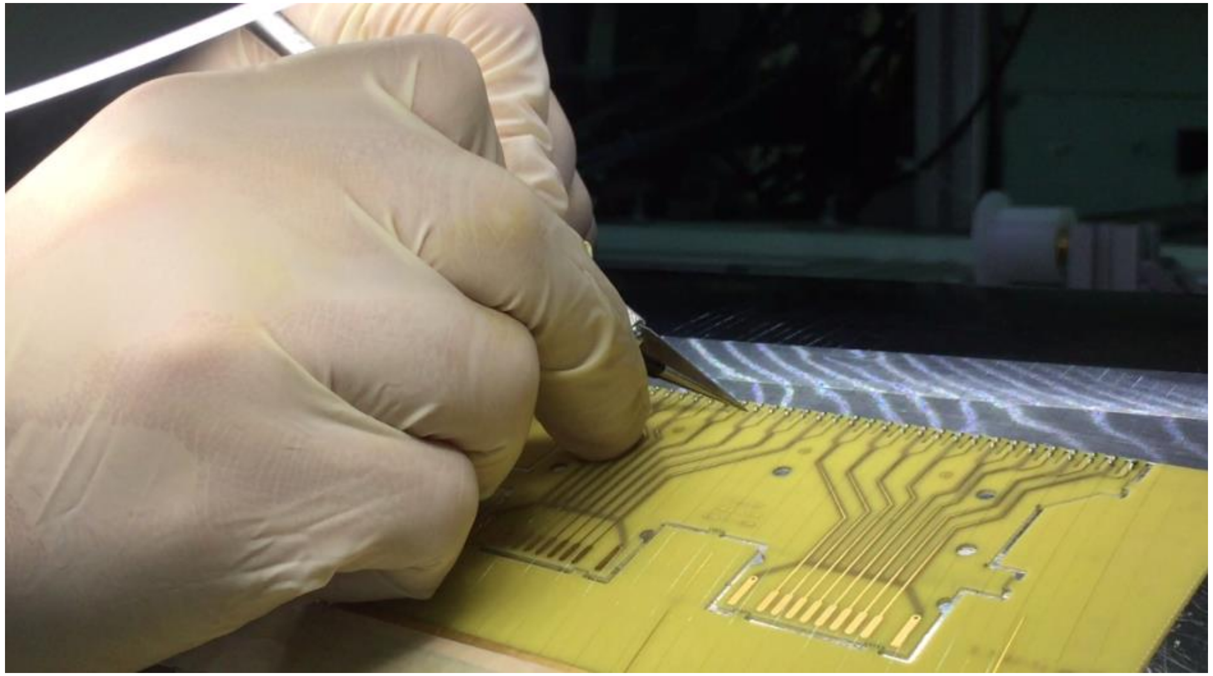

PRODUCTION PHASE

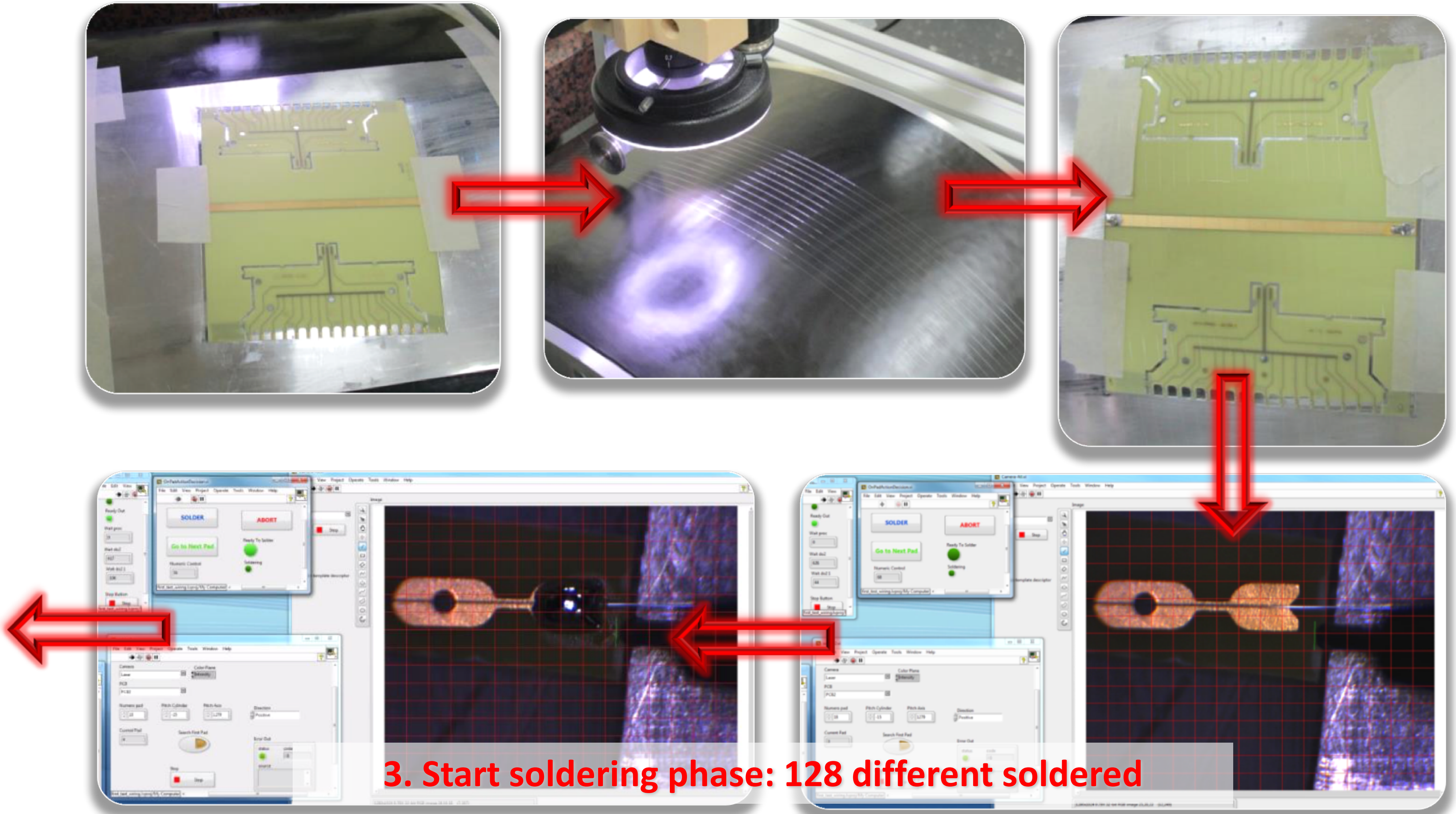

3. Start soldering phase: 128 different soldered

PRODUCTION PHASE

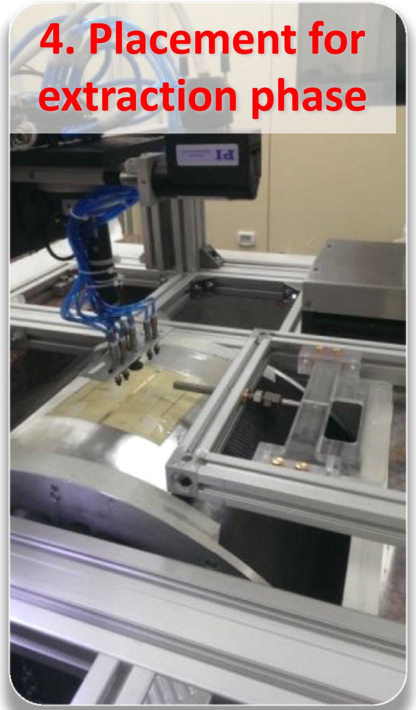

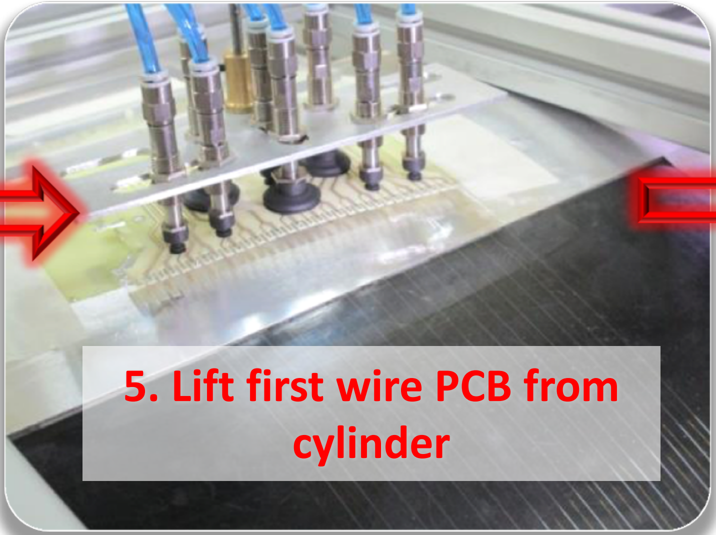

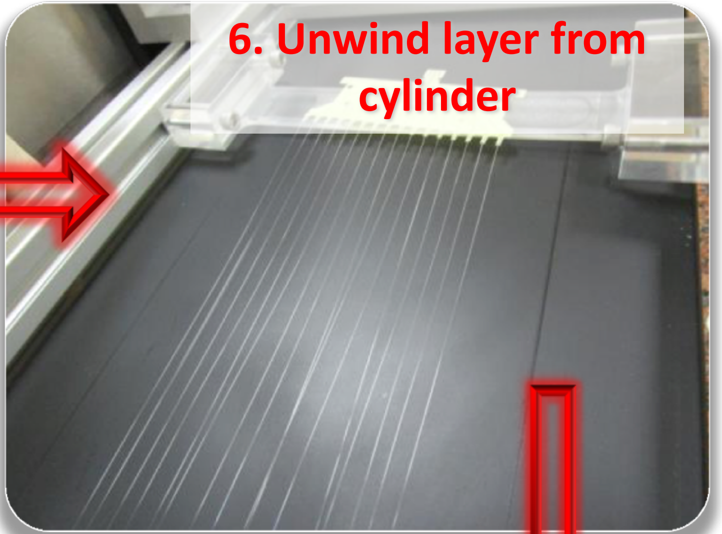

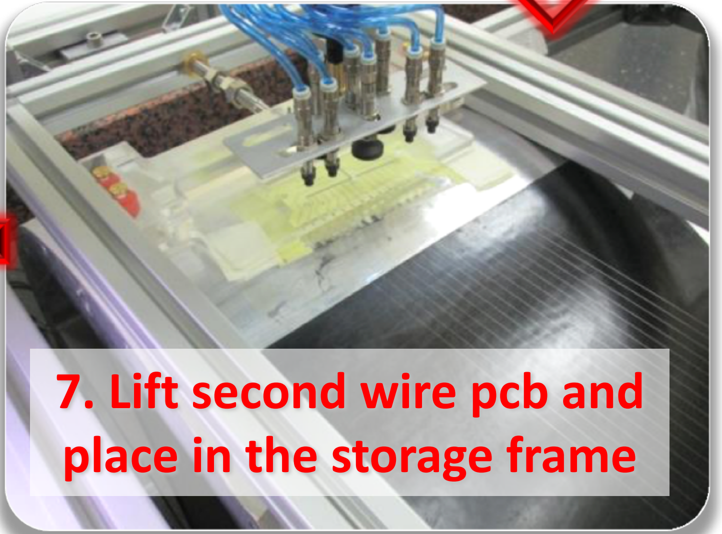

MEG II CDCH: aging

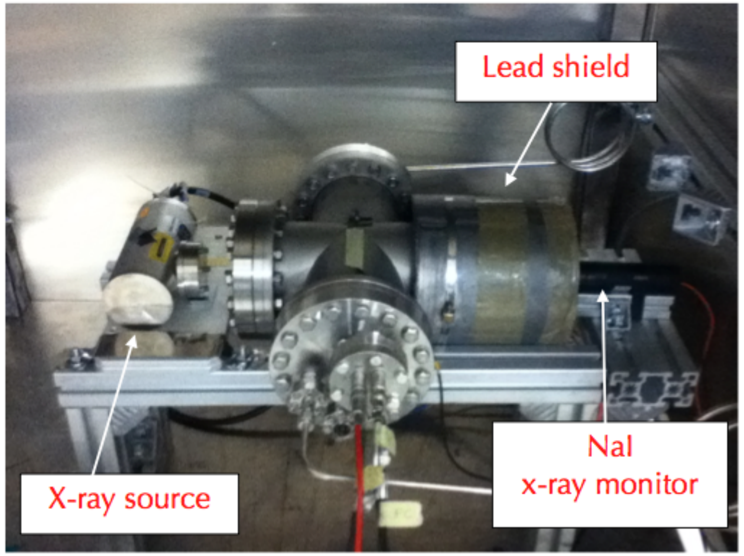

@ 7×10^7 μ/s and 10^5 gas gain

expect ≈ 6 nA/cm in the hottest point

≈ 0.32 C/cm

integrated over 3 years data taking

(however, @ $G = 10^5$, $dG/dV \approx$ 3-4%/Volt)

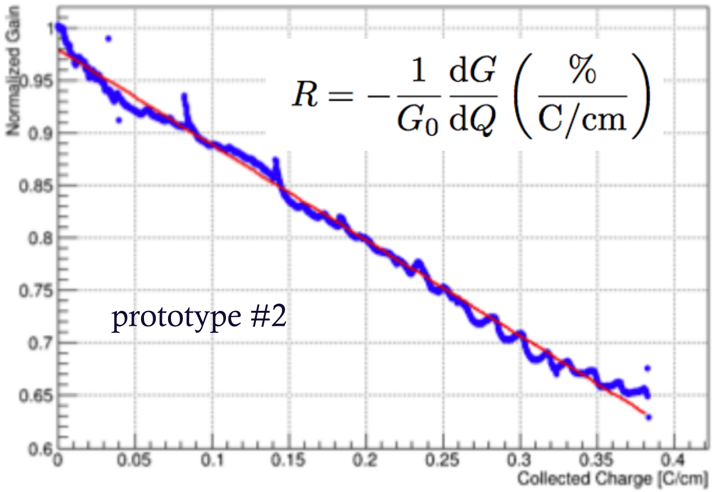

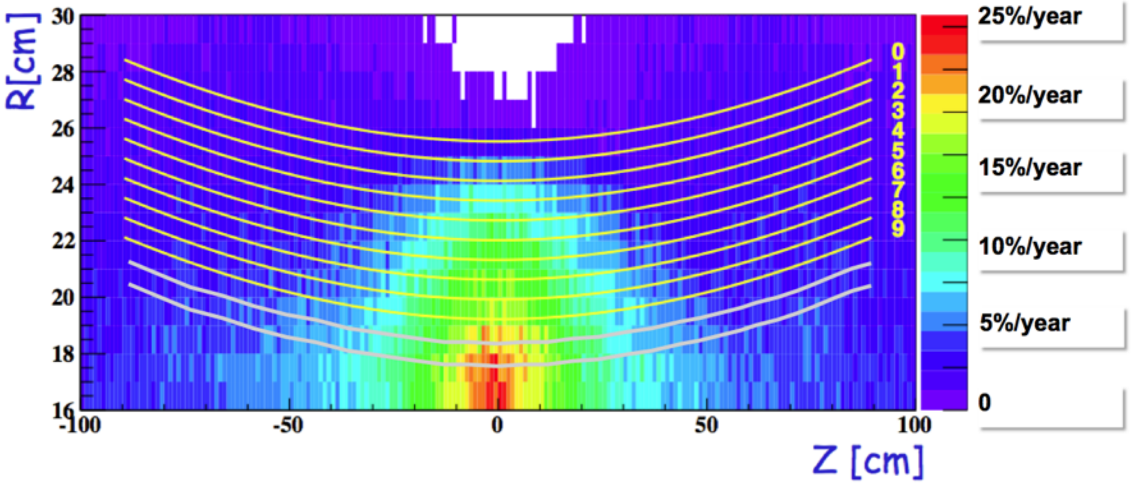

MEG-II DC: single hit resolution

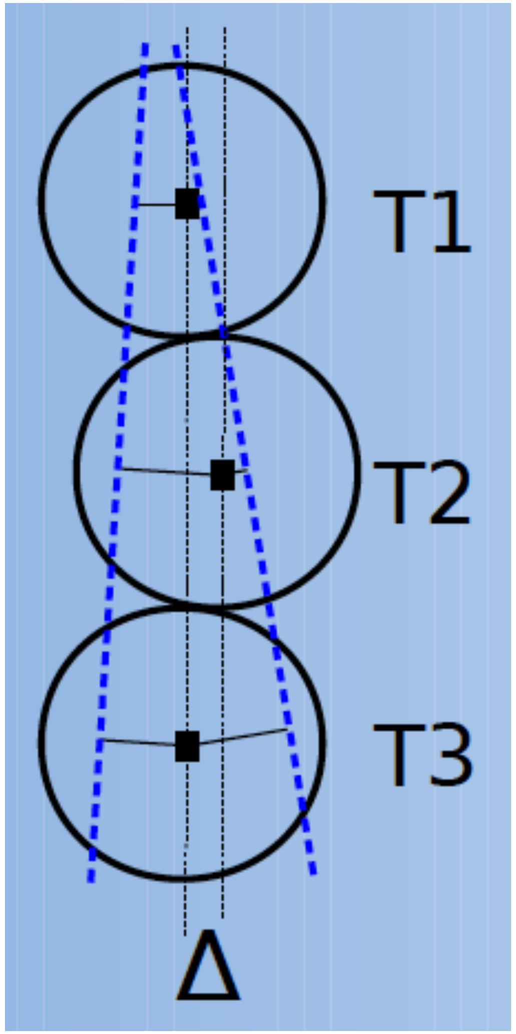

Staggered 3-tubes method with cosmic rays

85% He – 15% iC_4H_{10} : $\sigma_{drift} \approx 130\ \mu m$

averaged over all impact parameters and angles

(leading edge discrimination, no cluster timing)

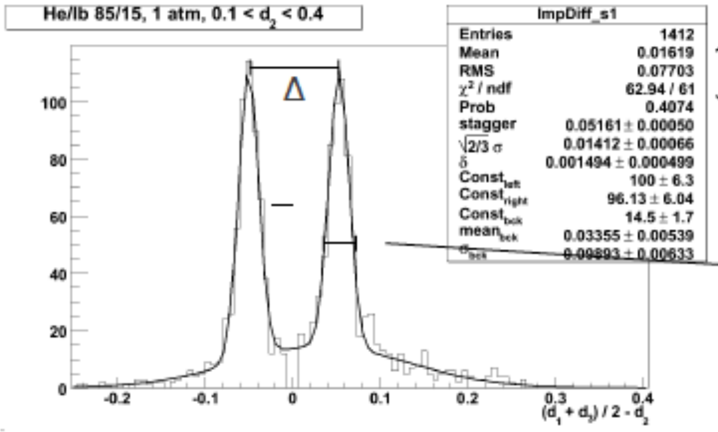

$$D = \frac{d_1 + d_3}{2} - d_2 \qquad \sigma_D = \sqrt{\frac{3}{2}}\sigma_d$$

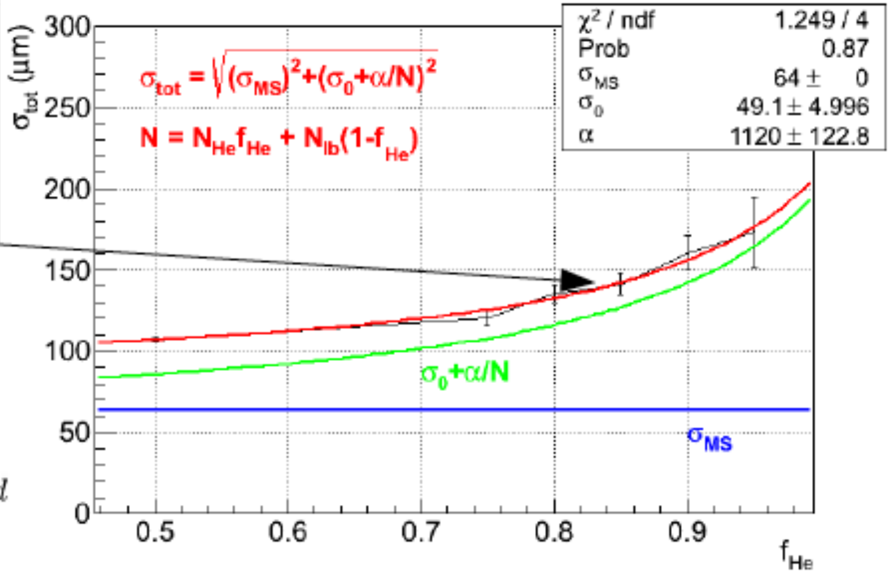

MEG-II DC: single hit resolution

Spatial resolution II

Staggered 3-cells method under Si telescope

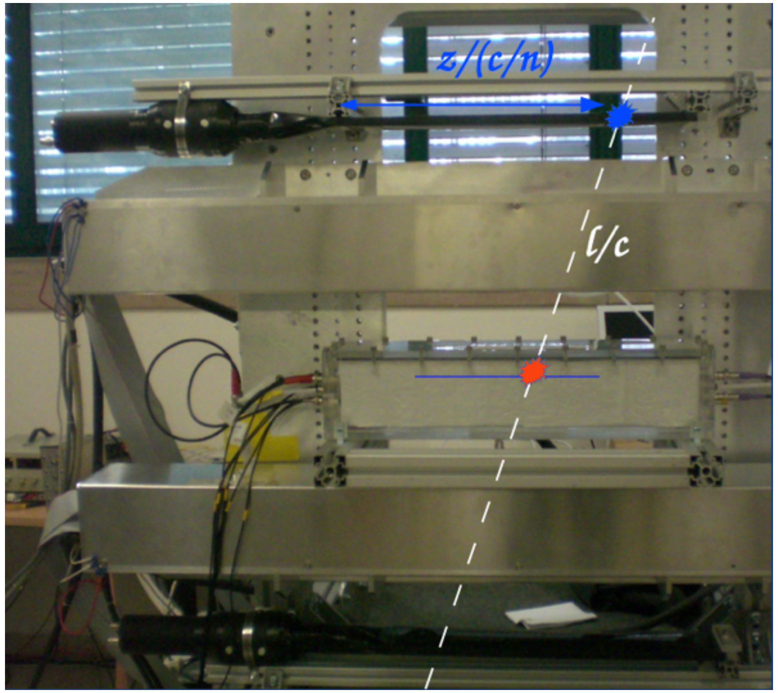

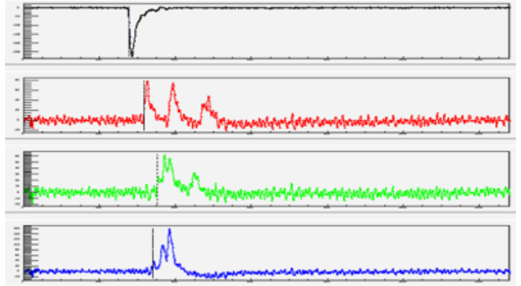

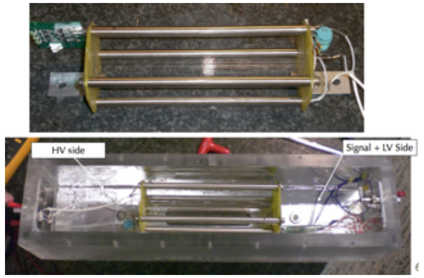

85% He – 15% iC_4H_{10}

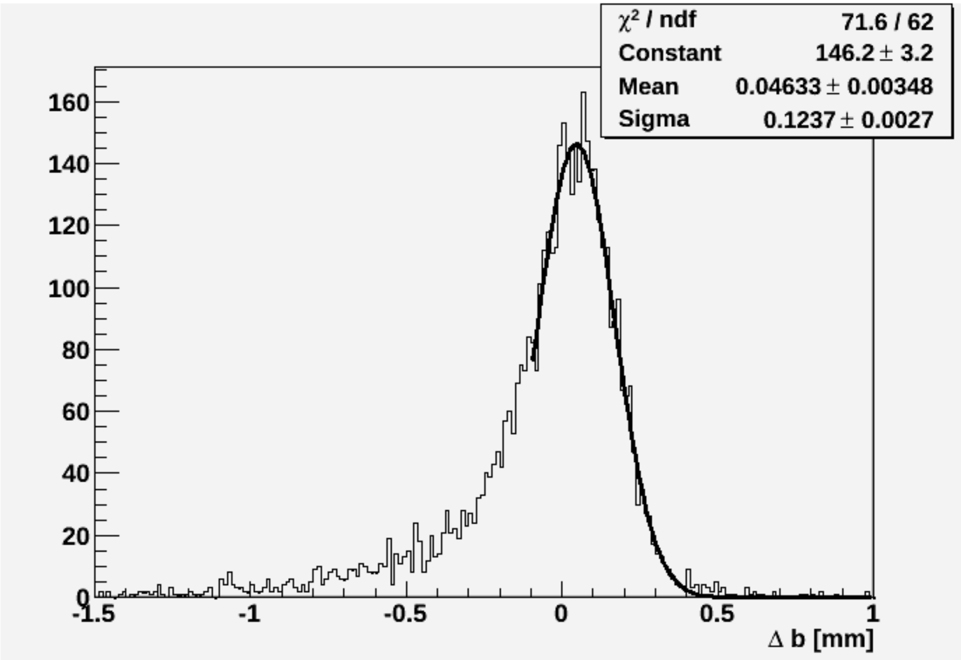

Average hit resolution σ_{drift} = 108 ± 5 μm

MEG-II DC: single hit resolution

Spatial resolution III

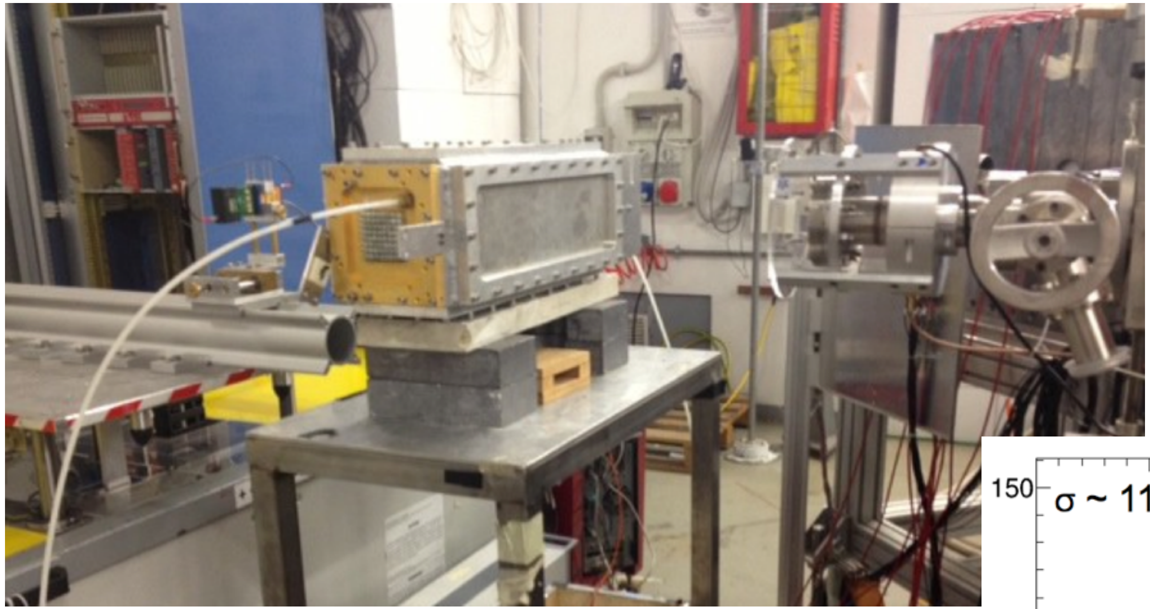

Beam test at BTF – LNF

normal incidence tracks

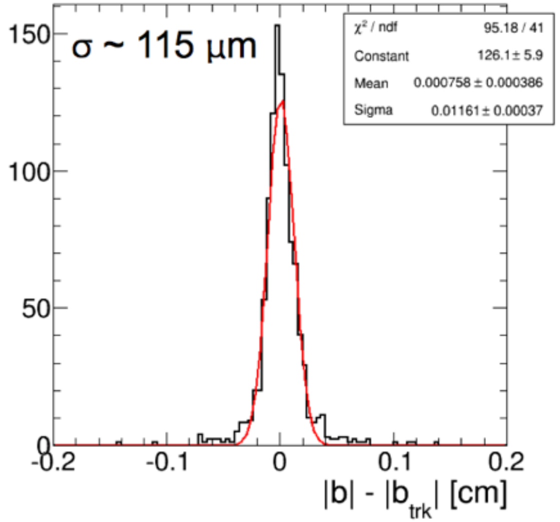

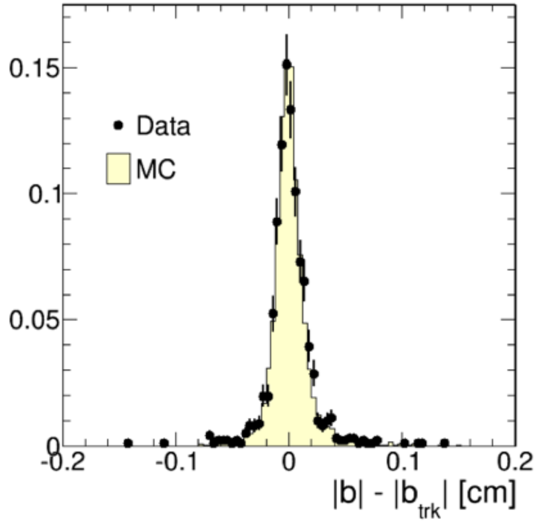

Average hit resolution

$\sigma_{drift} = 116 \pm 4\ \mu m$

Cluster Timing

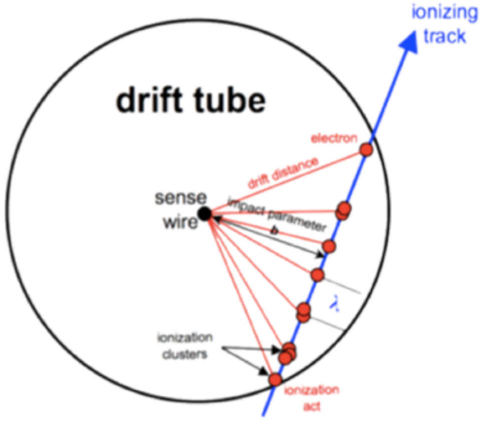

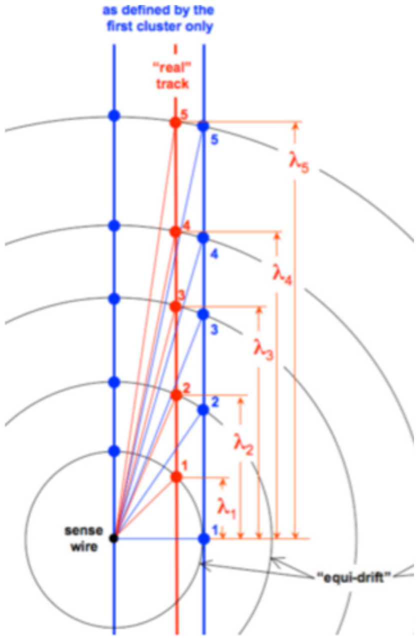

From the **ordered sequence of the electrons arrival times**, considering the average time separation between clusters and their time spread due to diffusion, **reconstruct the most probable sequence of clusters drift times:**

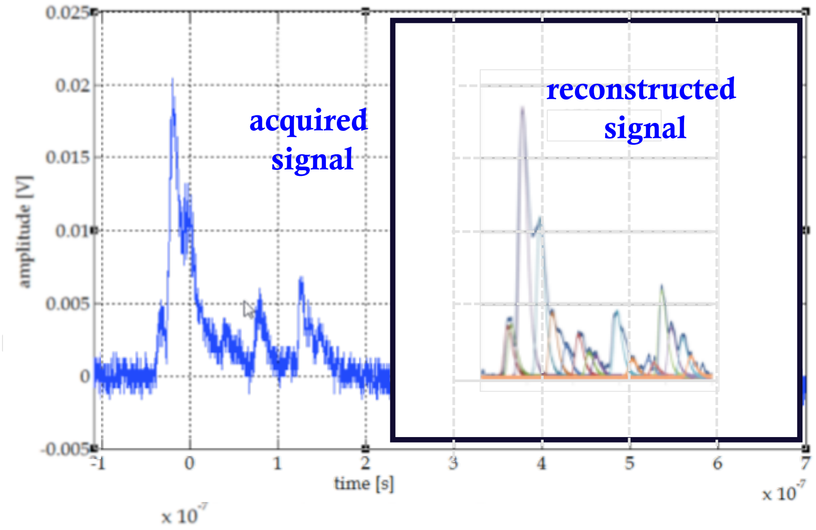

For any given first cluster (**FC**) drift time, the **cluster timing technique** exploits the drift time distribution of all successive clusters to determine the most probable impact parameter, thus reducing the **bias** and the average **drift distance resolution** with respect to what is obtained from with the FC only.

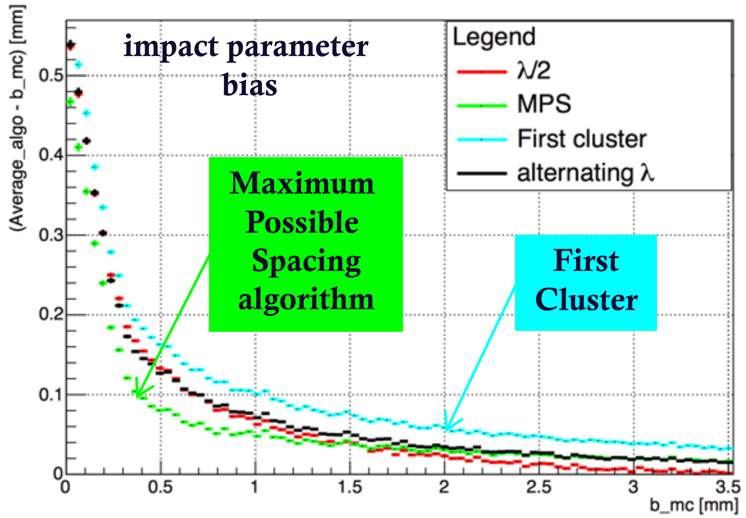

MEG-II DC: gas system

general layout

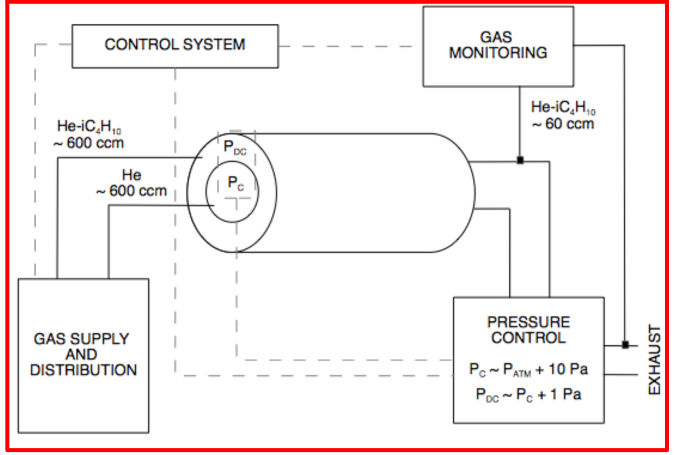

mixing and distribution | pressure control | monitoring

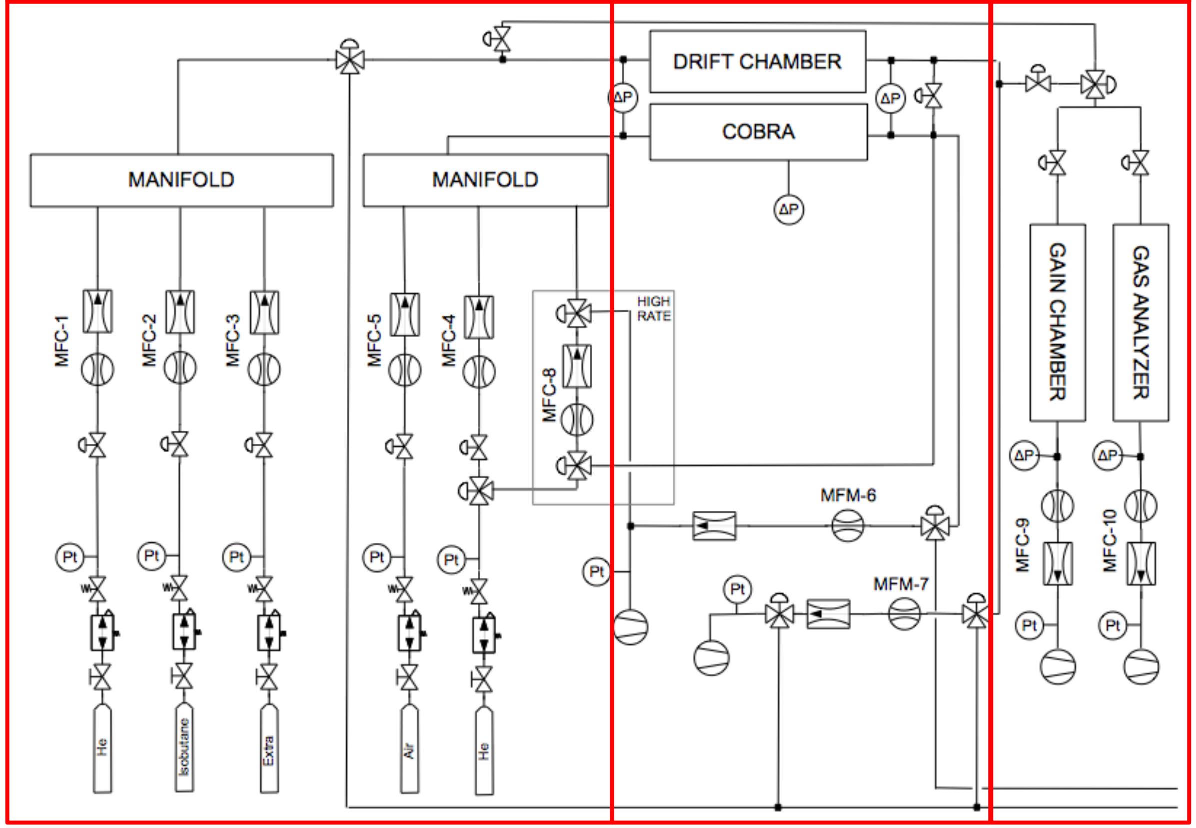

basic gas mixture:
85% He – 15% iC_4H_{10}
(+ H_2O vapor?)
DC volume ≈ 350 liters
1 volume exchange / 10 h

MEG II CDCH: HV distribution

6 boards ISEG

EHS F230p 305F SHV 16ch 3kV, 3mA
in a 10 slot crate

1 HV channel (≈ 1450 V) / 16 cells / sector / layer × 8 sectors × 10 layers = **80 channels**
instrumented active region (2/3 of chamber)
1 HV channel / 64 cells / 4 sectors / layer × 4 sectors × 10 layers = **10 channels**
not instrumented region (1/3 of chamber) only for field distribution
2 HV channels /2 double guard layers × 2 layers = **2 channels**
+ 4 spares = total 96 channels